Energy

FOSSIL

DOE/OR/03054-102
(DE84015652)

FULL-SCALE COLD-FLOW MODELLING OF THE SRC-I SLURRY FIRED HEATER AT CREARE, INC.

Mixing and 1^0 Downslope Studies

By
D. C. Mehta

Work Performed Under Contract No. AC05-78OR03054

International Coal Refining Company
Allentown, Pennsylvania

Technical Information Center
Office of Scientific and Technical Information
United States Department of Energy

DISCLAIMER

DISCLAIMER

This report has been reproduced directly from the best available copy.

Available from the National Technical Information Service, U. S. Department of Commerce, Springfield, Virginia 22161.

Price: Printed Copy A07
Microfiche A01

Codes are used for pricing all publications. The code is determined by the number of pages in the publication. Information pertaining to the pricing codes can be found in the current issues of the following publications, which are generally available in most libraries: *Energy Research Abstracts (ERA); Government Reports Announcements* and Index (*GRA* and I); *Scientific and Technical Abstract Reports (STAR);* and publication NTIS-PR-360 available from NTIS at the above address.

DOE/OR/03054-102
(DE84015652)
Distribution Category UC-89

FULL-SCALE COLD-FLOW MODELLING OF THE SRC-I SLURRY FIRED HEATER AT CREARE, INC. MIXING AND 1% DOWNSLOPE STUDIES

Prepared by
D. C. Mehta

INTERNATIONAL COAL REFINING COMPANY
P. O. Box 2752
Allentown, Pennsylvania 18001

for the

UNITED STATES DEPARTMENT OF ENERGY
Office of Solvent-Refined Coal Products
under Contract DE-AC05-78-OR-03054

TABLE OF CONTENTS

LIST OF TABLES

Page

LIST OF FIGURES

ABSTRACT

This report discusses the second phase of the slurry fired heater cold-flow modelling experiments at Creare, Inc. The experimental setup and operating conditions were selected to simulate a typical fired heater. The first half of the experimental series was designed to measure the extent of mixing between the liquid carpet and the slugs passing above it. The second series was performed in a 1° downslope configuration. This report covers the results of these experiments and their application to the fired heater design.

EXECUTIVE SUMMARY

One of the major pieces of equipment in the SRC-I Demonstration Plant is the slurry fired heater. Because of the absence of any plant data at comparable combinations of operating severity, a cold-flow modelling experimental program was initiated at Creare, Inc. The first phase of the test program confirmed the fired heater design and established reliable boundaries of flow rates for proper operation of the fired heater.

An experimental setup was designed and built at Creare to duplicate the piping arrangement and flow conditions of the fired heater. The pipe dimensions, flow rates, and fluid properties were selected to minimize areas of scale-up and extrapolation. This follow-up test program was developed to resolve concerns raised from the observations made in the first phase. Tests were conducted to establish the extent of mixing between the liquid carpet and the fast-moving liquid slugs above it. The other segment of the test program was designed to develop the flow regime and pressure drop data in the 1° downslope configuration.

The results demonstrated a significant amount of mixing between the liquid carpet and the liquid slugs for water and the 400-cP fluid at the design flow conditions. The extent of mixing improved with increasing liquid and gas velocities and decreasing liquid viscosities. Adequate mixing was observed at liquid flow rates as low as 50% of the design flow conditions.

Slug flow was observed at design conditions in the 1° downslope configuration. The liquid velocity corresponding to the transition from slug to stratified flow was significantly influenced by the liquid viscosity. The gas holdup measurements were in good agreement with predictions by the Hughmark correlation. However, the pressure drop data were less than 50% of the predicted values from the Hughmark correlation.

Although adequate mixing is expected in heater pipes, different techniques should be investigated to improve the extent of mixing.

Because the transition boundary in the 1° downslope configuration encroaches into the desired operating range of the flow rates, this boundary should be firmly established to allow a greater range of operating conditions.

INTRODUCTION

The slurry fired heater handles a mixture of coal, process solvent, and hydrogen-laden gas at temperatures of 480-760°F. Operating temperatures, pressures, and fluid velocities, as well as the presence of three-phase mixtures make the slurry fired heater one of the most complex pieces of equipment in the design of the SRC-I Demonstration Plant. The complexity of the design has led to a need for the verification of several assumptions made during the early design stages.

The design verification experiments were begun at Creare R&D, Inc. in January 1982 (Crowley et al., 1983). The experimental setup was a scaled replica of a one and one-half turn of the fired heater piping. The primary concern was the behavior of gas and liquid phases in the pipe at various combinations of operating conditions. The results of these earlier experiments confirmed the presence of the desired slug flow in the heater pipe. The experiments also indicated that a thick layer of liquid carpet flows at a relatively slower velocity than the slugs passing over it. The concern over the possible variance in heat transfer in the carpet and slugs and its influence on heat-related pipe stresses prompted ICRC to undertake experiments to quantify the extent of mixing between the liquid carpet and slugs passing over it.

The pipe configurations tested thus far have been 1° upslope and horizontal arrangements. The 1° upslope corresponded to the more likely heater design and the horizontal configuration was tested to provide two-phase data for comparison with the open literature. However, one of the possible, although less likely, pipe configurations involves a 1° downslope. This arrangement has been used in one of the coal liquefaction pilot plants and should be tested to develop design data. Therefore, the experimental setup was modified to develop the two-phase flow data in the 1° downslope configuration.

An overall perspective of the test program and the application of the results in the fired heater design are discussed in this report. An acceptable criterion for mixing between the liquid carpet and slugs is presented. The criterion is then used to establish flow rate boundaries to assure adequate thermal mixing in the heater pipes. A simplified

correlation is developed for calculating gas holdup in a 1° downslope configuration. The gas holdup data are also compared with predictions by the Hughmark correlation, which was used in the ICRC fired heater design to predict gas holdup.

FIRED HEATER DESIGN DETAILS

The preliminary design of the fired heater is based on data from the Ft. Lewis Pilot Plant, and represents an approximate 30-fold extrapolation to a 6.813-in. pipe in the demonstration plant. This phase of the program is an extension of the work initiated in Phase I. Many of the fired heater design details are listed in the report published on the earlier work (Mehta, 1983). Some design information is outlined here to provide a cursory perspective.

Each demonstration plant heater contains an 8-in. schedule 160 nominal size pipe with an i.d. of 6.813-in. and an overall length of about 3,000 ft. The pipe is laid out in a 10- x 40-ft racetrack arrangement with a 1° upward slope. A mixture of coal and process solvent enters the fired heater at about 500°F. The mixture at the entrance contains about 40 wt % coal, which goes into solution during the heating process. A hydrogen-rich gas mixture is added to the heater to prevent cracking and coking in the heater pipes. The temperature of the mixture rises to about 760°F at the exit of the fired heater. The overall superficial velocity is limited to 18 fps to minimize pipe erosion. The viscosity of the liquid phase is expected to range from 80 to 400 cP.

The major factors influencing the fired heater design are heat transfer coefficients, pressure drop, internal pipe wall temperatures, and the possibility of erosion. All of these factors affect design in different ways, and the final design would be an attempt to maximize the benefits of each of them. The operating conditions affecting these factors are flow regime, fluid velocities, gas holdup, and fluid properties. Pipe configuration and orientation also play a role in the operation of the fired heater.

The test program was initiated to resolve concerns resulting from the 30-fold extrapolation and to develop data that would assist in optimizing the fired heater design. This extension work investigated a third relevant pipe orientation and was designed to answer questions raised by the results of the initial work.

PROGRAM OBJECTIVES

The objectives of the test program were to:

- Measure the extent of mixing between liquid carpet and liquid slugs.
- Develop flow characterization data in the 1° downslope pipe configuration.
- Determine the allowable range of gas and slurry velocities to avoid flow stratification.
- Generate slug behavior data and measure two-phase pressure drop over the full range of operating conditions.
- Compare the flow behavior and pressure drop data with available predictive methods.

TEST PROGRAM

The overall experimental setup is shown in Figure 1. The test loop was a 6.75-in. i.d. transparent Lexan pipe arranged in a racetrack arrangement. The overall dimensions of the test loop were 10 x 40 ft, with a total length of about 150 ft. The 90° bends were made of carbon steel for ease of fabrication. The Lexan pipe was assembled in several 6-ft sections to provide flexibility in instrumenting the loop and monitoring the flow behavior. The rest of the major pieces of equipment included inlet plenum, separator tank, slurry preparation tank, slurry feed pump, and Freon compressor.

The primary instrumentation is illustrated in the figure and described in the earlier report. The liquid and gas phases selected for the experiments were to simulate the fired heater operating conditions.

The liquid phase was water with the viscosity modifier sodium carboxy methyl cellulose (SCMC). The concentration of SCMC could be varied to create liquid phase viscosities ranging from 1 to 400 cP. The selection of Freon 12 for the gas phase provided a comparable gas density of 1.9 lb/ft^3 at a loop pressure of 80 psia. The liquid and gas phase flow rates could be varied from zero to full design loads. Tables 1 and 2 list the operating conditions tested in each of the segments of the program.

The mixing experiments consisted of injections of color dye and salt solution for qualitative and quantitative representation, respectively. The color dye was injected into the carpet and a preselected downstream location was filmed at a very high speed for visual demonstration of mixing. The quantitative procedure was much more elaborate. The schematic of the instrumentation for the mixing experiments is shown in Figure 2. The salt solution was injected at one location and the liquid samples were withdrawn at a pipe location 20 diameters downstream. The injection was spread over 10 small pores to minimize the disturbance of the carpet, and was carried out continuously for 10 sec. The samples were collected at three elevations, top, middle, and bottom, to quantify the extent of mixing. The liquid samples were withdrawn every time the slug passed these locations and were collected in three separate containers. The relative concentration of salt in each of these samples compared with a theoretically calculated fully mixed concentration gave the degree of mixing. The mixing experiments were performed in the horizontal loop configuration. Even though the slug frequencies are comparable (Mehta, 1983), identical flow conditions generate longer and faster liquid slugs with a thinner liquid carpet in the 1° upslope than in the horizontal loop configuration. Therefore, the level of turbulence at the front and the back of a liquid slug would be greater in the 1° upslope configuration. Therefore, the extent of mixing in the 1° upslope configuration would be improved over the horizontal arrangement.

The experimental setup was modified for a 1° downslope configuration. The overall test plan was the same as the previous flow characterization tests. The gas and liquid superficial velocities were

varied to cover the design values down to a 33% load. The liquid velocities were changed as needed to establish the transition boundary between the slug and stratified flows. The liquid and gas phase superficial velocities, pressure drop across specific pipe sections, slug frequency, slug dimension, slug velocity, and liquid carpet height were monitored during each combination of operating conditions. Gas holdup was calculated from the data recorded in the test program. Two additional gas phase velocities were tested to definitively establish the transition boundary.

RESULTS AND DISCUSSION

Because the objectives of the mixing experiments and the 1° downslope experiments were completely independent of each other, the results from each of these portions are presented and evaluated separately.

Mixing Experiments

The liquid slug picks up a signifigant amount of fluid from the carpet anteriorly and sheds an almost equal amount of the fluid posteriorly. This process creates a great deal of turbulence and exchange of fluids at each end of the slug. The fluid exchange continues throughout the length of the fired heater pipe. An adequate level of mixing between the carpet and slug would minimize temperature variations at a given cross-section of the pipe. Therefore, a quantitative evaluation of the fluid exchange mechanism was undertaken to identify any possible problems.

The experimental setup is outlined in greater detail in the Creare report (Appendix A, Crowley et al., 1984). The sampling was initiated starting with the first slug reaching the sampling points after the injection began. The period of 10 sec allowed collection of samples from about 20 slugs. The expected salt concentration in the fully mixed liquid was calculated from the amount of salt injected and the liquid superficial velocity. The salt concentrations in the feed and the samples were measured using conductivity probes. The sampling technique employed resulted in an average salt concentration for each slug, and an overall average for the approximately 20 slugs sampled.

The concentration gradients were first tested for a single phase flow. Different liquid superficial velocities were set for the tests. The single phase fluid flow was also modeled using a computer program "FLUENT" which was developed by Creare. The program can calculate the salt concentrations and draw contours in any direction desired for observation.

The FLUENT program used a finite difference grid system to calculate salt concentrations at successive locations. A fully turbulent flow was assumed in the pipe. The calculations show that most of the salt tends to stay in the lower half of the pipe. The salt concentration at the middle of the pipe is about 10% of the maximum concentration.

The salt reaches up to the center of the pipe at the injection point and settles to the bottom at downstream locations. However, the FLUENT program applies only to single-phase situations and some steady-state two-phase situations. Nevertheless, the results from the FLUENT program provided an understanding of the path of the salt solution.

The results of the mixing experiments in the single- and two-phase flows are tabulated in Tables 3 and 4, respectively. The experimental loop is a closed loop operation, and therefore, the batch of liquid in the system retains some salt from preceding experiments. The concentrations shown in the tables are measured values minus the salt concentration in the recirculating liquid at the start of each test.

The salt concentration values of the samples from the middle and top of the pipe were compared to determine the extent of mixing. The movies taken to observe the mixing phenomena were not useful because rusting of the tanks from the presence of salt resulted in a colored background. The injection of a colored dye did not provide any contrasting effects to enhance the usefulness of the movies.

The liquid sample points were flush with the pipe wall instead of being inserted about ½ in. inside the pipe to avoid disturbing the flow regime. However, as a result, most of the sample liquid was collected from the boundary layer, especially for the side and top sample points. Therefore, the salt concentrations measured in the liquids collected from these two sample points would be affected by the experimental

technique. Because of this limitation, lower salt concentration values for these sample points compared with the bottom sample point would be acceptable. Relative salt concentrations of 67% for the side and 50% for the top sample points compared with the corresponding value for the bottom sample point are considered acceptable. The mixing data developed at Creare should be used primarily to establish the lower limits of the flow rates to attain a desired level of mixing.

The results consistently show certain trends in the extent of mixing between the liquid carpet and slugs:

- The extent of mixing improves with increasing liquid phase velocity. The salt concentration at the bottom of the pipe decreases with increasing liquid velocity.
- The increase in liquid phase viscosity reduces the extent of mixing.
- Increasing gas velocity increases the overall mixture velocity, which in turn enhances the level of turbulence in the pipe. The increased turbulence tends to improve the extent of mixing.
- Although slugs appeared to be present in the pipe, the results show that a small gas pocket was present above the liquid slugs during certain flow conditions. This phenomenon prevented the collection of adequate-sized samples from the sample location at the top of the pipe.
- The results demonstrate an acceptable level of mixing with water or with the 400-cP liquid at the design gas and liquid superficial velocities of 12 and 6 ft/sec, respectively.

One-Degree Downslope Experiments

The 1° downslope is the third pipe configuration investigated at Creare, and was derived from its use in one of the coal liquefaction pilot plants. These experiments would enable the evaluation of all major pipe configurations and would assist in selecting the most optimum fired heater design.

An additional set of instrumentation was added to the series of tests. An attempt was made to estimate carpet height and slug velocities with the use of two banks of conductivity probes placed at a fixed distance. One bank contained probes at pipe diameters of 25, 35, 45, 55, and 65%, and in the other bank, probes were placed at pipe diameters of 30, 40, 50, 60, and 70%. The probes were capable of identifying whether they were in contact with a liquid or a vapor phase. The overall carpet height monitoring would be within 5% of the pipe diameters. By maintaining a fixed distance between the two banks of probes, the slug velocities could be calculated. This instrumentation was relatively successful with water because it drained off the probe bank sufficiently rapidly. However, the viscous fluids did not drain quickly enough, and therefore, the results from the probe banks were inconsistent. The technique would be improved in the next phase of the experiments.

Flow Regime

The flow regime experiments included observing the prevailing flow regime at a given combination of gas and liquid phase superficial velocities and establishing a transition boundary between the slug and stratified flow. The observed flow regimes were recorded on movies for future evaluations. The gas velocity was set at a desired value and the liquid velocity was raised until the onset of slugging was observed. The results obtained in the series of experiments were then compared with those obtained with the 1° upslope and horizontal configurations.

Two additional gas velocities were tested for water and 80-cP fluid to develop greater confidence in the transition boundary. The results of the transition experiments are presented in Table 5, and these results along with those for horizontal and 1° upslope configurations are illustrated in Figure 3. As can be seen, the transition data for water and 80-cP fluid show a reverse trend compared with the other two pipe configurations. The liquid phase transition velocity decreases with an increase in gas phase velocity, whereas, for all other experiments, the transition velocity increases with an increase in gas velocity.

Creare presented a preliminary theory to explain the diverse nature of the transition boundaries. The theory, which is summarized below for perspective, is based upon a plot of curves of constant gas void fractions. It is reasoned that the critical Froude number, Fr, could locate the transition boundary on these plots.

$$Fr = \frac{V_{GS}\sqrt{\rho_G}}{\sqrt{D \cdot g_c \cdot \Delta\rho}} = a \cdot \varepsilon_G^{3/2} \qquad (1)$$

In the down-flow situation, the flow of the low-viscosity fluid is influenced more by the gravitational force than the interfacial shear stress and the momentum forces. The two limits of ε_G=0 and ε_G=1 were used to develop a plot in Figure 4 to illustrate the general nature of the transition boundaries for various pipe configurations. The plot compares the range of operating conditions tested at Creare to the transition boundaries, and demonstrates that the reverse trend in the slope of the transition boundary for water and 80-cP fluid in the downslope configuration is explainable.

Gas Holdup

Gas holdup in a pipe affects the heat and mass transfer between phases, as well as between the pipe wall and the fluids. The presence of a slow-moving liquid carpet results in a smaller gas holdup than indicated by the ratio of the gas and total superficial velocities. However, in the case of the downslope configuration, the liquid carpet has gravitational force as the additional driving potential. Therefore, the liquid carpet would be moving at a faster velocity than that in the horizontal or 1° upslope configurations, and this phenomenon would obviously result into a higher gas holdup in the downslope pipe configuration.

Gas holdup is a function of fluid properties and operating conditions, and has been very well correlated to the Lockhart-Martinelli (L-M) parameter X in previous ICRC slurry fired heater modelling investigations. The L-M parameter is an incorporation of physical properties such as gas density and viscosity, liquid density and viscosity, and operating conditions such as gas and liquid phase super-

ficial velocities. Equation 1 shows the relative contributions of these variables in the L-M parameter.

$$X = \left(\frac{\rho_L}{\rho_G}\right)^{0.4} \left(\frac{\mu_L}{\mu_G}\right)^{0.1} \left(\frac{V_{LS}}{V_{GS}}\right)^{0.9} \quad (2)$$

During the experiments at Creare, some of these variables were held constant; e.g., the liquid and gas phase densities were held at 62.3 and 1.9 lb/ft^3, respectively. Gas phase viscosity was also steady at 0.013 cP. As in the previous program, the liquid phase viscosity was varied from 1 to 80 to 400 cP. The combinations of gas and liquid velocities tested are listed in Table 2.

The technique to measure gas holdup is to isolate a specific section of the test loop and collect the liquid in that segment in a measuring tank. Although isolation of the portion of the test loop requires the use of quick-acting shutoff valves, for the pipe size of 6.75-in. in these experiments, the possibility of severe water hammer prevented the use of this technique. Instead, gas holdup was indirectly calculated with the use of a simple formula, in which it was correlated to two reliably measured variables of gas superficial velocity and slug velocity:

$$1/\varepsilon_G = V_S/V_{GS} \quad (3)$$

The slug characteristic data for the experiments are listed in Table 6, and the calculated values of the gas holdup are provided in Table 7. The gas holdup values were then correlated with the L-M parameter to develop the following equations:

For a 1° downslope pipe: $1/\varepsilon_G = 1.160 + 0.197\ X$ (4)

For a horizontal pipe: $1/\varepsilon_G = 1.295 + 0.194\ X$ (5)

For a 1° upslope pipe: $1/\varepsilon_G = 1.563 + 0.266\ X$ (6)

The equations for the horizontal and 1° upslope pipe configurations are presented for comparison. As expected, gas holdup decreases with a

change in pipe configuration to horizontal and decreases even more for a 1° upslope pipe configuration. It should be recognized that these equations were developed for the 6.75-in. pipe, and their usage with other pipe dimensions should take this into consideration. These correlations were developed by linear regression analysis using the least squares technique. Therefore, even though the data show some scatter, the coefficients in the equations are listed to four significant figures for accurate predictions. The primary objective of developing these equations was to have simplified correlations from the experimental data specifically for the SRC-I fired heater. A varying degree of accuracy was observed by using generalized correlations such as the Hughmark correlation.

The experimentally calculated values of gas holdup were then compared with the estimations using the Hughmark correlation (Hughmark, 1965), which is more generalized because it incorporates pipe diameter. The equations proposed by Hughmark are listed below:

$$\varepsilon_G = \frac{V_{GS}}{(1 + K_2)\ (V_{GS} + V_{LS})} \tag{7}$$

K_2 is a function of the modified Reynold's number Re_L'. It can be approximately correlated to Re_L', as shown in equations 7, 8 and 9:

$$Re_L' = \frac{D(V_{LS} + V_{GS}) \cdot \rho_L}{\mu_L} \tag{8}$$

$$K_2 = 1.8896 - 0.3074 \times \log Re_L' \quad @\ Re_L' < 2.7 \times 10^5 \tag{9}$$

$$K_2 = 0.22 \quad @\ Re_L' > 2.7 \times 10^5 \tag{10}$$

Comparisons of the measured and calculated values of gas holdups are listed in Table 7 and illustrated in Figure 5. The calculated values of the gas holdup by the Hughmark correlation are an average of 20% lower than the measured values for viscous fluids. The results from the Hughmark correlation are reasonable, but should be used with caution if the 1° downslope configuration is selected for the fired heater.

Pressure Drop

The presence of two-phase flow complicates the measurement of pressure drop in the test loop. The existence of intermittent flow and downslope configuration creates additional difficulties in the pressure drop measurements. Because continuous pressure monitors did not work consistently in the test facility at Creare, manual differential manometers were installed. The unsteady nature of the flow in the downslope configuration further complicated the measuring techniques.

The pressure drops were measured across three segments of the test loop: the 30-ft-long middle leg, a 10-ft-long turnaround covering two 90° bends, and the 30-ft-long last leg. The average pressure drop results for the straight pipe segments are presented in Table 8, and the raw data are presented in the Creare report in Appendix A.

Although single-phase pressure drops have been correlated by several models in the literature, there are very few correlations to describe the two-phase flow data. The Hughmark correlation, which was reasonably successful in predicting the Creare two-phase pressure drop data in the horizontal and 1° upslope configurations, predicted significantly higher (over 100%) pressure drops than the measured values for several combinations of flow rates. One possible explanation for the discrepancy could be related to the difficulty in measuring pressure drop.

The two-phase pressure drop correlations developed by Shu and Vermeulen and Ryan account for wall shear due to liquid and the entraining of liquid ahead of the slug. Both these correlations assume the liquid carpet velocity to be zero. The carpet velocity is particularly high in the downslope configuration, and therefore, these two correlations lead to large values for the acceleration term in the pressure drop predictions.

Creare presented a theory developed by Wallis to calculate the two-phase pressure drop. This generalized theory pertains primarily to slug flow, which is represented as a series of "unit cells" consisting of one gas bubble and one liquid slug. Figure 5 illustrates the unit cell and related parts of it. With the gas bubble at constant pressure

and its relative density and viscosity low, pressure drop occurs entirely in the liquid slug. Therefore, the pressure drop can be computed for a series of single-phase liquid slugs and accounts for turbulence in the front and back of each slug.

The details of the derivation are contained in the Creare report. The final expression to calculate the frictional pressure drop is as follows:

$$\frac{\Delta P_{TP}}{\Delta L} \leq \left\{\frac{32 \cdot \mu_L}{g_c \cdot D^2}\right\} \left\{V_{LS} + V_{GS}\left(1 - \frac{1}{b\,(1-E_\ell)}\right)\right\} \qquad (11)$$

where $\frac{\Delta P_{TP}}{\Delta L}$ = two-phase pressure drop per linear foot of pipe in lb/ft^3

$b = V_S/(V_{LS} + V_{GS})$

E_ℓ = average fraction of pipe cross-section occupied by liquid around the gas bubble.

The value of b for all the non-Newtonian fluids at Creare ranged from 1.4 to 1.6. The proportion of gas addition dictates the value of E_ℓ, which in turn determines whether the addition of gas flow would increase or decrease the two-phase pressure drop per linear foot of the pipe.

CONCLUSIONS

The conclusions for this phase of the test program are subdivided into mixing experiments and 1° downslope experiments.

Mixing Experiments

- There will be an acceptable level of mixing between liquid carpet and liquid slugs at the design of gas and liquid superficial velocities of 12 and 6 ft/sec, respectively. An acceptable level of mixing was observed with water or the 400-cP fluid at the design flow conditions.

- An acceptable level of mixing was observed for liquid flow rates as low as 50% of the design flow for water and 400-cP fluid.
- The extent of mixing improves with increasing liquid velocity, increasing gas velocity, and decreasing liquid viscosity.

One-Degree Downslope Experiments

- The flow regime will be slug flow at the design conditions of 6- and 12-ft/sec liquid and gas superficial velocities, respectively.
- Slug flow will not exist at mass loadings of two-thirds or lower of the gas and liquid velocities except for 400-cP fluid.
- The liquid velocity corresponding to the transition from slug to stratified flow is significantly influenced by the liquid viscosity. For water and 80-cP fluid, the transition velocity decreased with increasing gas velocity and liquid viscosity. However, the transition velocity for the 400-cP fluid increased with increasing gas velocity.
- Gas holdup was higher than horizontal and 1° upslope configurations at identical operating conditions.
- Gas holdup predictions by Hughmark correlation are in good agreement with the experimental results.
- A simplified correlation was developed equating the reciprocal of gas holdup to the Lockhart-Martinelli parameter for the SRC-I fired heater design.
- The measured pressure drops were 30-50% lower than those used in the fired heater design.
- The observed pressure drop could not be satisfactorily predicted by the Hughmark correlation currently used in the design.
- The two-phase pressure drop increased with increasing gas and liquid velocities and liquid viscosity.

RECOMMENDATIONS

The experiments in this phase indicated adequate mixing between the liquid carpet and slugs at loads as low as 50% of the design conditions. The results also showed that slug flow exists for high gas and liquid velocities. The following recommendations are made to enhance fired heater operation:

- Different techniques should be investigated to improve the extent of mixing. The penalty of pressure drop accompanying these techniques should be carefully examined.
- The transition zone between slug and stratified flow should be investigated over a larger range of operating conditions, since this zone is significantly influenced by liquid viscosity in the downslope configuration.
- The two-phase pressure drop correlation shown in equation 11 incorporates the contributions of several factors affecting pressure drop and shows a good fit with the data (Appendix A). The equation is applicable to diverse operating conditions and pipe arrangements. Therefore, equation 11 is recommended for predicting two-phase pressure drop.

LITERATURE CITED

Crowley, C. J., B. R. Patel, and R. G. Sam. 1983. Cold flow modeling test program. Creare final report. July.

Crowley, C. J., B. R. Patel, R. G. Sam, and G. B. Wallis. 1984. Technical memorandum on mixing and downslope configuration experiments. Creare final report. February.

Hughmark, G. A. 1965. Holdup and heat transfer in horizontal slug gas-liquid flow. Chemical Engineering Science 20:1007-1010.

Mehta, D. C. 1983. Full-scale cold flow modelling of the SRC-I slurry fired heater at Creare, Inc. December.

NOMENCLATURE

a	Constant in equation 1
b	Ratio of slug velocity to total superficial velocity
C_0	Salt concentration at bottom of pipe (% by wt)
$C_{0.5}$	Salt concentration at middle of pipe (% by wt)
$C_{1.0}$	Salt concentration at top of pipe (% by wt)
C_F	Salt concentration in fully mixed fluid (% by wt)
D	Pipe diameter (ft)
E_ℓ	Average fraction of pipe cross-section occupied by liquid around bubble
F_r	Critical Froude number
g_c	Gravitational acceleration (ft/sec^2)
K_2	Hughmark parameter
ΔL	Length of pipe (ft)
L_L	Liquid slug length (ft)
ΔP_{TP}	Two-phase pressure drop (lb/ft^2)
Re_L	Modified liquid Reynolds number
V_{GS}	Gas superficial velocity (ft/sec)
V_{LS}	Liquid superficial velocity (ft/sec)
V_S	Slug velocity (ft/sec)
V_T	Transition velocity (ft/sec)
X	Lockhart-Martinelli parameter
ε_G	Gas holdup
μ_G	Gas viscosity (cP)
υ_S	Slug frequency (1/sec)
ρ_G	Gas density (lb/ft^3)
ρ_L	Liquid density (lb/ft^3)
$\Delta\rho$	Difference between liquid and gas densities ($\rho_L - \rho_G$ · lb/ft^3)
θ	Angle of pipe inclination (degree)

Table 1

Range of Operating Variables for Mixing Experiments

Operating variable	Range of values
Superficial liquid velocity (ft/sec)	2, 4, and 6
Superficial gas velocity (ft/sec)	4, 8, and 12
Liquid viscosity (cP)	1 and 400
Gas density (lb/ft^3)	1.9
Loop inclination angle (°)	0

Table 2

Range of Operating Variables
for 1° Downslope Loop Configuration

Operating variable	Range of values
Superficial liquid velocity (ft/sec)	V_T[a], 2, 4, and 6
Superficial gas velocity (ft/sec)	4, 6[b], 8, 10[b], and 12
Liquid viscosity (cP)	1, 80, and 400
Gas density (lb/ft^3)	1.9
Loop inclincation angle (°)	-1

[a] V_T - liquid velocity at which flow regime changes from slug to stratified flow.
[b] These gas superficial velocities were tested only to measure transition liquid velocity, V_T.

Table 3

Single-Phase Flow Mixing Results

μ_L (cP)	V_{LS} (ft/sec)	Measured salt concentration			Fully mixed salt concentration (%)
		C_0	$C_{0.5}$	$C_{1.0}$	C_F
1	2	5.92	1.59	0	3.29
	4	2.03	0.48	0.03	1.46
	6	1.67	0.73	0.24	1.06
400	2	15.60	0.22	0.25	3.08
	4	7.16	0.71	0.41	2.81
	6	2.99	0.31	0	0.70

Table 4

Two-Phase Flow Mixing Results

μ_L (cP)	V_{GS} (ft/sec)	V_{LS} (ft/sec)	Salt concentrations (%)			
			C_0	$C_{0.5}$	$C_{1.0}$	C_F
1	4	2	3.59	0.05	ns[a]	3.33
	4	4	2.36	1.91	1.59	1.77
	4	6	2.06	1.56	0.70	1.26
	8	2	2.55	1.73	ns	3.24
	8	4	0.97	0.82	0.46	1.29
	8	6	0.89	0.66	0.50	1.18
	12	2	1.48	1.27	ns	3.06
	12	4	1.38	0.98	ns	1.57
	12	6	1.10	0.81	0.57	1.19
400	4	2	8.38	0.08	0	2.53
	4	4	4.60	1.06	0.44	2.00
	4	6	4.01	0.38	0.20	0.63
	8	2	3.61	1.11	1.24	2.66
	8	4	1.62	0.07	0.16	1.73
	8	6	0.95	0.86	0.92	1.68
	12	2	3.77	2.31	ns	3.98
	12	4	1.15	0.36	0.33	1.73
	12	6	0.47	0.51	0.20	1.00

[a] ns - no liquid could be collected as sample.

Table 5

Transition Velocity from Slug to Stratified Flow
for One-Degree Downslope Configuration

θ (degree)	μ_L (cP)	V_{GS} (ft/sec)	V_T (ft/sec)
-1	1	4.0	4.9
		6.0	4.0
		8.0	3.4
		10.0	3.2
		11.9	2.8
	80	4.0	3.6
		6.0	3.1
		8.1	2.7
		10.0	2.3
		11.9	2.1
	400	4.1	1.2
		7.8	1.5
		12.0	1.7

Table 6

Slug Characteristics in 1° Downslope Pipe

μ_L (cP)	V_{GS} (ft/sec)	V_{LS} (ft/sec)	V_S (ft/sec)	υ_S (1/sec)	L_L (ft)
1	4.1	6.0	15.2	0.62	2.9
	8.1	4.0	16.0	0.21	2.4
	8.0	6.0	19.2	0.61	2.4
	11.9	2.8	--	--	--
	11.8	4.0	22.0	0.11	2.2
	11.5	6.0	23.8	0.30	1.6
80	4.1	4.0	12.2	0.34	4.3
	4.1	6.0	16.4	0.79	7.8
	8.2	4.0	15.2	0.26	2.7
	8.0	6.0	20.5	0.70	3.4
	11.8	4.0	18.9	0.21	1.8
	11.5	6.0	22.7	0.25	2.0
400	4.0	2.0	8.0	0.36	4.8
	4.1	4.0	12.3	0.38	11.3
	8.0	2.0	13.5	0.30	2.9
	8.1	4.0	19.2	0.56	3.6
	8.1	5.9	21.6	0.74	3.3
	11.9	2.0	19.7	0.05	1.5
	11.4	4.0	22.7	0.18	2.5
	10.9	6.0	27.2	0.31	1.8

Table 7

Gas Holdup in 1° Downslope Pipe

μ_L (cP)	V_{GS} (ft/sec)	V_{LS} (ft/sec)	Gas holdup		
			Measured	Hughmark	ICRC
1	4.1	6.0	0.270	0.333	0.346
	8.1	4.0	0.506	0.549	0.552
	8.0	6.0	0.417	0.468	0.474
	11.9	2.8	--	0.664	0.669
	11.8	4.0	0.536	0.612	0.616
	11.5	6.0	0.483	0.539	0.542
80	4.1	4.0	0.336	0.290	0.331
	4.1	6.0	0.250	0.237	0.260
	8.2	4.0	0.539	0.398	0.463
	8.0	6.0	0.390	0.342	0.380
	11.8	4.0	0.624	0.451	0.532
	11.5	6.0	0.507	0.400	0.450
400	4.0	2.0	0.500	0.333	0.424
	4.1	4.0	0.333	0.258	0.299
	8.0	2.0	0.593	0.414	0.555
	8.1	4.0	0.422	0.351	0.426
	8.1	5.9	0.375	0.307	0.352
	11.9	2.0	0.604	0.453	0.621
	11.4	4.0	0.502	0.395	0.492
	10.9	6.0	0.401	0.359	0.405

Table 8

Two-Phase Pressure Drop in 1° Downslope Pipe

μ_L (cP)	V_{GS} (ft/sec)	V_{LS} (ft/sec)	$\Delta P_{TP}/\Delta L$ (lb/ft^3)
1	4.1	6.0	0.77
	8.1	4.0	0.90
	8.0	6.0	1.67
	11.8	4.0	1.81
	11.5	6.0	2.84
80	4.1	4.0	0.47
	4.1	6.0	1.23
	8.2	4.0	1.16
	8.0	6.0	2.05
	11.8	4.0	1.56
	11.5	6.0	2.87
400	4.0	2.0	1.44
	4.1	4.0	2.76
	4.0	6.0	4.05
	8.0	2.0	2.04
	8.1	4.0	3.22
	8.1	5.9	5.54
	11.9	2.0	2.62
	11.4	4.0	4.22
	10.9	6.0	6.69

FIGURE 1

EXPERIMENTAL SET-UP

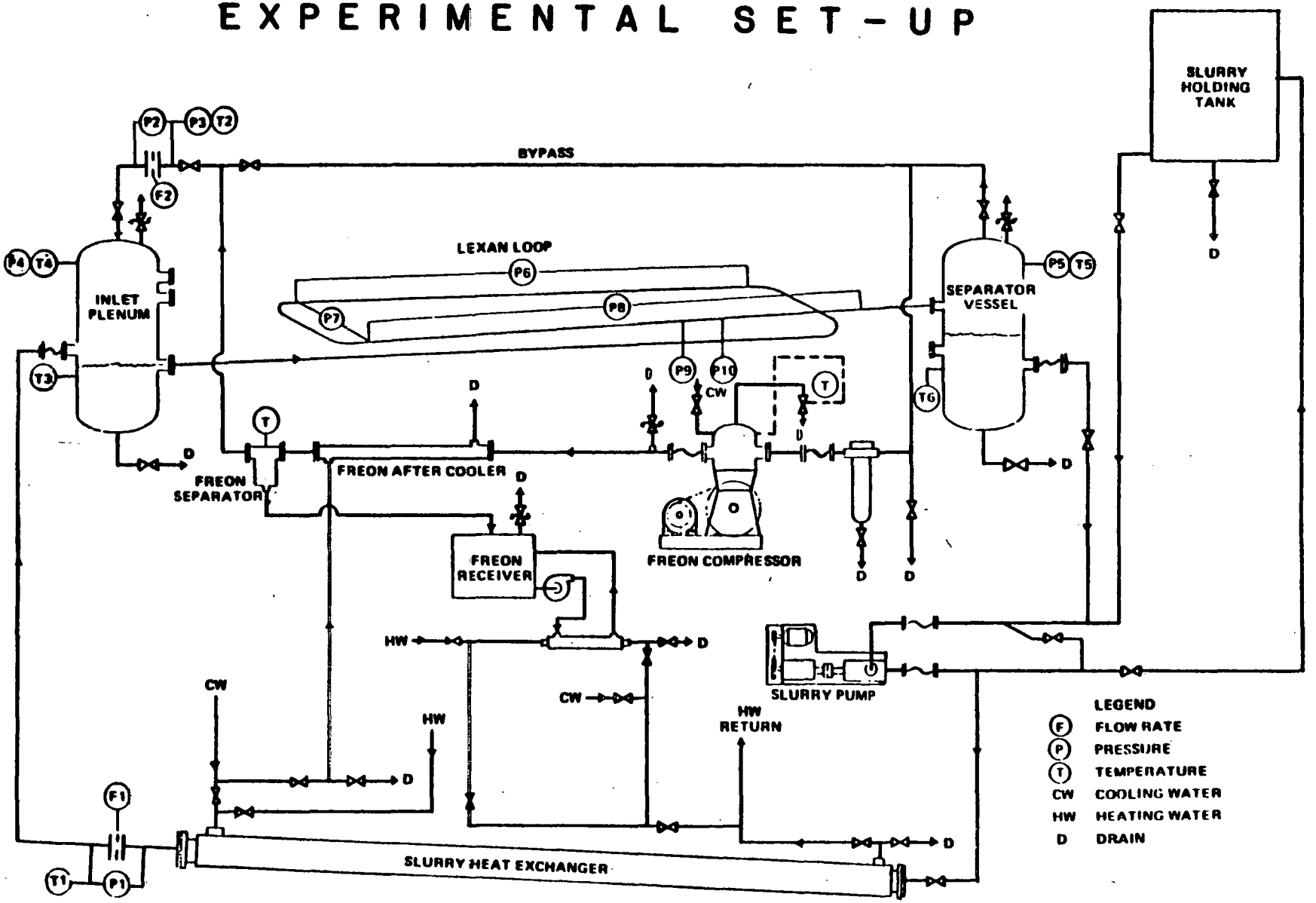

FIGURE 2

SCHEMATIC OF INSTRUMENTATION FOR THE MIXING EXPERIMENTS

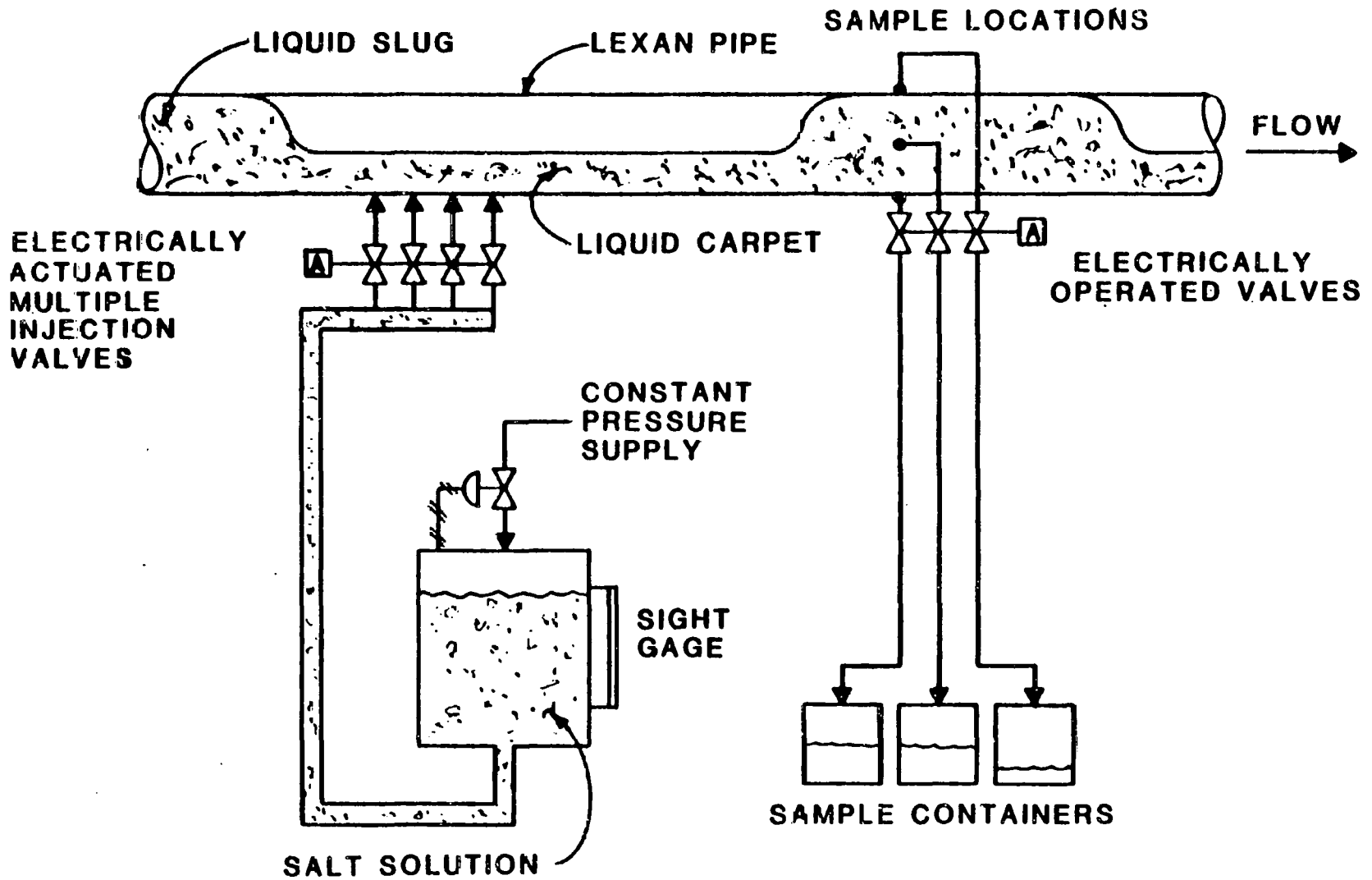

FIGURE 3

TRANSITION LIQUID VELOCITY
FROM SLUG TO STRATIFIED FLOW

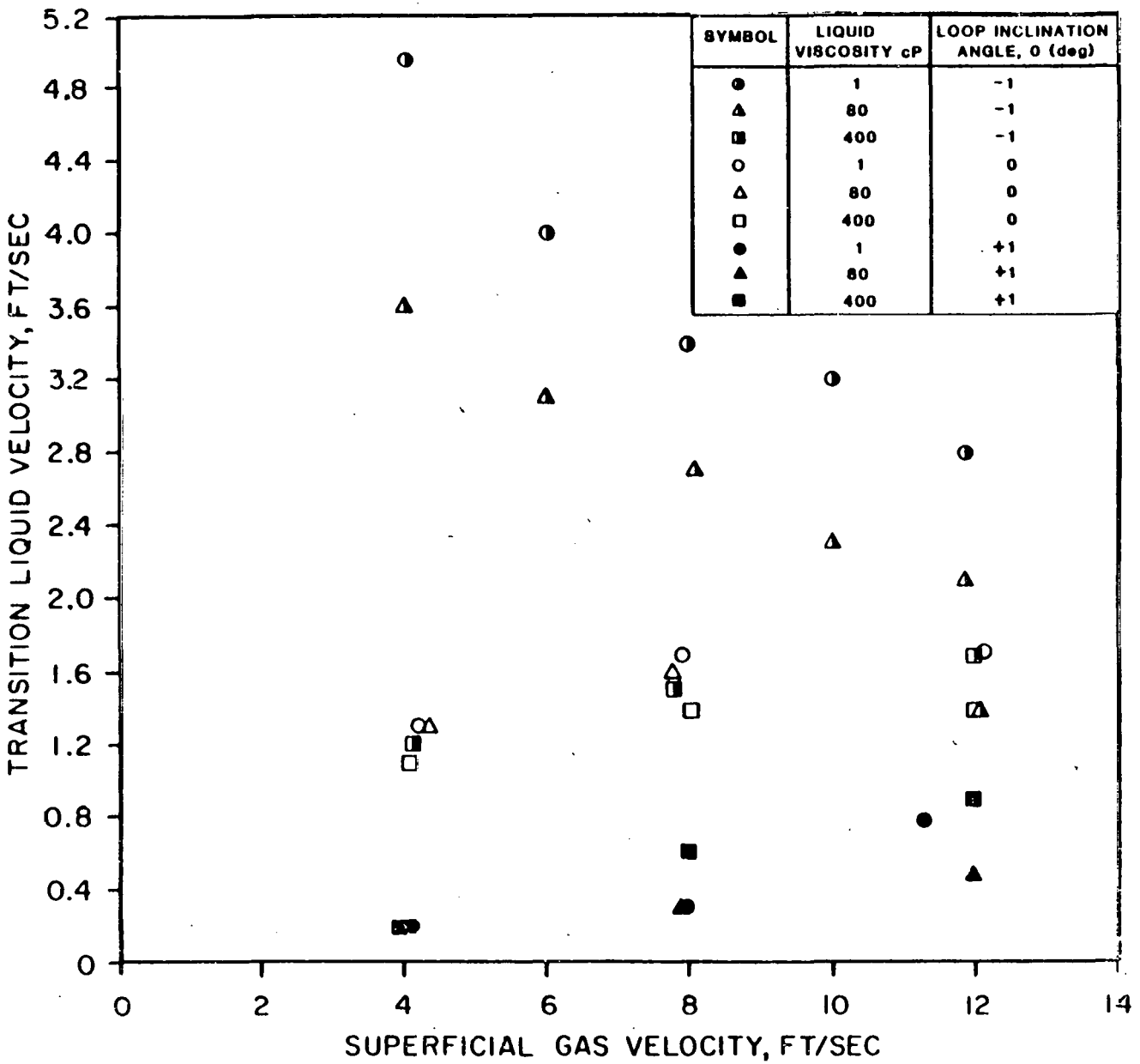

FIGURE 4

SCHEMETIC OF TRANSITION BOUNDARIES FOR VARIOUS PIPE INCLINATIONS AND LIQUID VISCOSITIES

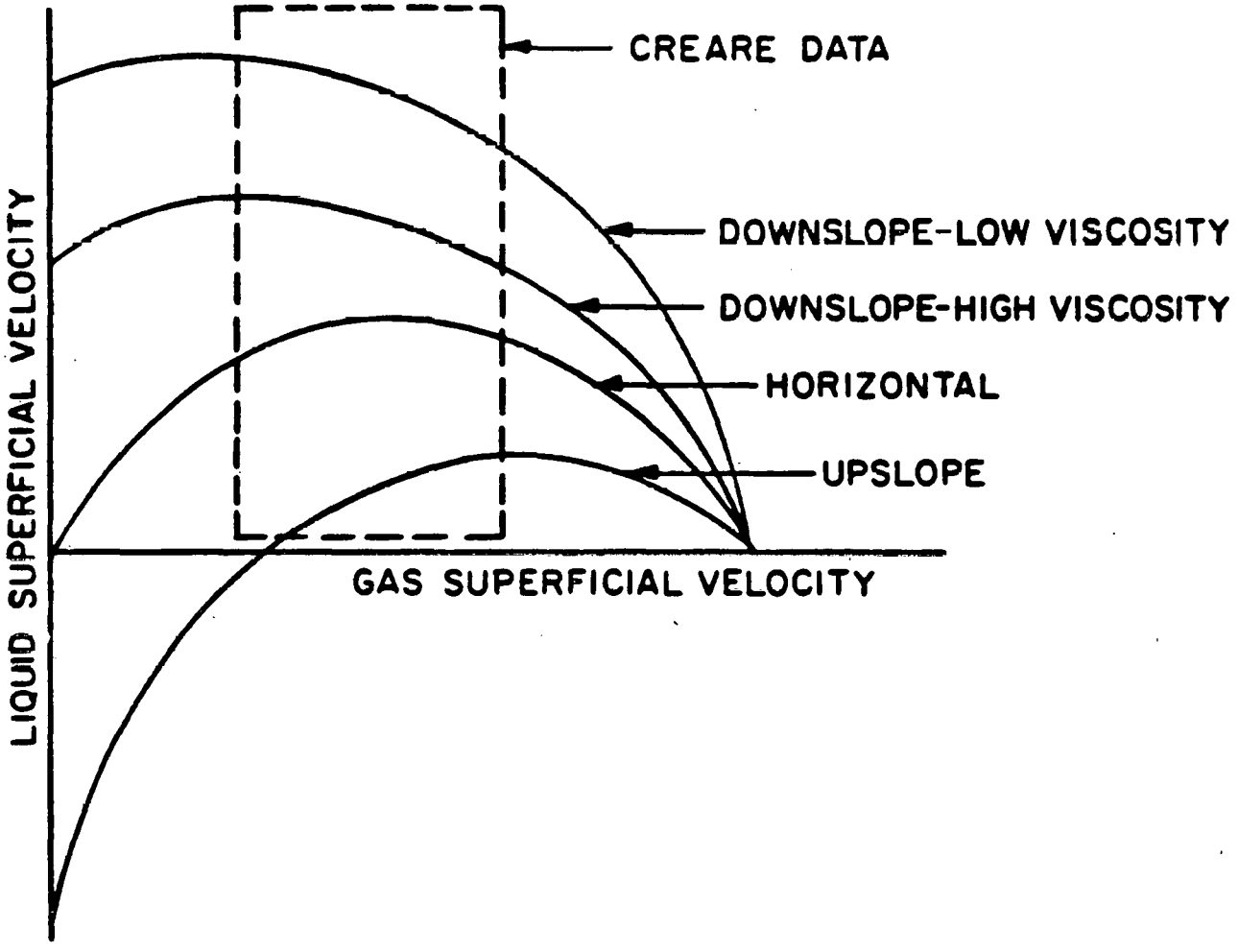

FIGURE 5

COMPARISON OF GAS HOLDUP
MEASURED VS. HUGHMARK CORRELATION
-1 DEGREE PIPE INCLINATION

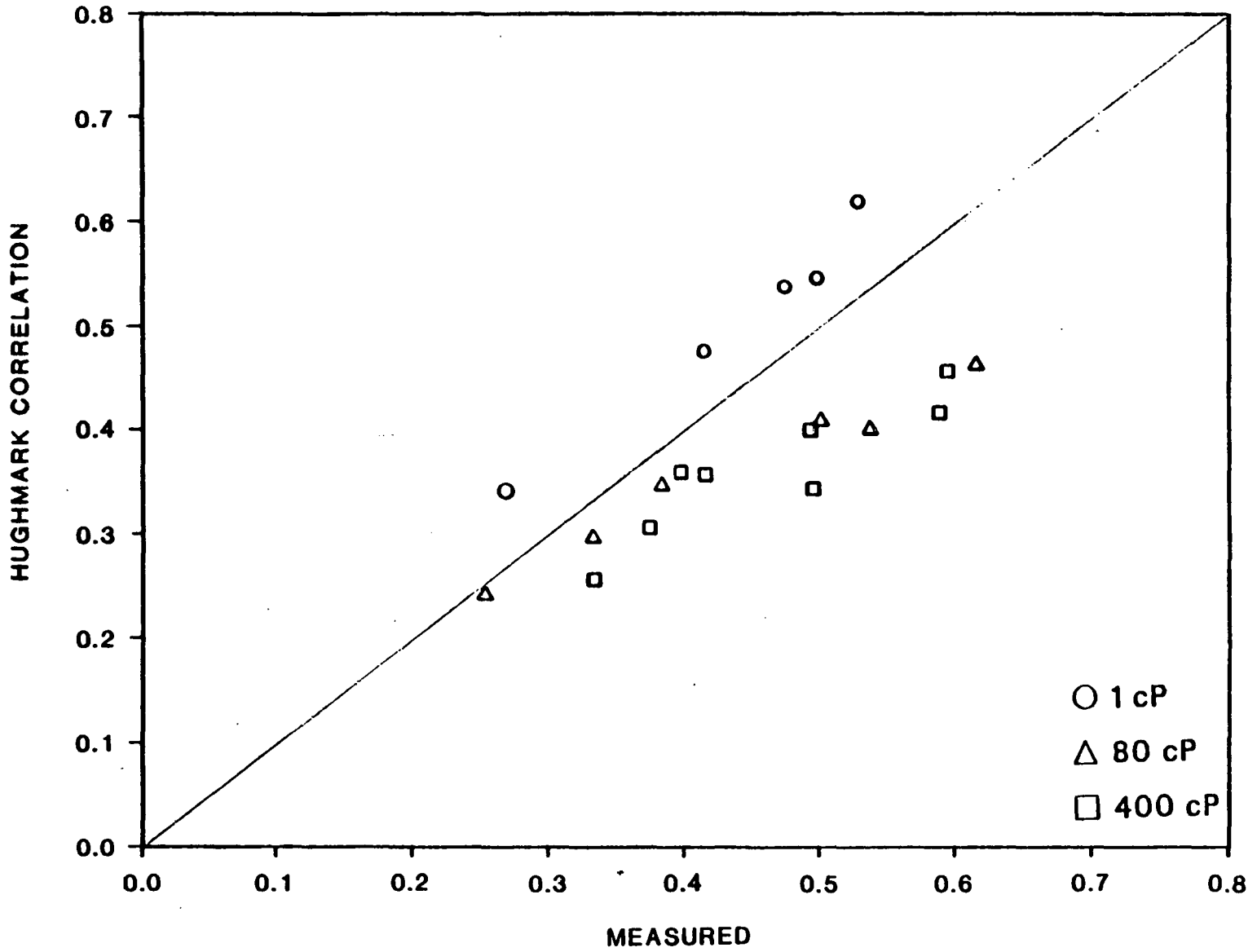

THIS PAGE

WAS INTENTIONALLY

LEFT BLANK

APPENDIX A

Creare Technical Memorandum

MIXING AND DOWNSLOPE CONFIGURATION EXPERIMENTS

Richard G. Sam
Graham B. Wallis
Christopher J. Crowley
Bharatan R. Patel

TABLE OF CONTENTS

LIST OF FIGURES

Figure

LIST OF TABLES

TABLE

NOMENCLATURE

B	constant in Eq. 20
C	constant in Eq. 3
C_o	ratio of slug velocity, V_s, to total superficial velocity, J
D	pipe diameter
E_ℓ	average fraction of pipe cross-section occupied by liquid around bubble
f	friction factor
f_s	slug frequency
Fr	Froude number, $j_g\sqrt{\rho_g}/\sqrt{Dg\Delta\rho}$
g	gravitational acceleration
G	overall mass flux, $\rho_\ell j_\ell + \rho_g j_g$
H	vertical height in pipe
j_g	superficial gas velocity
j_ℓ	superficial liquid velocity
$j_{\ell t}$	transitional superficial liquid velocity
J	total superficial velocity, $j_\ell + j_g$
L	length for pressure drop measurement
L_b	bubble length
L_s	slug length
L_{sa}	average slug length
n	power law index
$\Delta P_{m\ell}$	middle leg pressure drop
ΔP_b	bend pressure drop
$\Delta P_{\ell\ell}$	last leg pressure drop
Re_ℓ	liquid Reynolds number, $\rho_\ell D j_\ell/\mu_\ell$
Re_m	mixture Reynolds number, $\rho_m D j_\ell/\mu_m$
V	average liquid velocity

V_c average carpet velocity

$V_{c\ell}$ slug centerline velocity

V_m mixture velocity

V_s slug velocity

X measured, slug tracer concentration

X_T calculated, fully-mixed, slug tracer concentration

α gas void fraction

θ loop inclination angle

μ_ℓ liquid viscosity

μ_m mixture viscosity

ρ_g gas density

ρ_ℓ liquid density

ρ_m mixture density

$\Delta\rho$ density difference, $\rho_\ell - \rho_g$

THIS PAGE

WAS INTENTIONALLY

LEFT BLANK

1 INTRODUCTION

This report describes additional work performed for the International Coal Refining Company under subcontract 01-13105, Slurry Fired Heater Cold Flow Modeling, R&D Program Area 12.4.2. Creare R&D Inc. has recently completed the first phase of the Cold Flow Modeling Test Program (CFMTP) with the primary objectives of identifying and quantifying the flow regimes expected to occur at prototypical operating conditions in the SRC-1 Demonstration Plant coal slurry/hydrogen gas heaters and of obtaining heat transfer data to address the issues of local tube coking and burnout. Reference [1] is a comprehensive summary of the work performed to date.

Experiments have shown that a slug flow regime occurs for the operating conditions of interest. Visual observations have indicated the existence of a liquid carpet between the slugs as thick as 1/2 of the pipe diameter. In addition, observations have been made which suggest that the carpet moves significantly slower than the slugs. The concern is that there might be insufficient mixing between the liquid in the slugs and the carpet which would lead to severe temperature gradients within the liquid. Non-uniform slurry temperatures would have an adverse effect on fired heater performance. Therefore, this program was performed to assess the extent of mixing between the liquid in the carpet and the liquid in the slugs.

The previous CFMTP experiments were performed with a +1° upslope loop inclination angle as well as with a horizontal loop configuration. The horizontal loop data were obtained in order to make comparisons with existing data in the literature, the majority of which were obtained with small diameter, horizontal pipes. The +1° upslope configuration represents the most likely design for the SRC-1 Demonstration Plant heaters. However, a -1° downslope configuration is also a viable option for the fired heaters. Therefore, this program was also performed to generate flow regime and pressure drop data in the -1° downslope configuration.

The following sections present the mixing and downslope configuration experimental results.

2 MIXING EXPERIMENTS

2.1 Objective and Approach

The experimental objective was to determine the extent of mixing between the liquid carpet and slugs in the horizontal loop configuration. In order to meet this objective, experiments were performed with Freon 12 as the gas phase and either water or the 400 cP water/polymer solution (WPS) as the liquid phase over a range of gas and liquid superficial velocities. Single-phase liquid tests were also done to determine the limiting behavior with zero gas flow.

Both qualitative and quantitative results were obtained. The qualitative results include movies which illustrate the mixing between the slugs and the carpet. The quantitative results were obtained by injecting a tracer into the liquid carpet and measuring the tracer concentration profile in the slugs. The following sections summarize the experimental methods (Section 2.2), single-phase flow results (Section 2.3), and two-phase flow results (Section 2.4).

2.2 Experimental Facility, Procedure, and Instrumentation

Experimental Facility

The quantitative mixing results were obtained by injecting a sodium chloride/test liquid solution tracer into the liquid carpet and sampling liquid from the slugs to determine the tracer concentration. The injection location was 14 ft. 2 1/2 in. from the inlet end of the last leg of the Lexan loop and the sampling location was 11 ft. downstream of the injection point, as shown in Figure 1. The tracer was injected through 10, 1 in. diameter holes at the bottom of the Lexan tube as shown in Figure 2. The holes were sized to minimize the liquid carpet disturbance due to the injection flow rate. Solenoid valves in each injection line were actuated simultaneously to initiate and terminate injection. The injection duration was controlled automatically by an adjustable timer (0.1 - 20 sec. duration).

Each injection line was connected to a 2 in. diameter manifold which in turn was connected to a 125 gal. tracer supply tank (see Figure 3). The tracer supply tank pressure was maintained well above the loop operating pressure using a compressed air supply. The amount of injected tracer was varied by changing the tracer supply tank pressure, the solenoid valve open time, and by adjusting the ball valves between the solenoid valves and the injection points. The amount of injected tracer was determined using the sight gauge on the tracer supply tank.

Liquid was extracted from the loop approximately 11 ft. downstream of the injection location as shown in Figure 1. Samples were taken from the top, bottom, and side of the Lexan tube (see Figure 4). Again, remotely actuated, adjustable open time solenoid valves were used. Each of the three sampling lines was plumbed to an individual container (not shown).

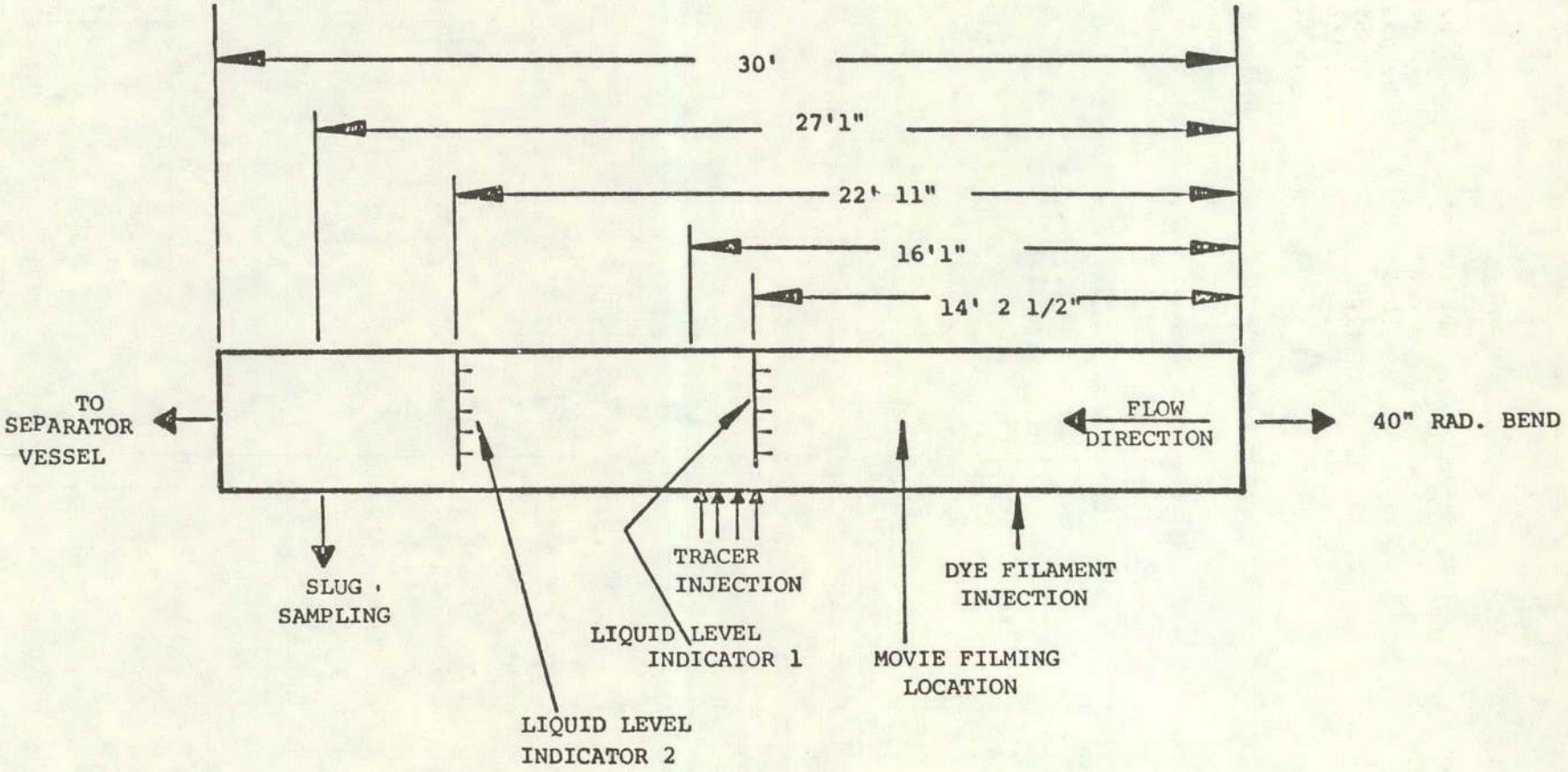

Figure 1. MEASUREMENT LOCATIONS IN LAST LEXAN LEG

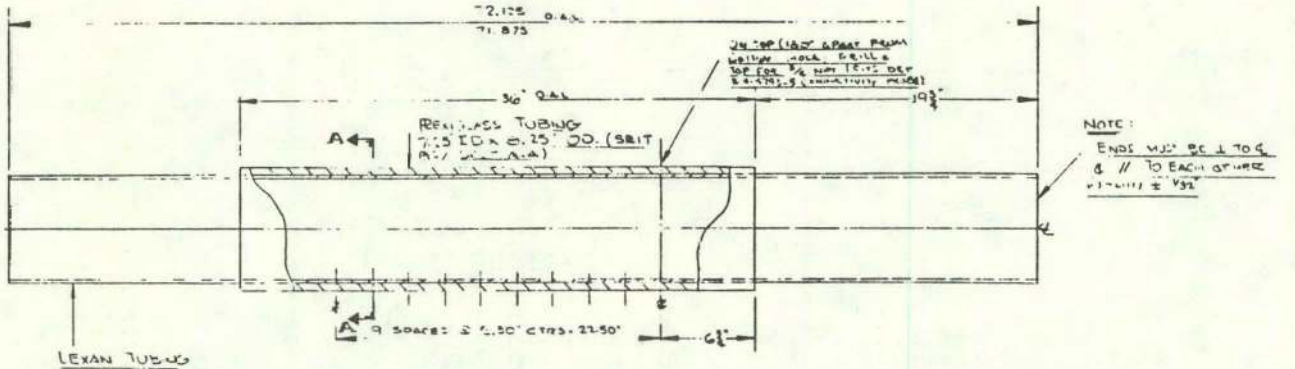

DETAIL "A"
(1) REQ'D AS SHOWN
SCALE 3" = 12"

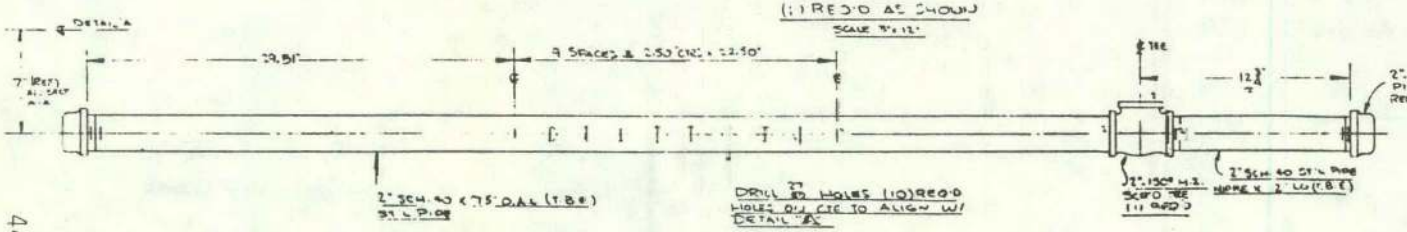

DETAIL "B"
(1) REQ'D AS SHOWN
SCALE: 3" = 12"

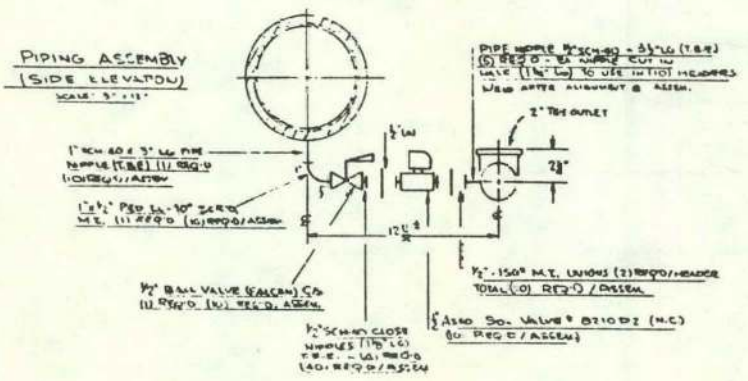

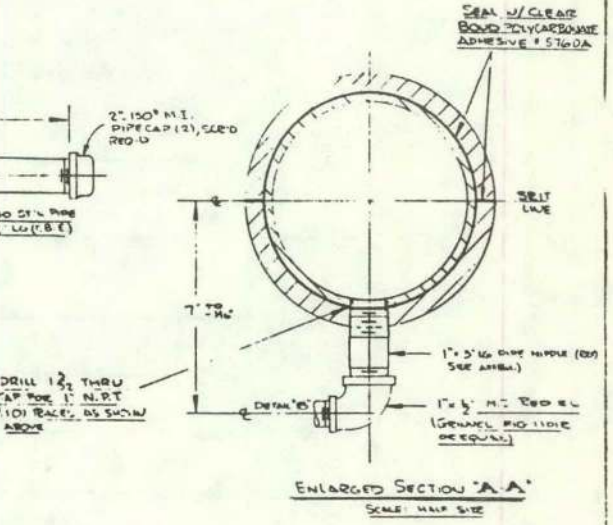

ENLARGED SECTION "A-A"
SCALE: HALF SIZE

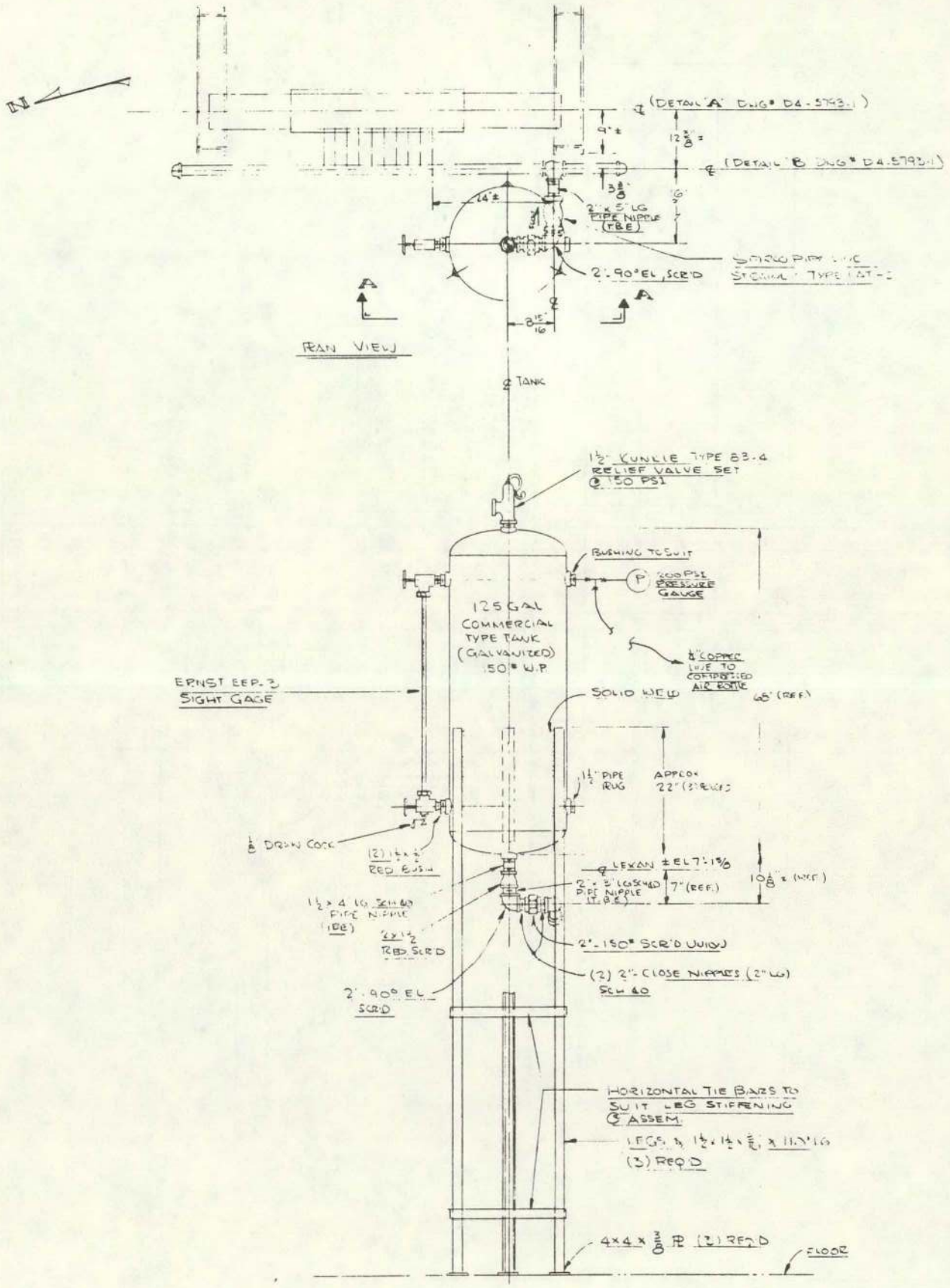

ELEVATION @ 'A-A'

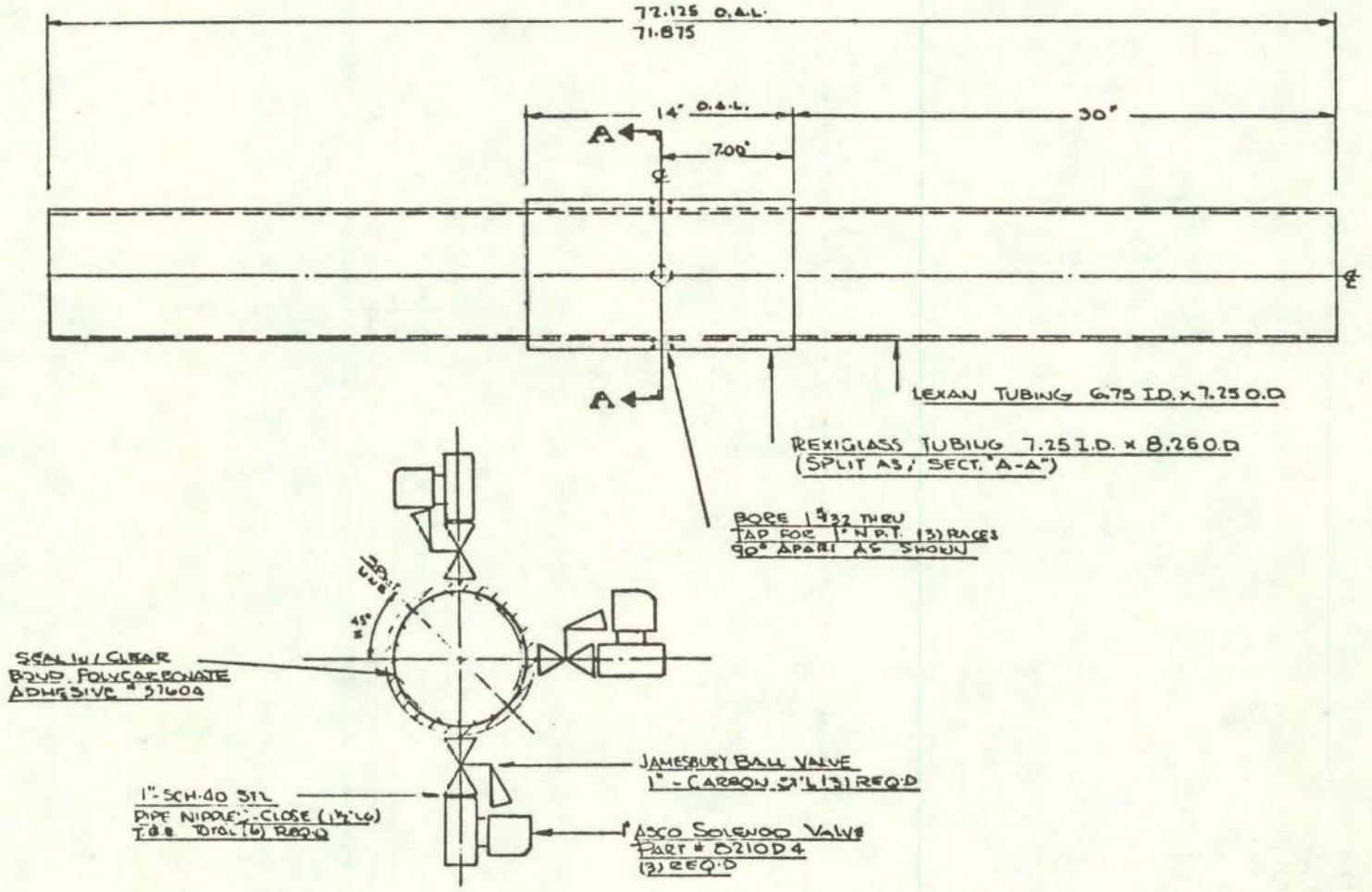

Figure 4. SAMPLING SECTION DETAILS

Procedure

The first step was to set the desired test conditions. This involved setting the gas and liquid flow rates for the two-phase flow tests or the liquid flow rate for the single-phase flow tests. Next, the sampling lines were flushed by actuating the sampling valves. To begin the test, the injection solenoid valves were actuated. Each slug that passed the injection point was sampled (for the 20 sec. injection duration). After the injection was terminated, the amount of tracer injected was determined by observing the supply tank level change using the sight gauge. Next, the liquid in the loop was allowed to circulate until the injected tracer had fully mixed with the loop inventory (experimentally verified by periodic sampling and concentration measurement). After the loop concentration had reached equilibrium, the sampling tubes were again flushed to remove the possibly high concentration liquid from the previous test. Finally, a sample was taken to determine the new background concentration of the system liquid inventory.

Instrumentation

Test conditions were determined and recorded with the instrumentation/data acquisition system previously used for the CFMTP and described in reference [1]. The tracer concentration of samples extracted from the liquid flow was determined using a Beckman type RA6 conductivity meter with a range of 100 mmho/cm and an accuracy of ± 2 mmho/cm. The conductivity meter was calibrated (and checked several times during the experiments) against NBS traceable standards.

2.3 Single-Phase Flow Results

The single-phase flow tests were performed with water or the 400 cP WPS and liquid velocities of 2, 4, and 6 ft/sec which are equivalent to the superficial liquid velocities used for the two-phase flow tests. The results are shown in Figures 5 and 6 for water and the 400 cP WPS respectively (and included in Table A-1, Appendix A). The data are presented in terms of the measured concentration (minus the background concentration), X, normalized with the concentration that would exist if complete mixing had occurred, X_T, as a function of the location, H/D, from which the sample was taken (H^T = pipe height, D = pipe diameter; therefore, H/D = 0, 0.5, and 1.0 correspond to the bottom, middle, and top sampling locations respectively). The water data indicate that the concentration at the bottom of the pipe is 40% to 80% higher than the value that would exist if complete mixing had occurred (complete mixing would be characterized by a uniform concentration ratio across the pipe). Comparing the results for the two test liquids suggests that better mixing occurs with water than with the 400 cP WPS.

Salt mass balances using two different methods were made for each of the single-phase flow tests. The first salt mass balance method was to calculate the expected increase in the total liquid inventory salt concentration for the known amount of salt injected and compare it with the measured concentration before and after each test.

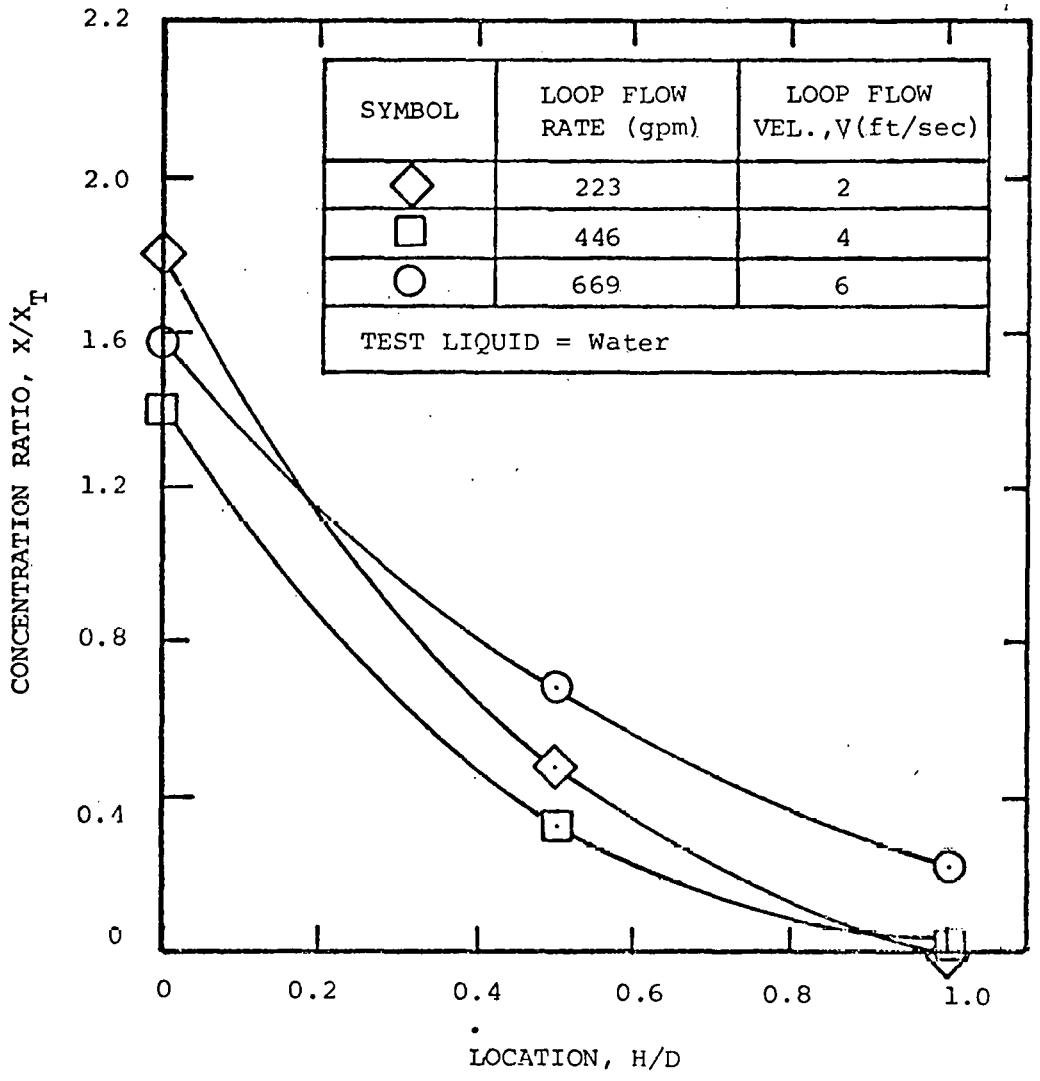

Figure 5. SINGLE-PHASE FLOW MIXING RESULTS OBTAINED WITH WATER

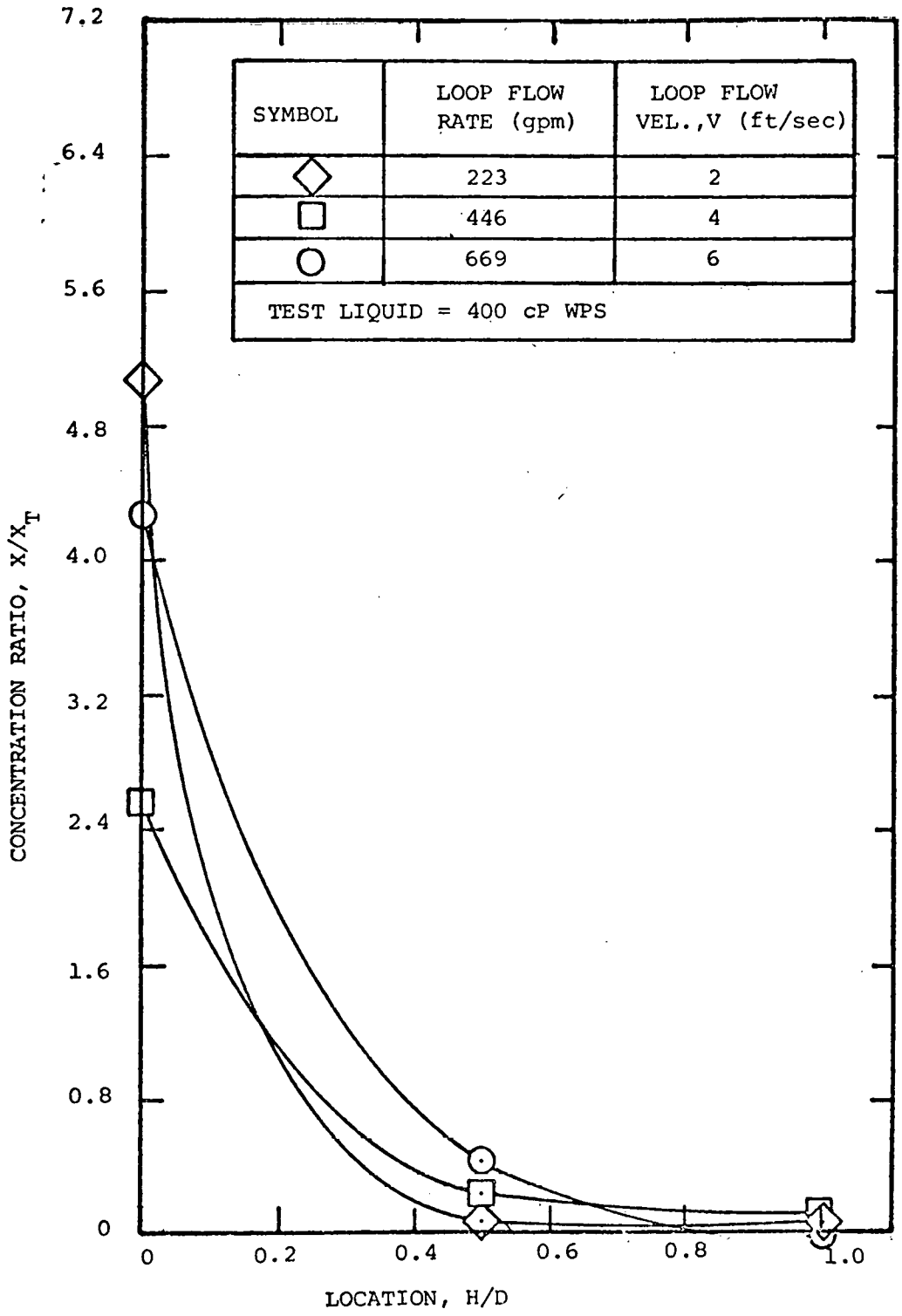

Figure 6. SINGLE-PHASE FLOW MIXING RESULTS OBTAINED WITH 400 cP WPS

For the second method, it was assumed that the concentration varied in the vertical direction only and that the bottom, side and top measurements were characteristic of the average concentration in the bottom, middle and top sections of the pipe. The mass flow rates through the bottom, middle, and top sections were calculated assuming that the velocity profile could be represented by the 1/7 power law turbulent flow profile. The salt flow rate through each section was determined by multiplying the measured concentration by the calculated mass flow rate. The actual salt injection rate was compared with the sum of the calculated salt flow rates through each of the pipe sections.

Table 1 summarizes the salt mass balance results using each of the methods described above. Results of the first method indicate that at least 90% of the salt can be accounted for which verifies the measurement method accuracy. The second method does not account for most of the injected salt which suggests that the assumption of a vertical concentration gradient only is inappropriate. In order to understand what concentration gradient assumption was appropriate, a calculation was made using the three dimensional code Fluent.

Table 2 summarizes the test conditions for which the Fluent calculation was made. The finite difference grid set up to analyze this problem is illustrated in Figures 7 and 8. The calculation was made assuming a fully turbulent velocity profile existed at the first injection plane. Results of the calculation after 600 iterations are shown in Figures 9 and 10. Figure 9 shows the salt concentration profile at the center of the pipe between the injection and sampling locations. Figure 10 shows the salt concentration profile at the sampling plane which indicates that a vertical concentration gradient should exist.

Comparison of the Fluent calculation results and the data is made in Table 3. The poor agreement between the calculation and the data is suspected to a result of the assumption of a fully developed turbulent velocity profile at the first injection plane. It is postulated that the bends upstream of the injection location impart a circumferential velocity component to the flow which could explain the discrepancy between the calculation and the data. Although this explanation was not investigated by performing an additional calculation which included the effect of the bends, visual observations of the flow were made which confirmed that the bends did impart a "swirl" to the flow.

2.4 Two-Phase Flow Results

The two-phase flow mixing experiments were performed using the tracer injection/sampling technique for each of the conditions given in Table 4. Motion picture movies (submitted with this report) illustrating the interaction between the slugs and the carpet were made for the test conditions given in Table 5. This section begins with a description of the results determined from the movies followed by a discussion of the injection/sampling data.

The movies were taken of a 2 ft. section of the last straight leg of the loop 10 ft. from the upstream bend. A dye filament was injected at the bottom of the pipe as shown in Figure 1. The movies show that the dye filament flows relatively undisturbed in the carpet between slugs. However, for essentially all of the conditions recorded on film, the dye filament would burst upward near the trailing edge of a passing slug. This observation is illustrated schematically in Figure 11.

TABLE 1
PERCENT OF SALT INJECTED NOT ACCOUNTED FOR IN MASS BALANCE

TEST LIQUID	LIQ. VEL. (ft/sec)	METHOD	
		1	2
Water	2		28
	4		46
	6	2.6	19
400 cP WPS	2		60
	4	2.4	11
	6	-8.2	-42

TABLE 2
FLUENT CALCULATION CONDITIONS

Liquid Type	Water
Liquid Flow Rate	446 gpm
Liquid Velocity	4 ft/sec
Salt/Water Injection Rate	24.5 gpm
Salt/Water Injection Concentration	25%

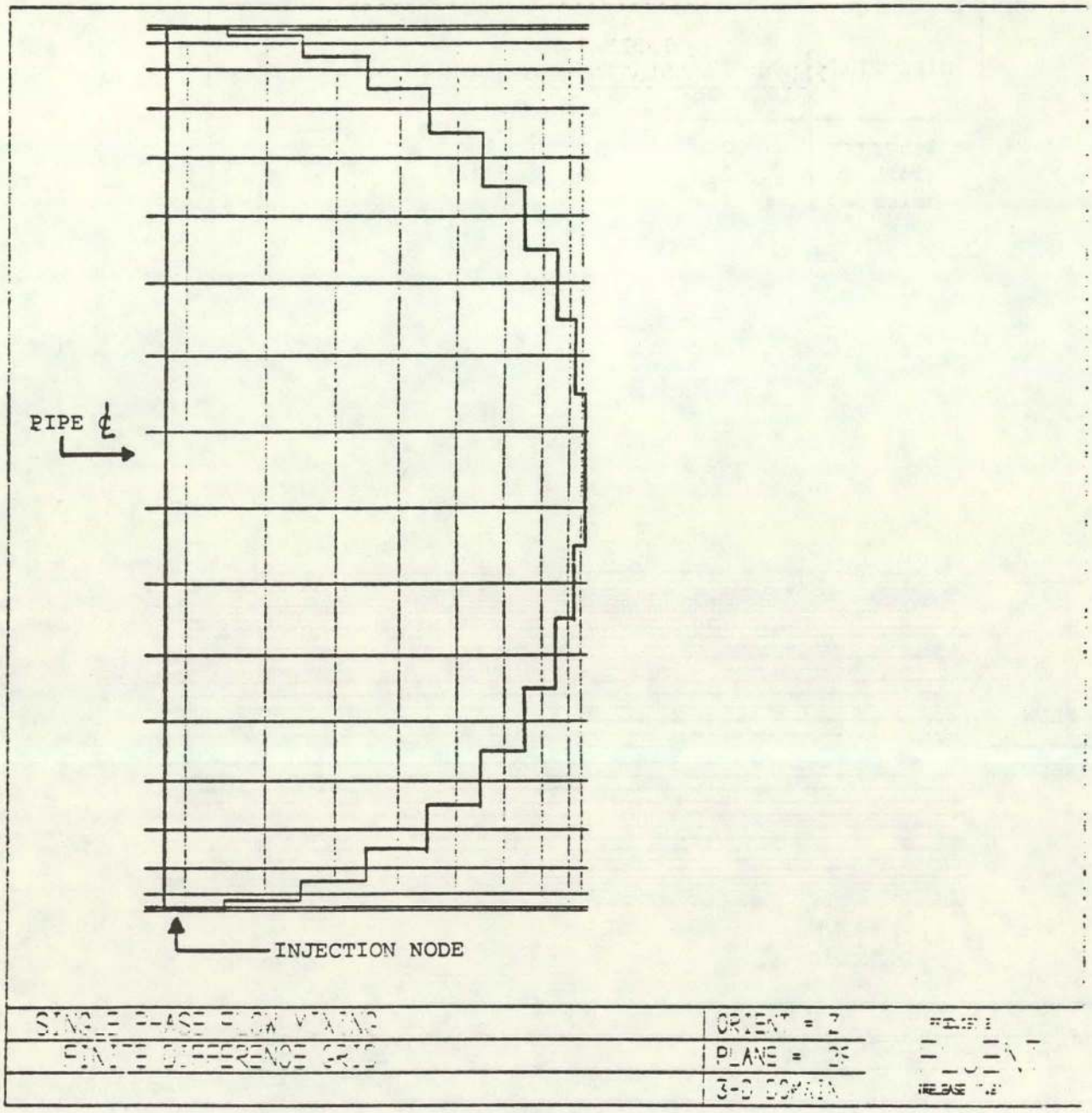

Figure 7. END VIEW OF FINITE DIFFERENCE GRID USED IN FLUENT CALCULATIONS

DIRECTION	NUMBER OF NODES
length	30
width	12
height	22

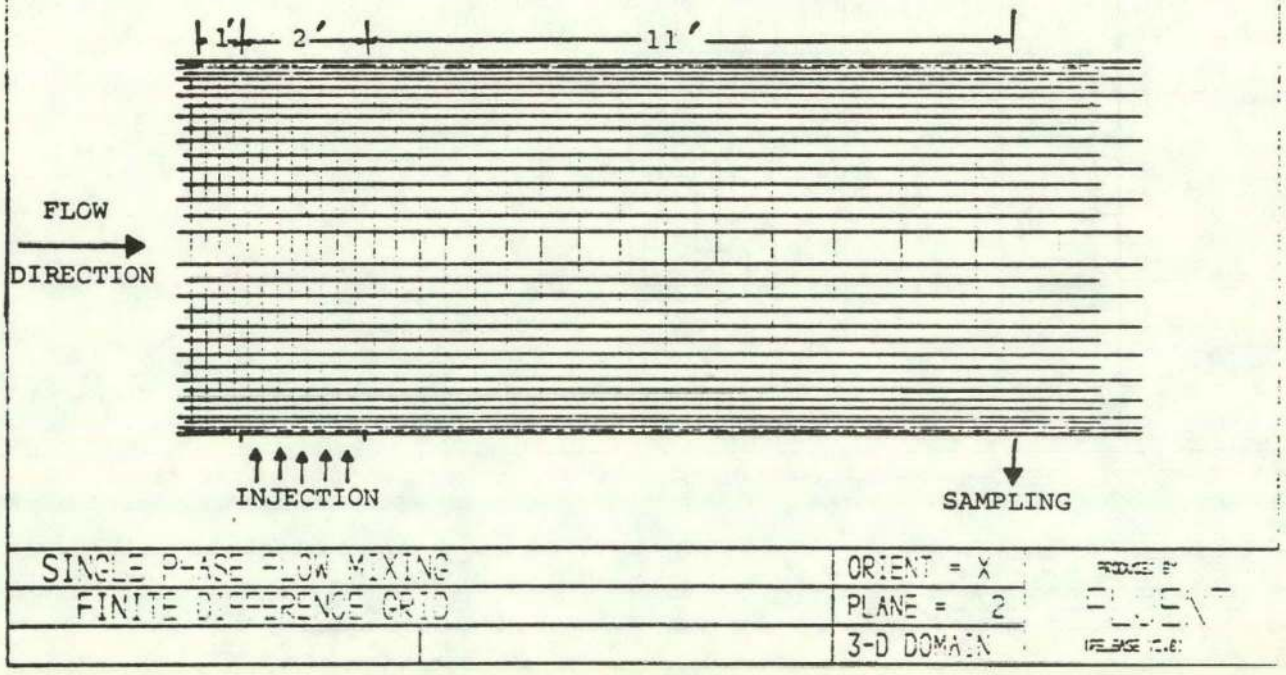

Figure 8. SIDE VIEW OF FINITE DIFFERENCE GRID USED IN FLUENT CALCULATIONS

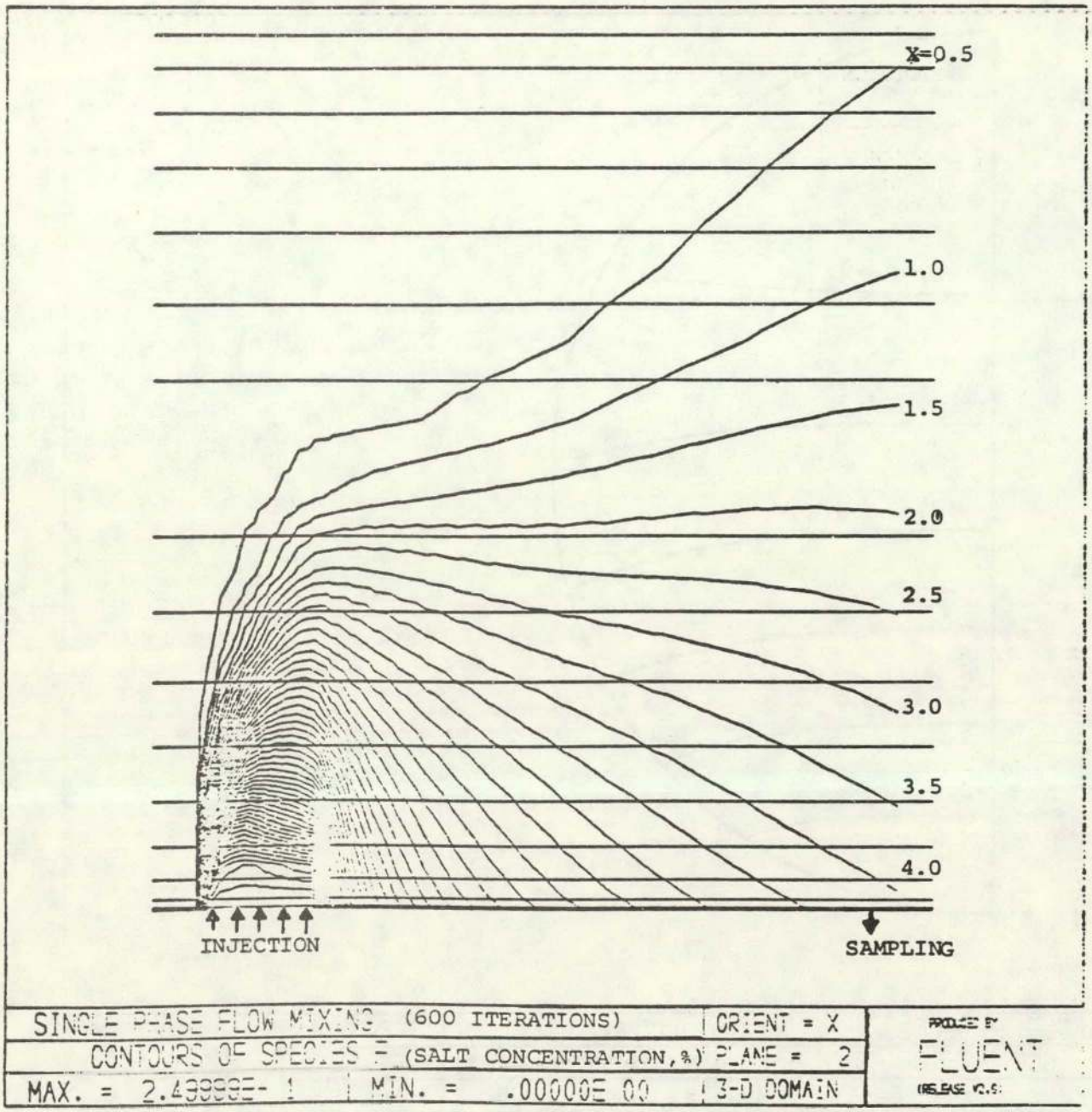

Figure 9. SALT CONCENTRATION PROFILE BETWEEN INJECTION AND SAMPLING LOCATIONS

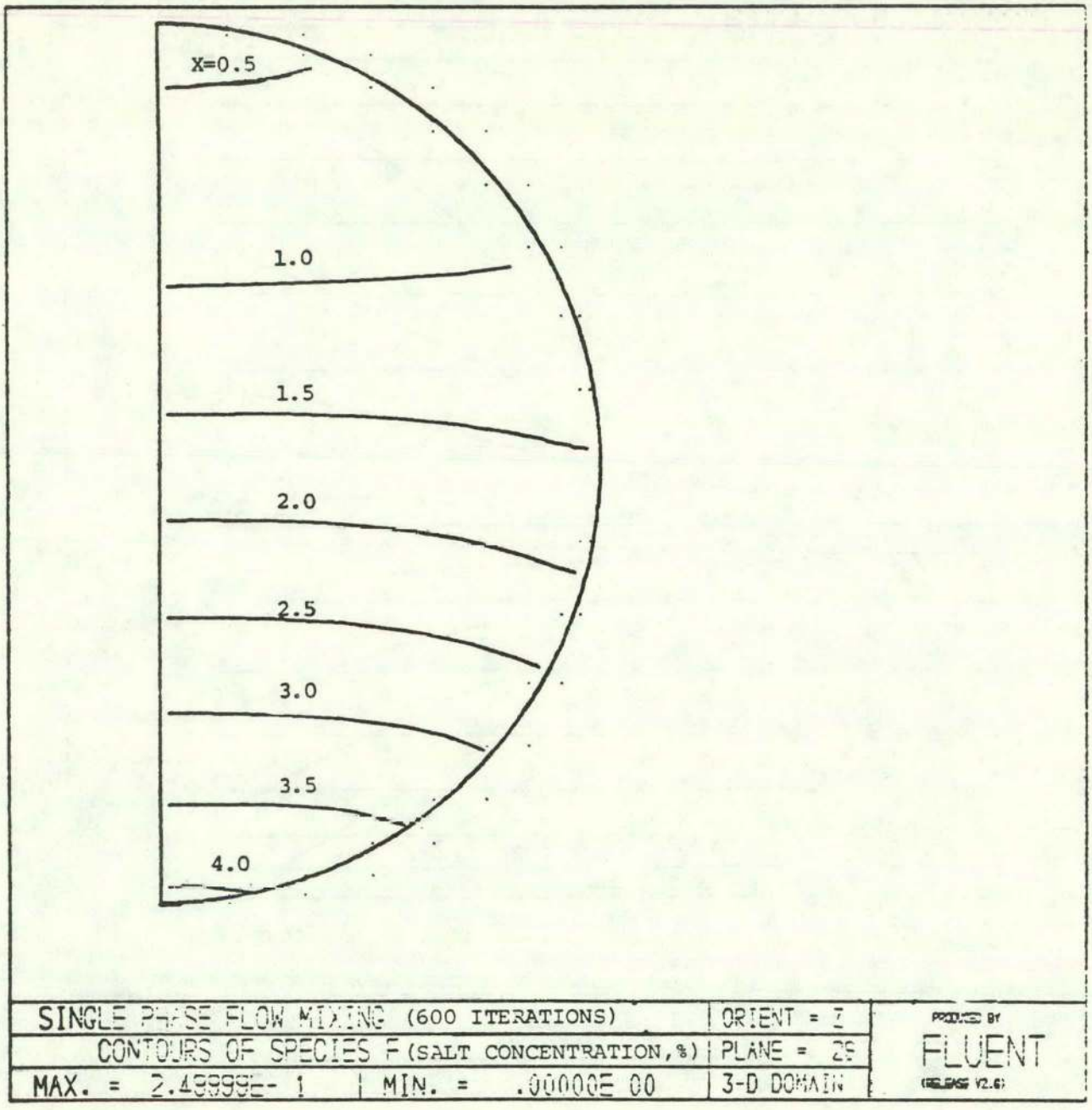

Figure 10. CROSS-SECTIONAL VIEW OF SALT CONCENTRATION PROFILE AT SAMPLING LOCATION

TABLE 3
COMPARISON OF FLUENT CALCULATION
RESULTS AND MEASURED DATA

LOCATION	SALT CONCENTRATION, X (%)	
	CALCULATED	MEASURED
Top	0.5 - 1.0	0
Middle	1.5	0.5 ± 0.3
Bottom	3.0 - 4.0	2.0 ± 0.3

TABLE 4
TWO-PHASE FLOW MIXING TEST MATRIX

Loop Inclination Angle (deg.)	0 (horizontal)
Gas Phase	
Type	Freon 12
Density (lbm/ft^3)	1.9
Superficial Gas Velocities (ft/sec)	4, 8, 12
Liquid Phase	
Type	W, WPS
Superficial Liquid Velocities (ft/sec)	2, 4, 6
Total Number of Tests	18

W = Water
WPS - Non-Newtonian water/polymer solution with viscosity of 400 cP at a shear rate of 213 sec^{-1}.

TABLE 5
TEST CONDITIONS FOR FILMING

ROLL NUMBER	FILM NUMBER	SUPERFICIAL GAS VEL., j_g (ft/sec)	SUPERFICIAL LIQ. VEL., j_ℓ (ft/sec)
B1	1	8	4
	2	8	4
	3	8	6
	4	8	6
	5	11	6
	6	11	6
B2	7	12	4
	8	12	4
	9	4	4
	10	4	4
	11	4	6
	12	4	6

The observed motion of the dye filament might be explained by the following analysis. The flow pattern can be "brought to rest" by imagining the pipe wall to be moving at the slug velocity, $-V_s$:

$$V_s = C_o J = C_o (j_\ell + j_g) \qquad (1)$$

If the slug is long enough for a single-phase liquid velocity profile to develop, the local velocities in this frame of reference can be derived by superimposing $-C_o J$. The result depends on whether $C_o J$ is greater or less than the single-phase flow liquid centerline velocity, $V_{c\ell}$ as illustrated in Figure 12.

A recirculation region should exist if $C_o J < V_{c\ell}$ even for the unconventional slugs observed in these tests (see Figure 13). In this case, some of the carpet liquid flows up and over the recirculation region. In fact, the carpet liquid flows all around the "recirculation bubble" being mostly on the walls.

In laminar viscous flow, $V_{c\ell} = 2J$ and therefore recirculation occurs if $C_o < 2$. In laminar flow of a non-Newtonian power law liquid,

$$V_{c\ell} = J\,(3n+1)/(n+1) \qquad (2)$$

where n is the power law index. Therefore, in the range of interest for the 400 cP WPS (n = 0.54-0.60), $V_{c\ell}$ = 1.7 to 1.75 J and some recirculation will occur if the slug is long, since C_o lies mostly between 1.4 and 1.6 in these tests. This result is consistent with the observations of the dye bursting upward and in the direction of the flow, as was illustrated in Figure 11.

The two-phase flow mixing results obtained with the tracer injection/sampling technique are presented in Figures 14-19 (and included in Table A-2, Appendix A). The data are plotted in terms of the concentration ratio, X/X_T, and sampling location, H/D. Each figure includes data for a single liquid type and superficial velocity, with a range of superficial gas velocities. The single-phase flow results are also included for comparison.

Essentially all of the data indicate that for a given liquid type and superficial velocity, the extent of mixing increases as the superficial gas velocity is increased. This statement implies (and the data confirm) that better mixing occurs with two-phase flow than with single-phase flow. Therefore, the single-phase flow behavior could be considered as a conservative design criterion.

A comparison of the water and the 400 cP WPS data indicates that better mixing is achieved with water than with the 400 cP WPS. This result is not surprising given that the water is certainly in the turbulent flow regime whereas the high viscosity of the 400 cP WPS implies a low Reynolds number indicative of a laminar flow regime.

For many of the test conditions, there are no data plotted corresponding to the location H/D = 1.0. The reason is that for these conditions, there was a very high void fraction at the top of the slugs which made it impossible to extract a liquid sample of sufficient size to measure the tracer concentration.

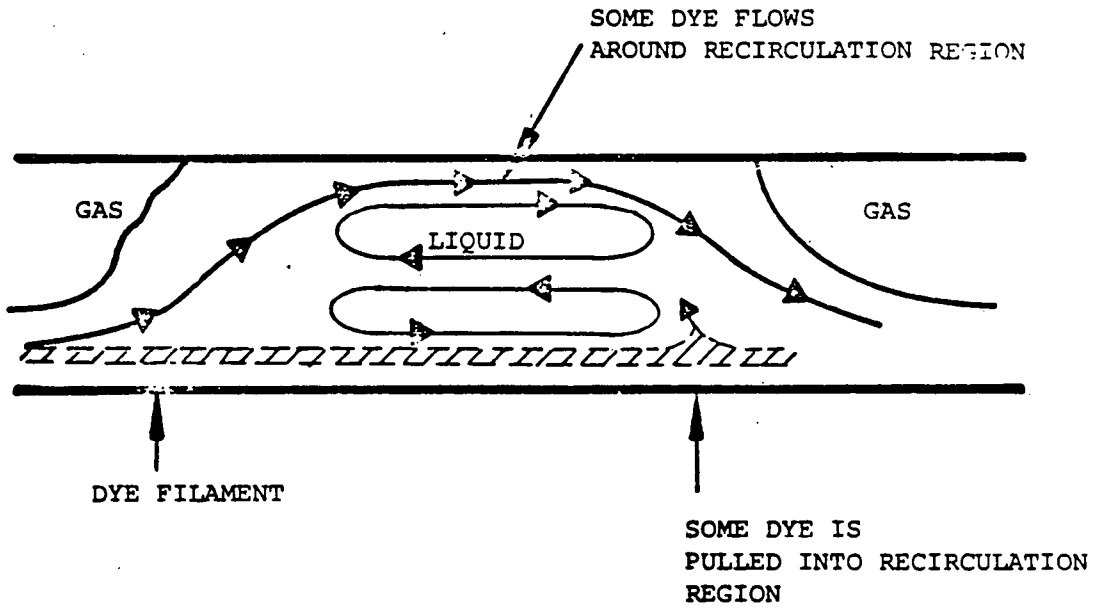

Figure 11. FLOW PATH FOLLOWED BY INJECTED DYE

(Note: Flow pattern is drawn as if pipe wall were moving to the right at the slug velocity and gas bubbles are stationary)

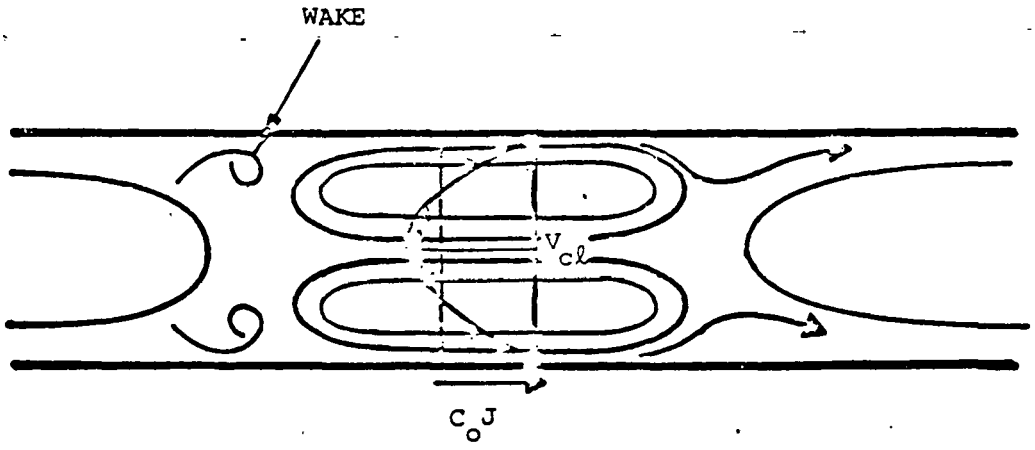

A. $C_oJ<V_{c\ell}$

RECIRCULATION REGION

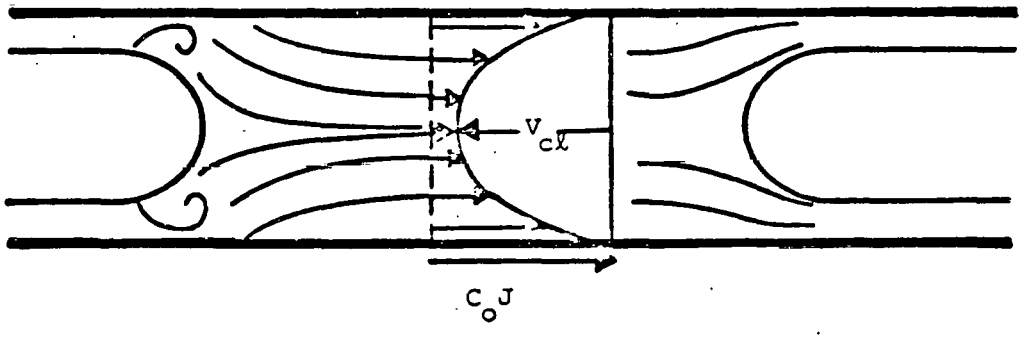

B. $C_oJ>V_{c\ell}$

NO RECIRCULATION

Figure 12. VELOCITY PROFILES AND STREAMLINES WITH VARYING C_oJ

(Note: Flow pattern is drawn as if pipe wall were moving to the right at the slug velocity and gas bubbles are stationary)

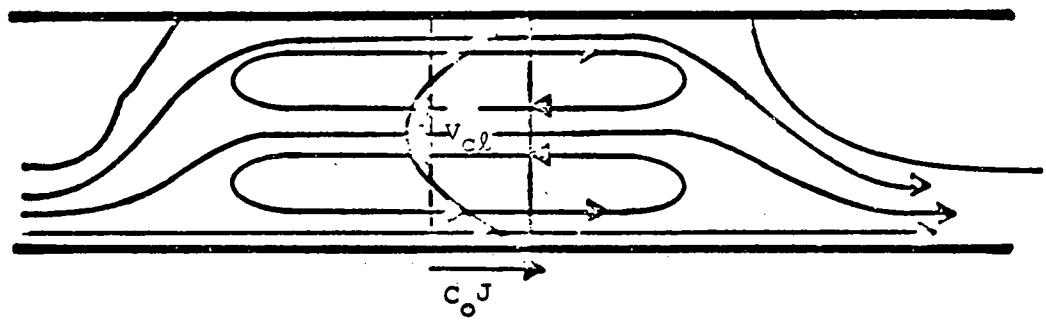

Figure 13. VELOCITY PROFILE AND STREAMINES FOR UNCONVENTIONAL SLUG

(Note: Flow pattern is drawn as if pipe wall were moving to the right at the slug velocity and gas bubbles are stationary)

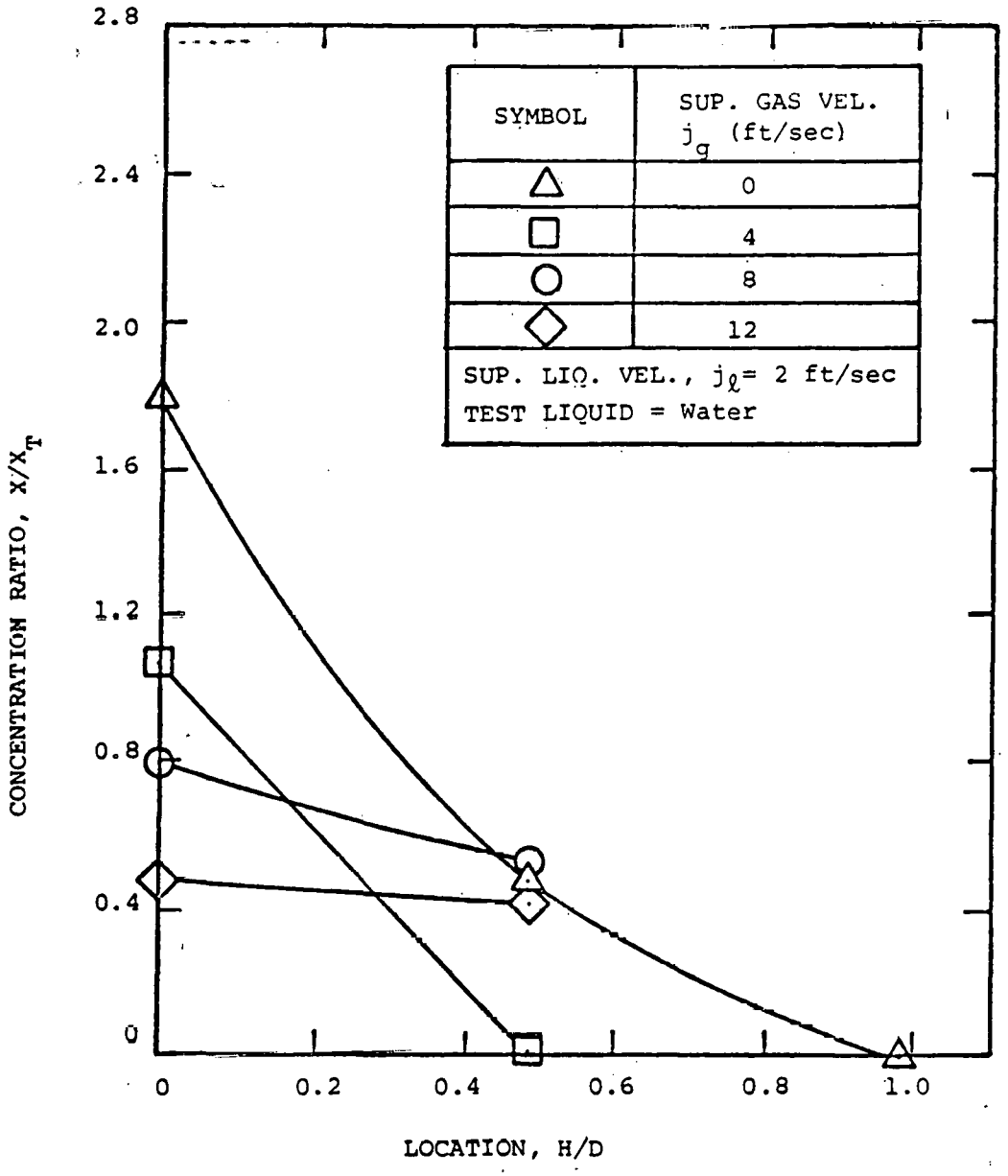

Figure 14. TWO-PHASE MIXING RESULTS OBTAINED WITH WATER AND j_ℓ = 2 ft/sec

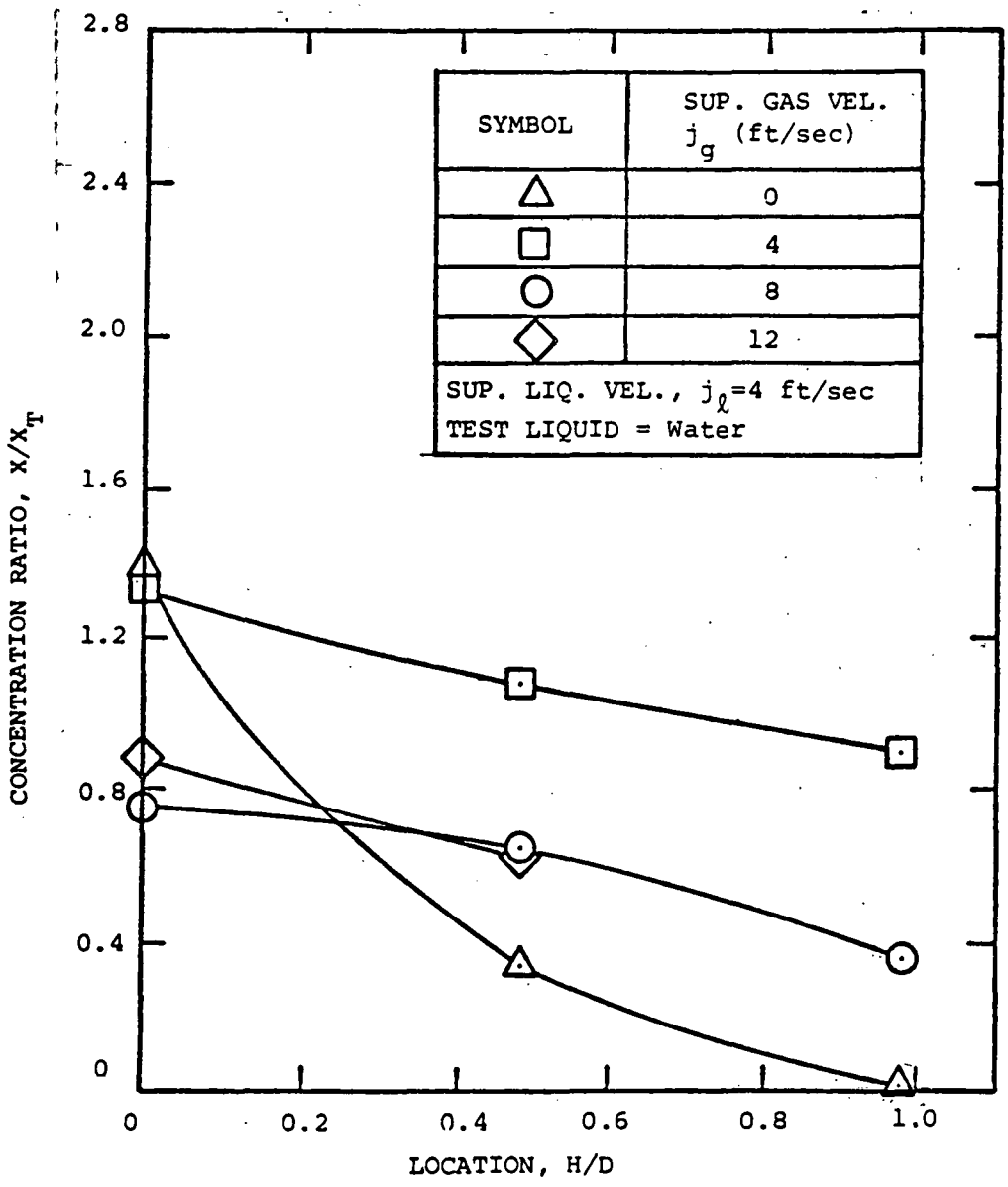

Figure 15. TWO-PHASE MIXING RESULTS OBTAINED WITH WATER AND j_ℓ = 4 ft/sec

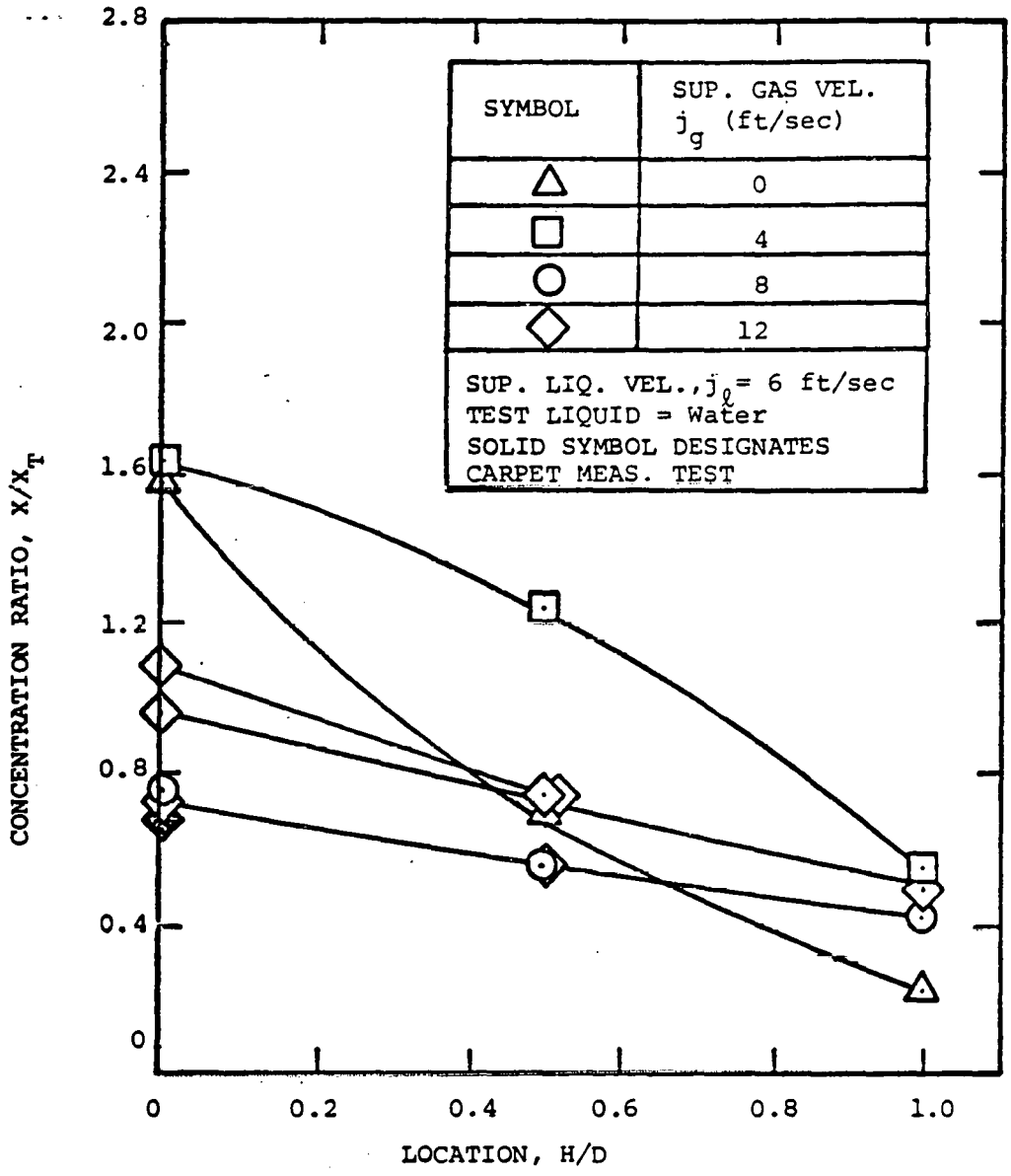

Figure 16. TWO-PHASE MIXING RESULTS OBTAINED WITH WATER AND j_ℓ = 6 ft/sec

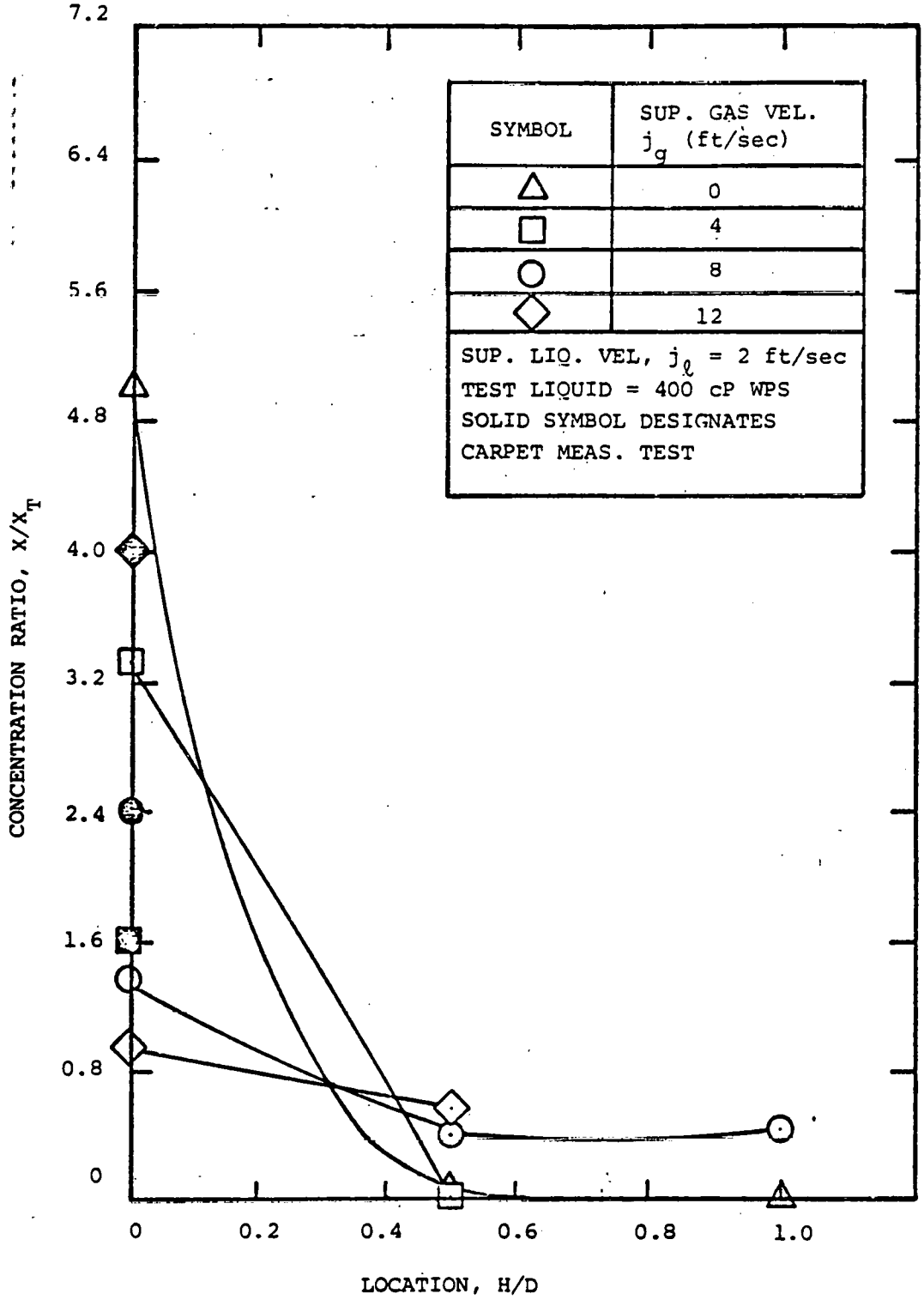

Figure 17. TWO-PHASE MIXING RESULTS OBTAINED WITH 400 cP WPS AND j_ℓ = 2 ft/sec

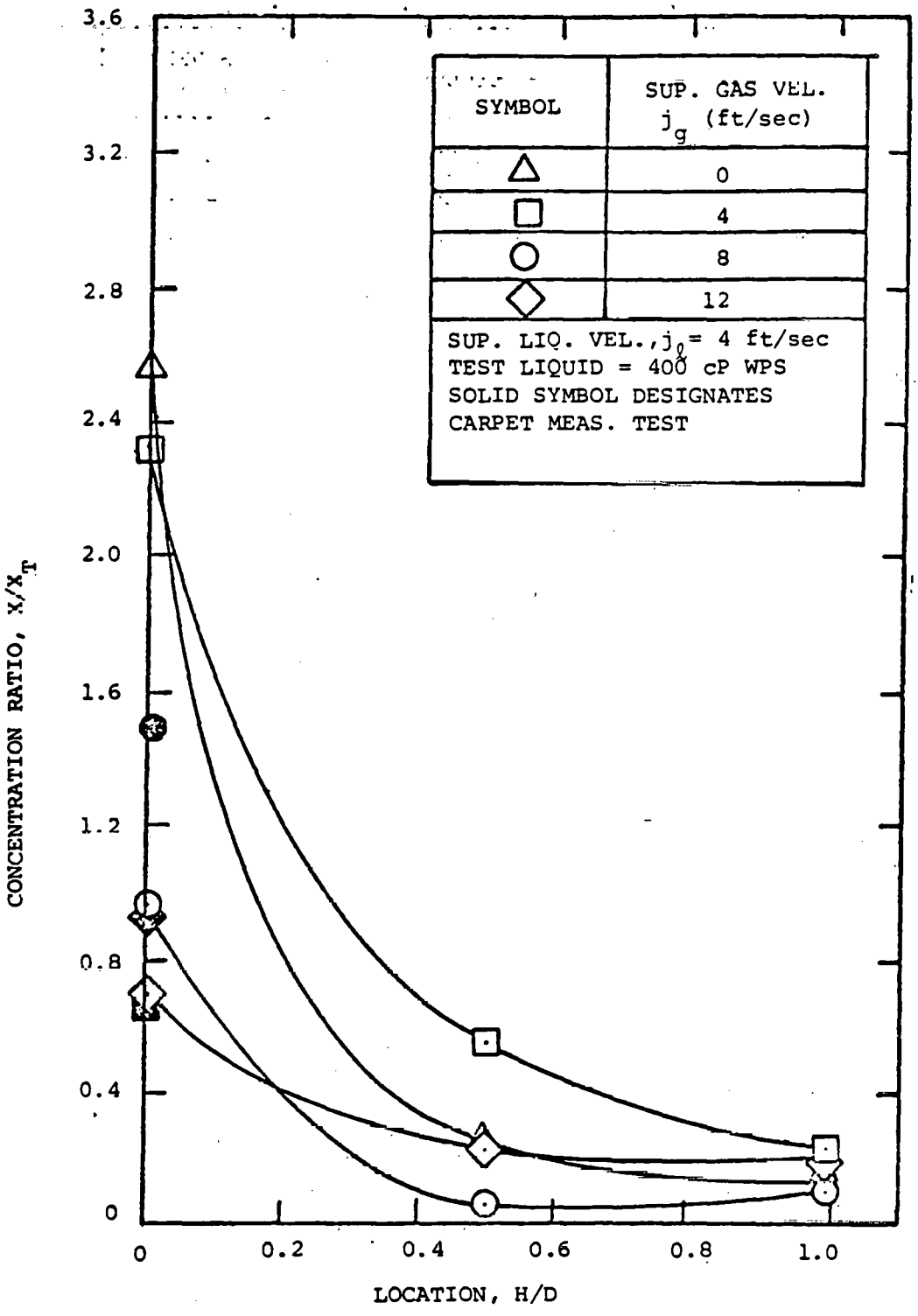

Figure 18. TWO-PHASE MIXING RESULTS OBTAINED WITH 400 cP WPS AND j_ℓ = 4 ft/sec

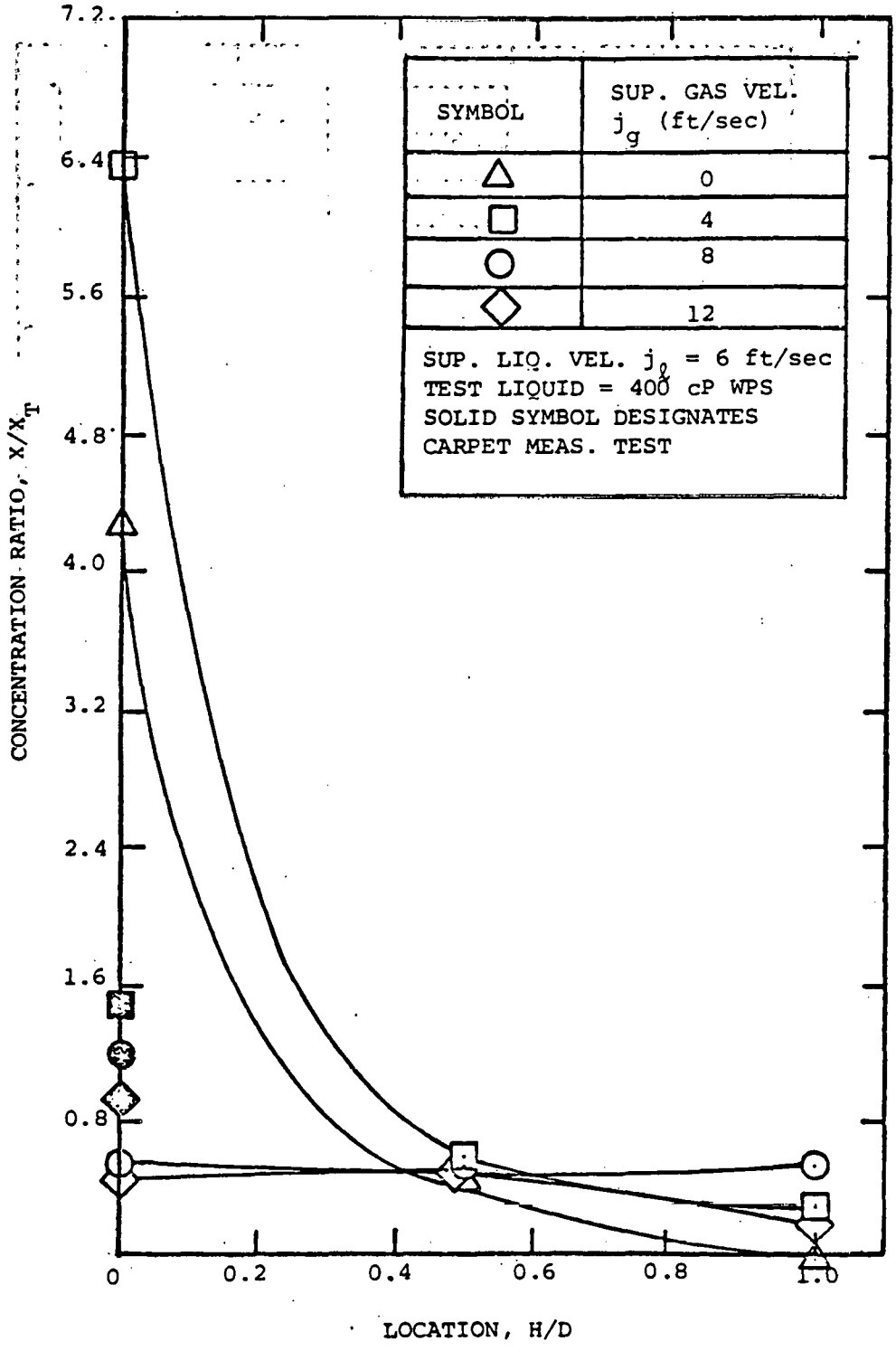

Figure 19. TWO-PHASE MIXING RESULTS OBTAINED WITH 400 cP WPS AND j_ℓ = 6 ft/sec

Close visual observations from above the pipe indicated that the high void fraction region resembled a "tunnel" as illustrated in Figure 20. Apparently, in some cases, a slug-annular flow regime is approached.

Some of the data indicate an average concentration ratio across the pipe of less than 1.0. This implies that the carpet concentration must be higher than the slug concentration. In order to verify this, additional tests were performed to determine the carpet concentration for some conditions. The results are included with the slug data and distinguished by the solid symbols. The carpet data are shown to be consistent with the slug data; i.e., if the average slug concentration is low, the carpet concentration is high and vice versa.

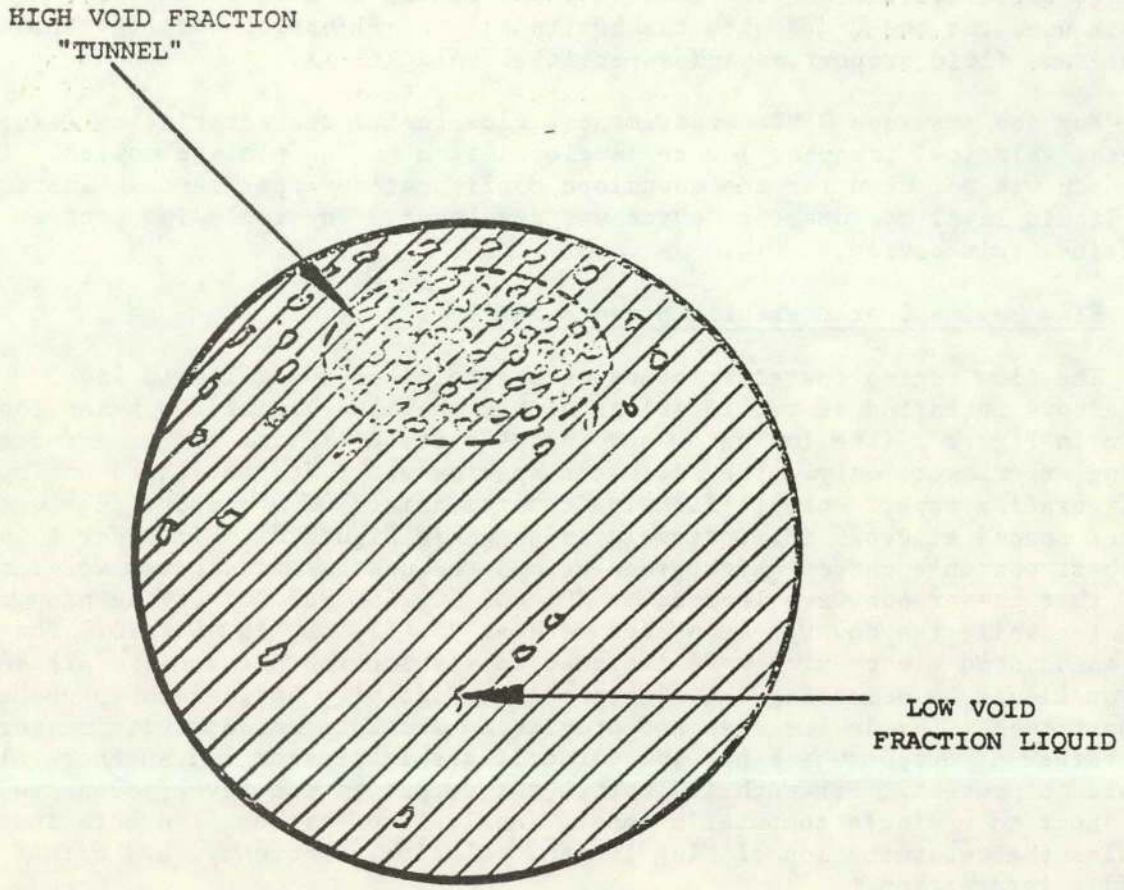

Figure 20. CROSS-SECTION OF SLUG ILLUSTRATING VOID FRACTION

3 DOWNSLOPE CONFIGURATION EXPERIMENTS

3.1 Objective

The objective of the experiments was to develop flow regime and pressure drop data with a -1° downslope configuration. The test matrix for the downslope configuration experiments is shown in Table 6. It is identical to the test matrix used for the CFMTP with the horizontal and +1°upslope configurations (i.e. same fluid properties and superficial velocities).

For the previous CFMTP experiments, flow regime characteristics (slug length, velocity, frequency) were developed from motion picture movies. This approach was not used for the downslope configuration experiments. Instead, a new liquid level measurement device was developed. The following section describes this device.

3.2 Flow Regime Characteristic Measurement Device

The flow regime characteristics were determined using liquid level indicators installed at two locations within the last leg of the Lexan loop as shown in Figure 1 (The indicator spacing of 8 ft. 8 1/2 in. was used for the mixing experiments only. The indicator spacing was 5 ft. for the downslope configuration experiments). Each indicator consists of a support tube with five probes spaced at 0.675 in. intervals as shown in Figure 21. In order to provide the best possible carpet height resolution, the upstream indicator was installed such that the probes were located at 30, 40, 50, 60, and 70% of the pipe inner diameter while the downstream probes were at 25, 35, 45, 55, 65% ID. The probes and associated electronics were designed to distinguish between the presence of gas or liquid by measuring the electrical conductivity between the probe tip and support tube. The device does not provide an absolute conductivity measurement, but rather an output which has one value if gas is present and another value if liquid is present. For each indicator, the output of the five probes are summed and input to a single computer channel. Analysis of traces from both indicators enables the determination of slug length, velocity, frequency, and carpet profile information.

Flow regime characteristic data were obtained during the mixing experiments (horizontal loop configuration) with the liquid level indicators to compare with data previously obtained from movies in order to verify the new measurement technique. The new data are shown to be consistent with the previous results in Appendix B. The following section presents the flow regime characteristic data obtained with the downslope configuration.

3.3 Flow Regime Characteristics

This section presents slug velocity and frequency data obtained with water, 80 cP WPS, and 400 cP WPS. The data are not analyzed in detail, but simply compared with the corresponding results obtained in the horizontal and +1° upslope configurations. The data are also included in Appendix A, Table A-3.

Figures 22, 23, and 24 present slug velocity as a function of the total superficial velocity for water, 80 cP WPS, and 400 cP WPS respectively. Although there is significant scatter in the data, it appears that the slug velocity for a given total superficial velocity increases slightly with

TABLE 6
DOWNSLOPE CONFIGURATION TEST MATRIX

Loop Inclination Angle (deg.)	-1
Gas Phase	
Type	Freon 12
Density (lbm/ft^3)	1.9
Superficial Gas Velocities (ft/sec)	4, 8, 12
Liquid Phase	
Type	W, WPS 1, WPS 2
Superficial Liquid Velocities (ft/sec)	v_t, 2, 4, 6
Total Number of Tests	36

W = Water
WPS 1 = Non-Newtonian water/polymer solution with viscosity of 80 cP at a shear rate of 213 sec^{-1}.
WPS 2 = Non-Newtonian water/polymer solution with viscosity of 400 cP at a shear rate of 213 sec^{-1}.
v_t = Liquid superficial velocity at transition from stratified to slug flow (if achievable).

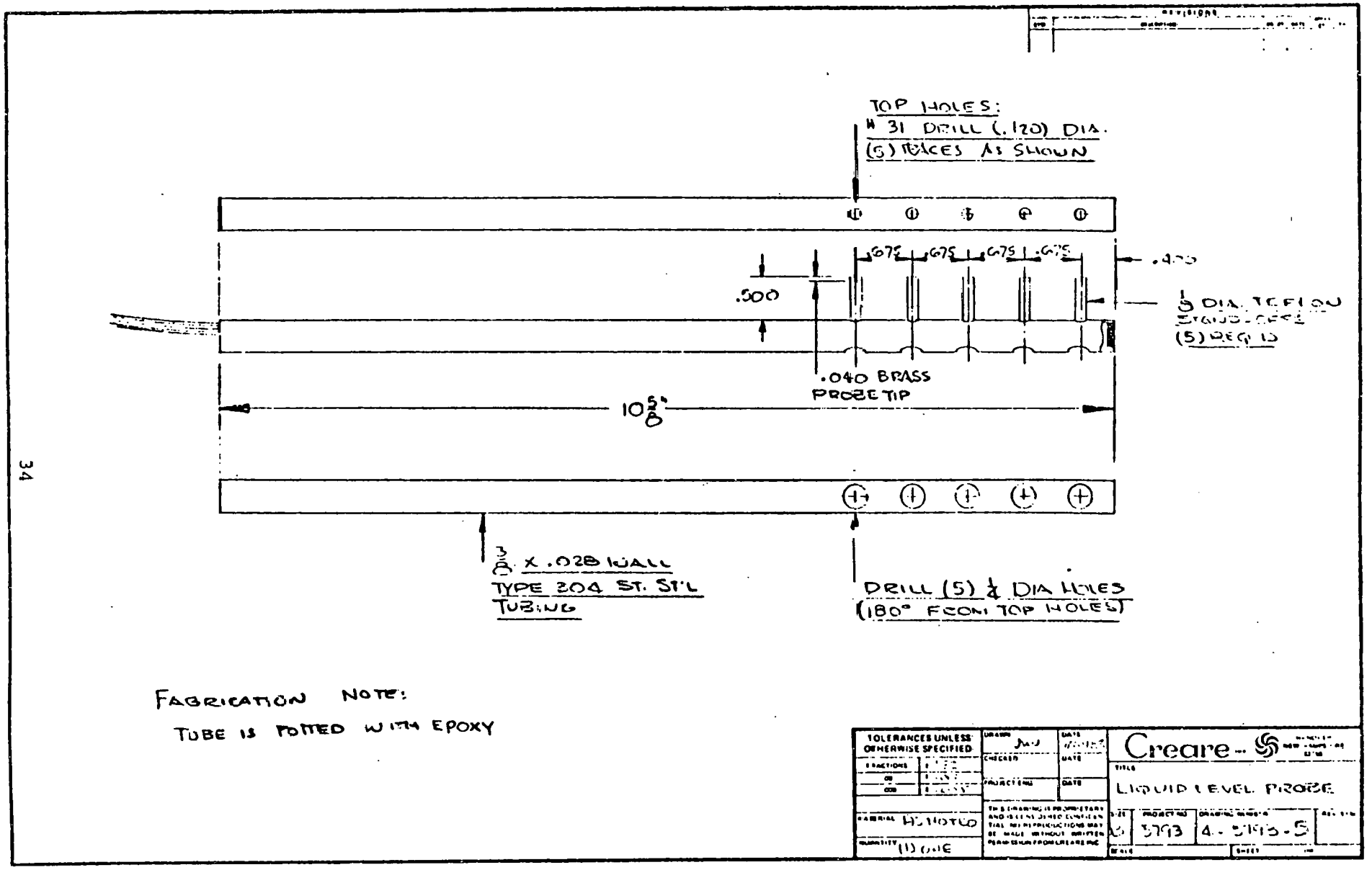

Figure 21. LIQUID LEVEL PROBE DETAILS

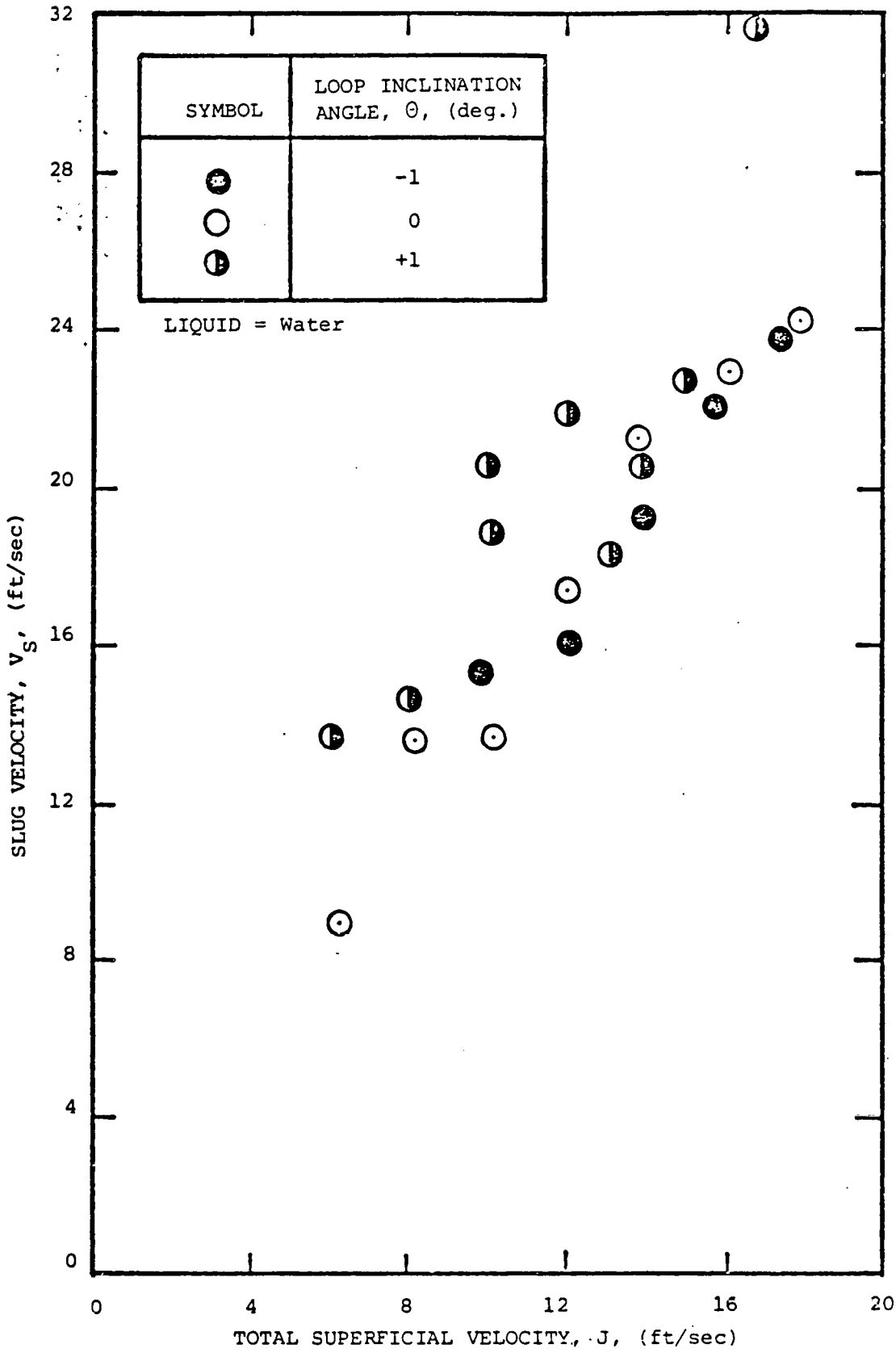

Figure 22. SLUG VELOCITY DATA OBTAINED WITH WATER

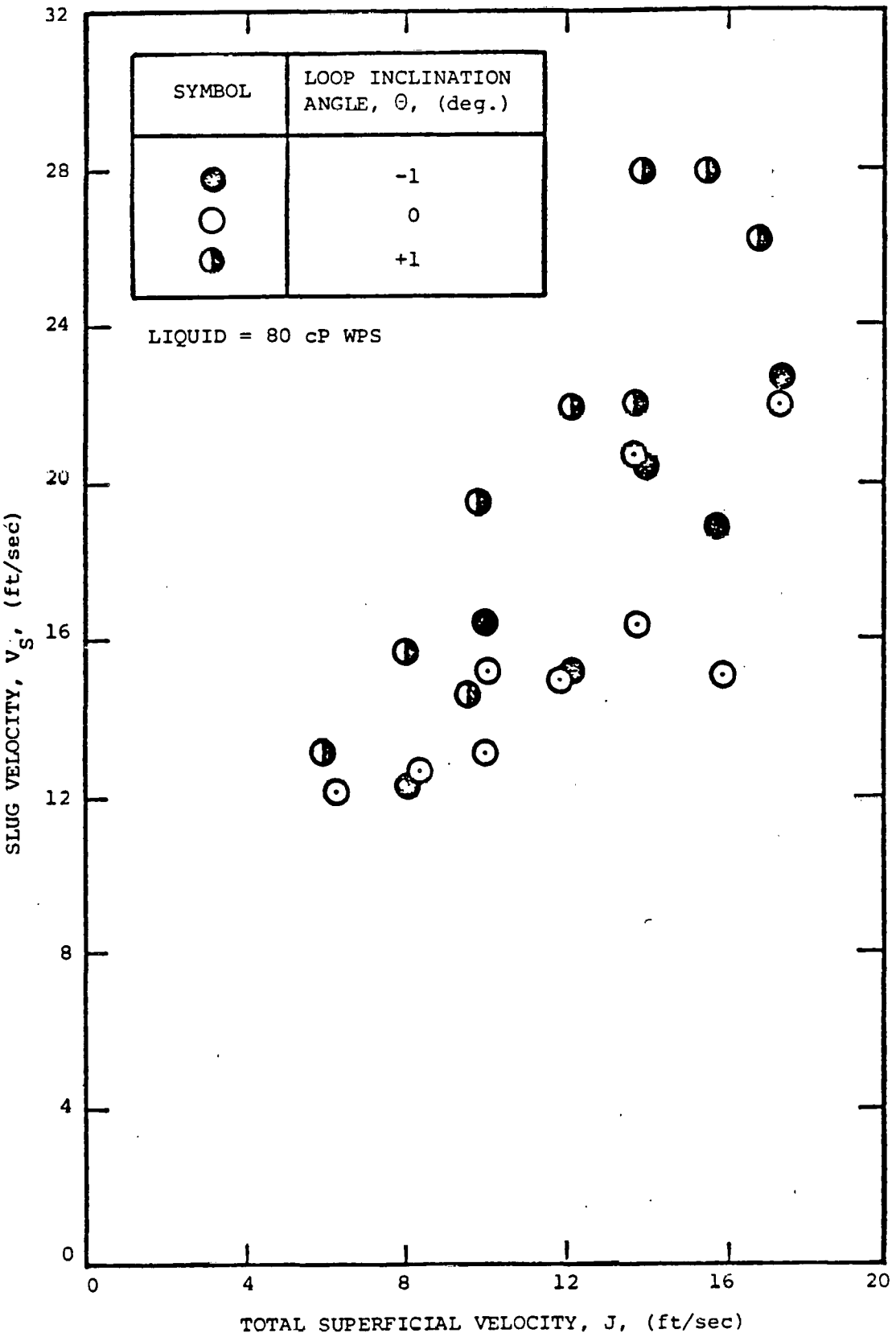

Figure 23. SLUG VELOCITY DATA OBTAINED WITH 80 cP WPS

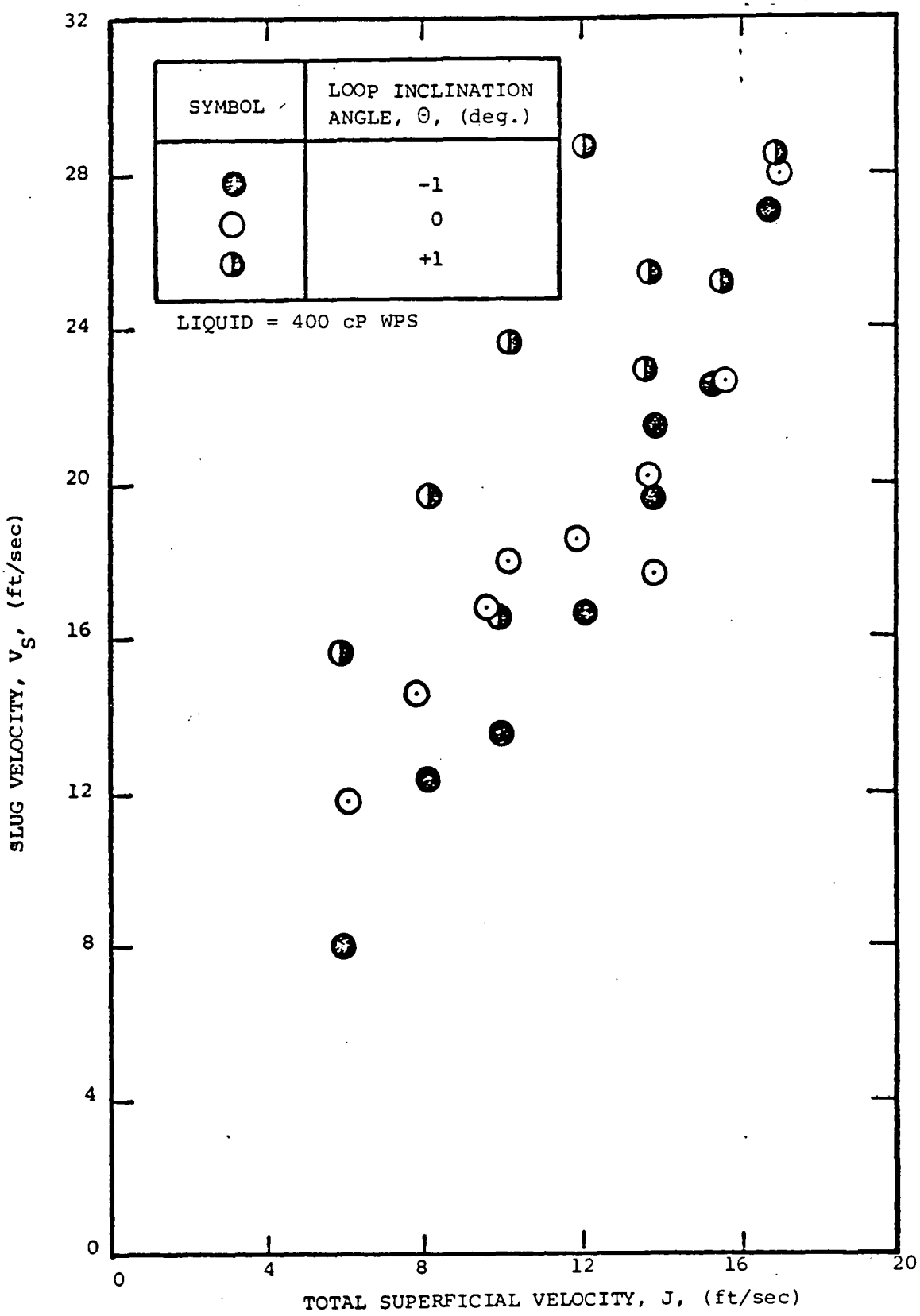

Figure 24. SLUG VELOCITY DATA OBTAINED WITH 400 cP WPS

increasing liquid viscosity. The slug velocity also appears to be slightly greater for the upslope configuration than for either the horizontal or the downslope configurations. It should be noted that the velocities of slugs recorded for a given test condition can vary by as much as ± 25%, due to variations in the instantaneous loop hold up. Therefore, the data in Figures 22, 23, and 24 represent average values.

Slug frequency data are plotted as a function of the superficial liquid velocity with the superficial gas velocity and loop inclination angle as parameters for water, 80 cP WPS, and 400 cP WPS in Figures 25, 26, and 27. The slug frequency is shown to increase with increasing superficial liquid velocity and possibly decrease with increasing superficial gas velocity. However, there is no significant effect of liquid type or loop inclination angle.

Slug length data are also tabulated in Appendix A (Table A-3) but have not been presented in this section due to the lack of interesting trends.

3.4 Slug Flow/Stratified Flow Transition Data

Experiments have been performed with each liquid and a range of superficial gas velocities to define the transition boundary between slug flow and stratified flow. The test procedure was identical to that used for previous CFMTP experiments and involved setting a particular value of superficial gas velocity and adjusting the superficial liquid velocity until the onset of slugging was reached (characterized by a very occasional slug). For the previous CFMTP experiments, the resulting transitional superficial liquid velocities were not sensitive to how they were obtained. That is, the result did not depend on whether it was arrived at by increasing or decreasing the liquid flow rate.

The downslope transition data are included in Table A-4, Appendix A, and compared with the horizontal and upslope configuration results in Figure 28. Note that additional experiments were performed with water and the 80 cP WPS at superficial gas velocities of 6 and 10 ft/sec in order to improve the transition boundary definition. The figure shows that the transitional superficial liquid velocities obtained with water are slightly higher than the transitional velocities obtained with the 80 cP WPS and are not only much higher than the results obtained with the 400 cP WPS, but show the opposite trend (transition liquid velocity decreases with increasing gas velocity for water or 80 cP WPS while transition liquid velocity increases with increasing gas velocity for 400 cP WPS). In addition, except for the results obtained with the 400 cP WPS, the downslope data are significantly different than the horizontal or upslope data. The preliminary theory described below has been developed to explain the data trends.

The basis of the theory is a plot of curves of constant void fraction, α, for stratified flow on a map with coordinates of superficial liquid velocity and superficial gas velocity. If these curves are known, it is possible to locate the transition curve which is hypothesized to be described by a critical Froude number, Fr,

$$Fr = \frac{j_g\sqrt{\rho_g}}{\sqrt{Dg\Delta\rho}} = C\,\alpha^{3/2} \qquad (3)$$

where C is in the range of 0.5 to 1.

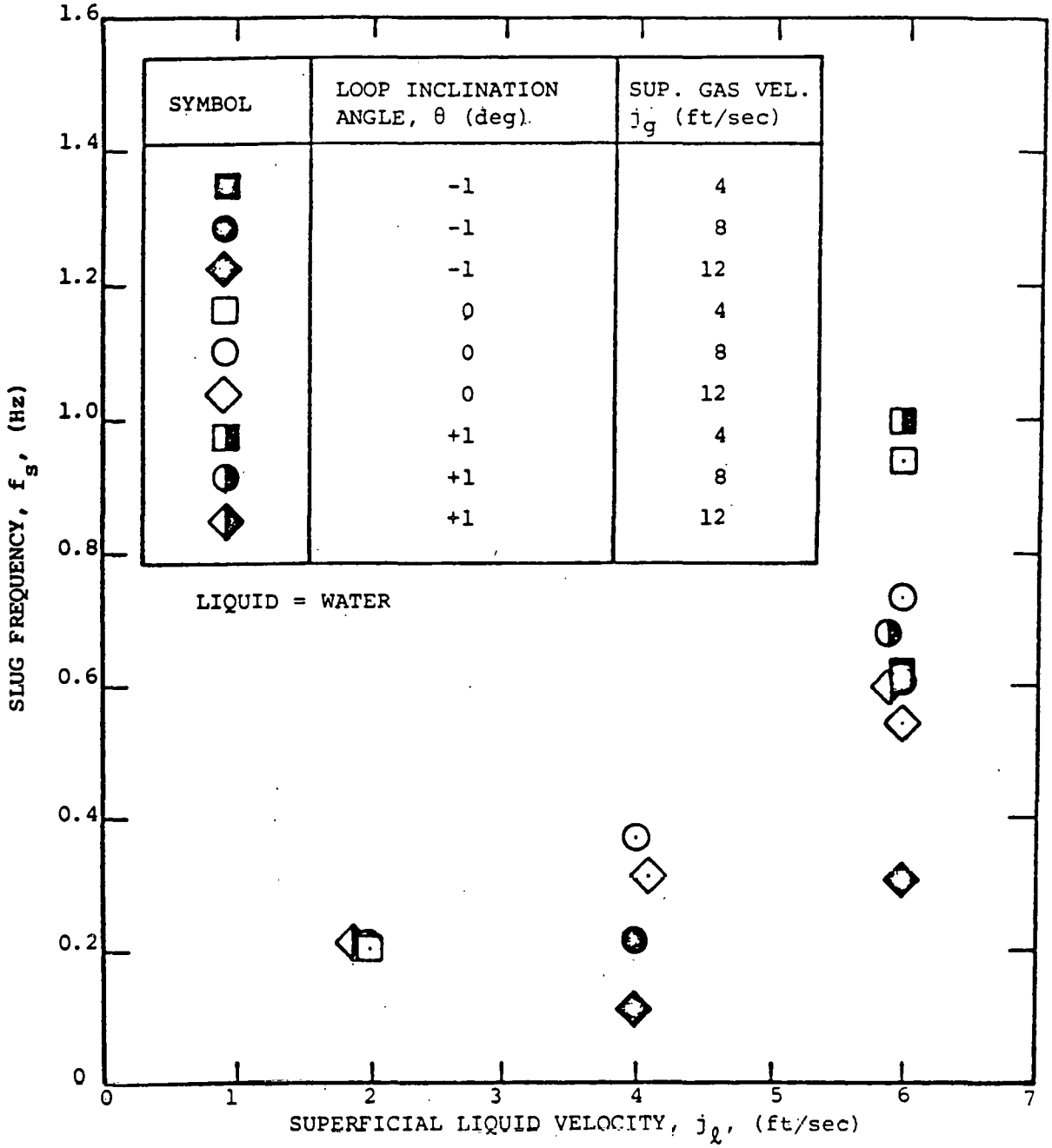

Figure 25. SLUG FREQUENCY DATA OBTAINED WITH WATER

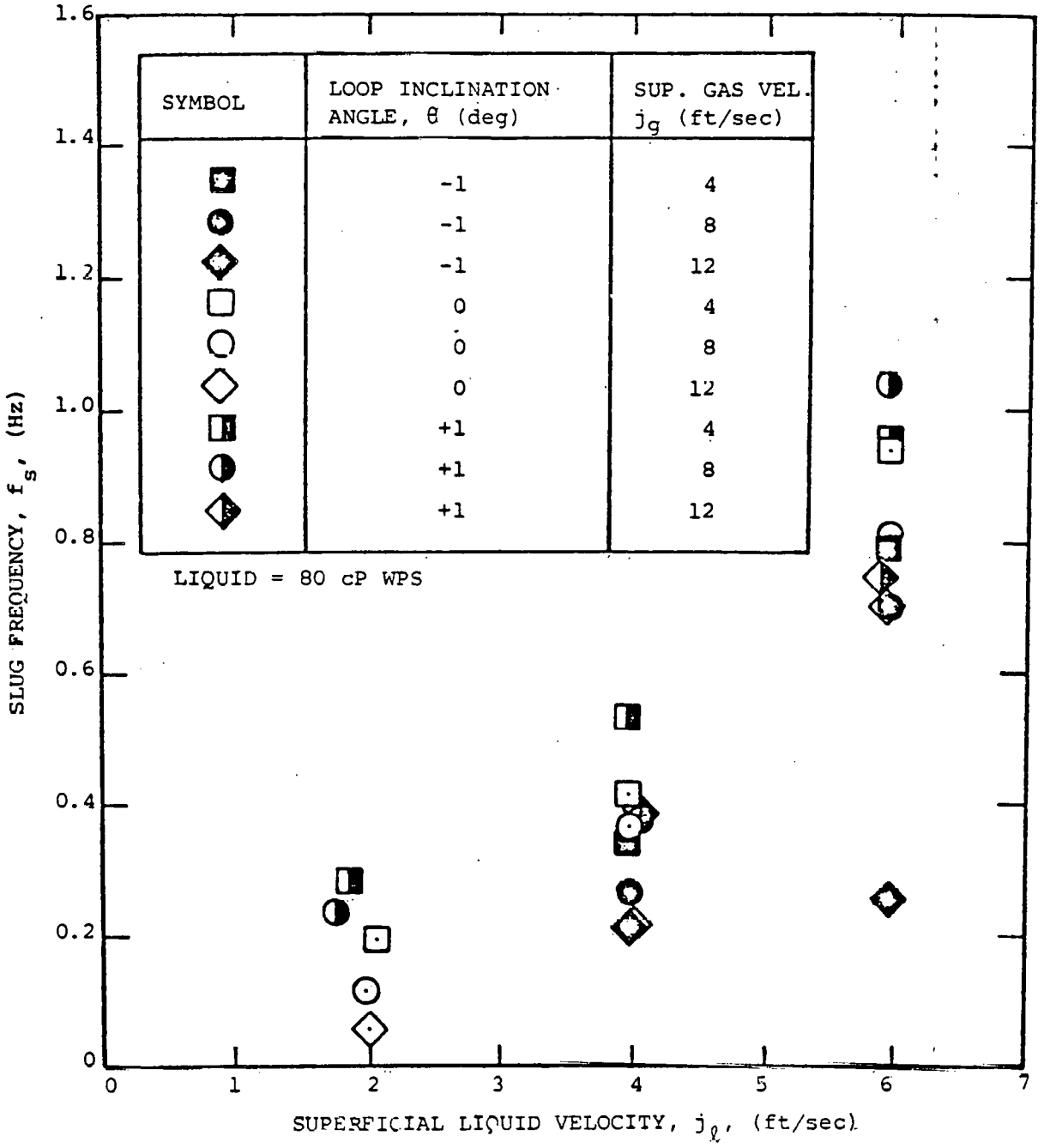

Figure 26. SLUG FREQUENCY DATA OBTAINED WITH 80 cP WPS

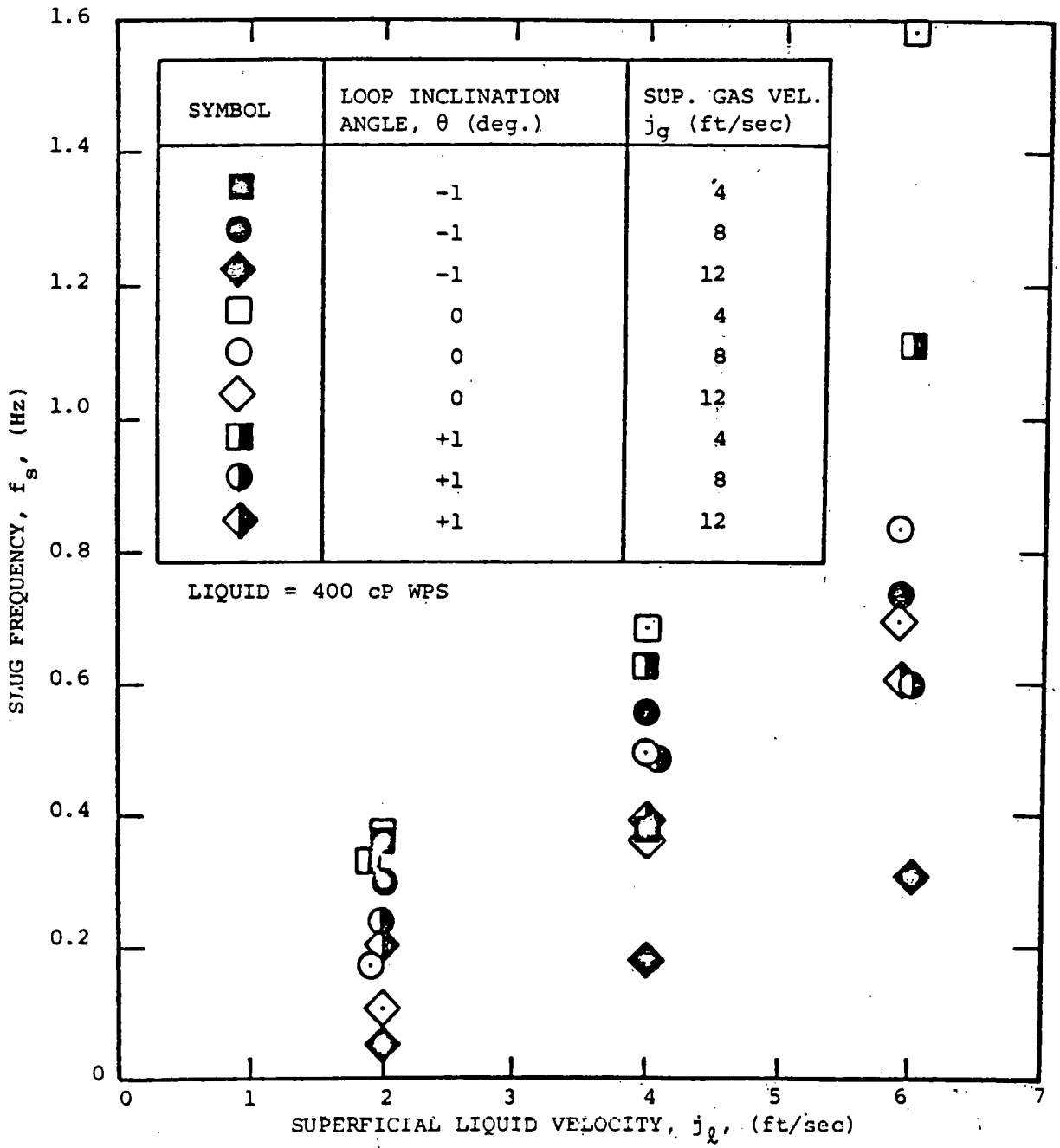

Figure 27. SLUG FREQUENCY DATA OBTAINED WITH 400 cP WPS

In downflow (Figure 29), the liquid flows under the influence of gravity (at low gas velocities when the interfacial shear stress is small) and α is almost unaffected until j_g is sufficiently large. The single-phase flow limits at $j_g = 0$ can be derived from open channel flow theory using the limit of Eq. 3 with $\alpha = 1$. These limits give an idea of the scale of the picture. If the liquid is more viscous and laminar, the intercepts of the constant α curves on the j_g axis move towards the origin, dragging the rest of the pattern with them (see Figure 30). The limit for a very viscous liquid gives a pattern similar to horizontal flow.

As shown in Figure 31 for horizontal flow, lines of constant α start from the origin since both phases are driven by the pressure gradient and the associated shear stress field. The transition curve also starts at the origin.

In upflow, the intercepts of the constant α curves on the j_g axis lie below the origin (see Figure 32). This drags the transition curve down and it crosses the j_g axis at some point.

The trends and numerical values of the data seem consistent with the composite curves sketched in Figure 33. An attempt to use Martinelli's correlation to predict the constant α lines for horizontal Freon/water flow gave results within the measured range. A better prediction would be obtained if the actual carpet depth data were used. Additional calculations and work to develop this theory are planned in the next program.

3.5 Pressure Drop Data

Measurements of the pressure drop across the loop middle leg, bend, and last leg have been made for each of the test conditions given in Table 6 as well as during the mixing experiments.

Appendix C includes a comparison of the new data obtained during the mixing experiments with old data previously obtained in a horizontal loop configuration. The comparison illustrates the good repeatability of the data.

The downslope data are compared with the horizontal and upslope configuration data in Figures 34-41, (and included in Table A-5, Appendix A). The results do not demonstrate any significant effect of loop inclination. It should be noted that the upslope and downslope configuration data have been reduced by subtracting the liquid hydrostatic head due to the elevation difference between the two measurement points from each manometer reading. The following paragraphs present some preliminary analytical considerations based on homogeneous flow theory and slug flow theory.

Homogeneous Flow

One of the simplest two-phase flow models is based on the assumption of homogeneous flow of the two phases. In turbulent flow, the pressure gradient due to friction is:

$$\frac{\Delta P}{L} = \frac{2f}{D} \rho_m V_m^2 = \frac{2f}{D} GJ \qquad (4)$$

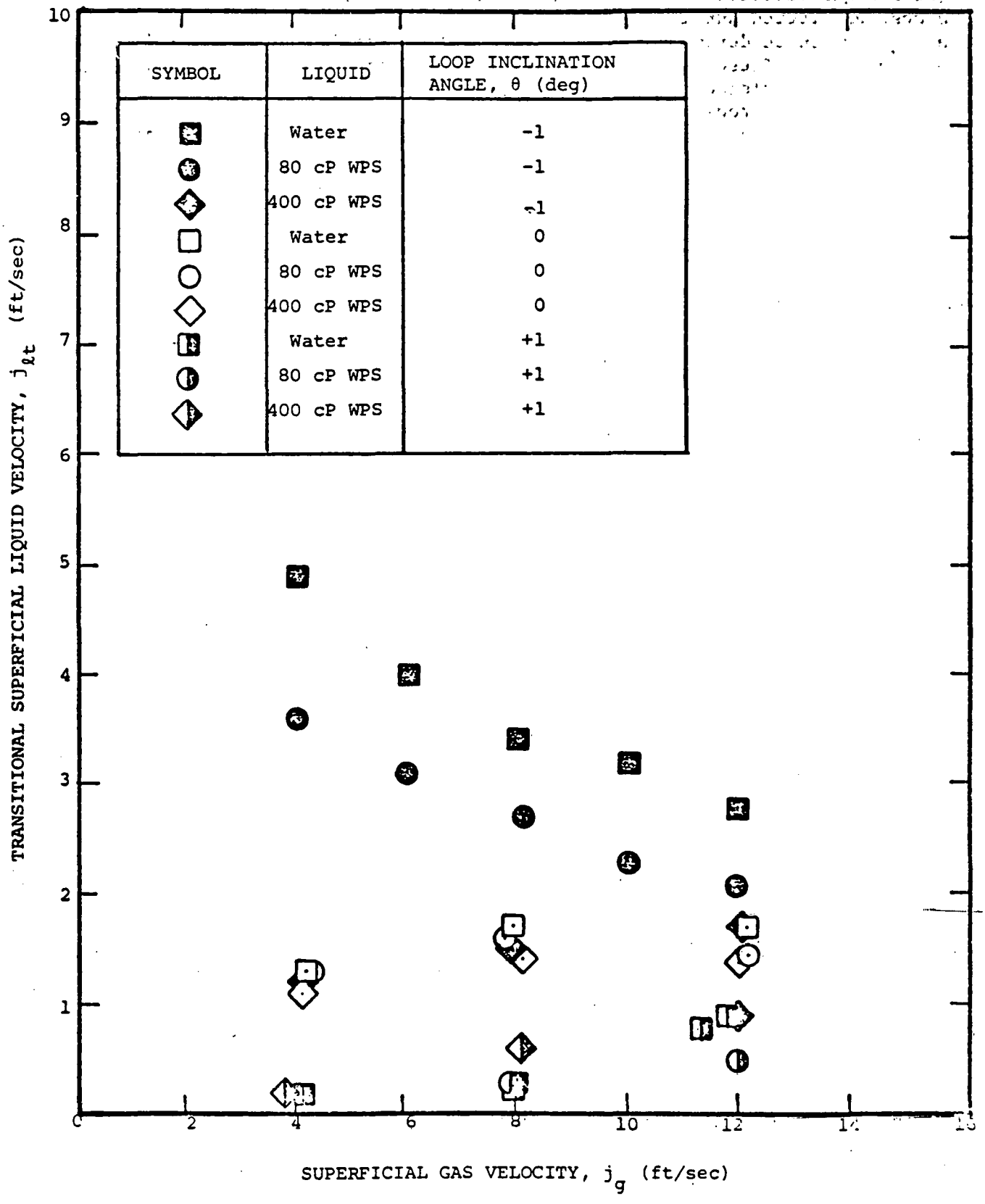

Figure 28. SLUG FLOW/STRATIFIED FLOW TRANSITION DATA

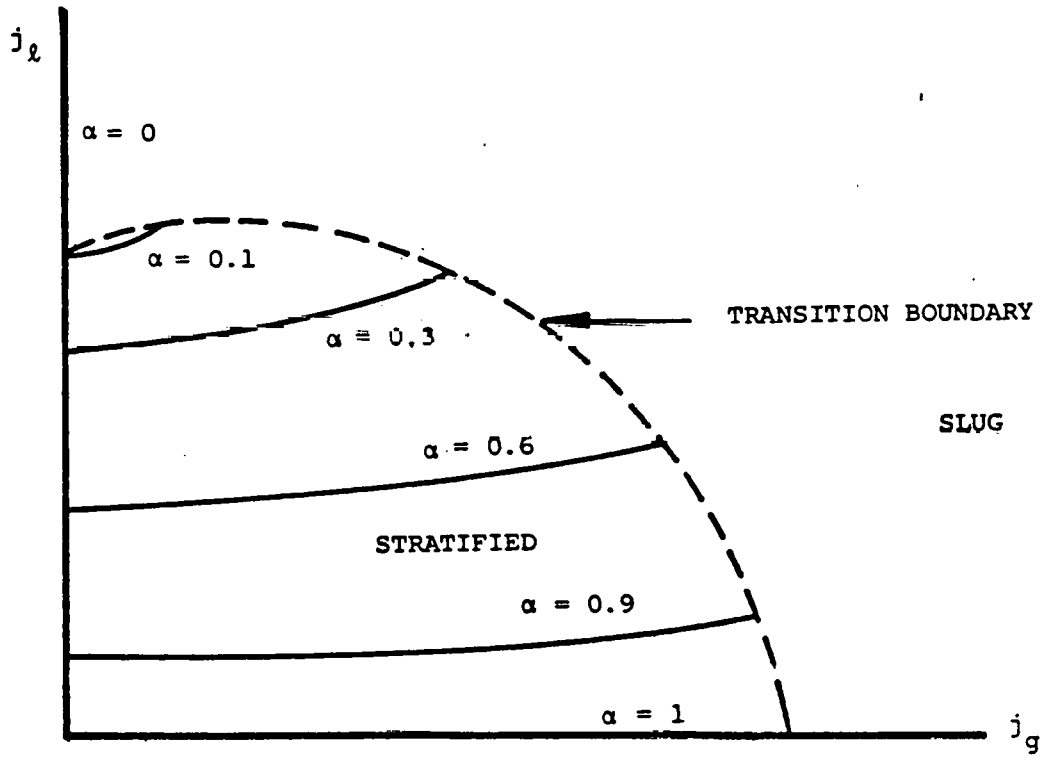

Figure 29. TRANSITION BOUNDARY FOR INCLINED DOWNFLOW

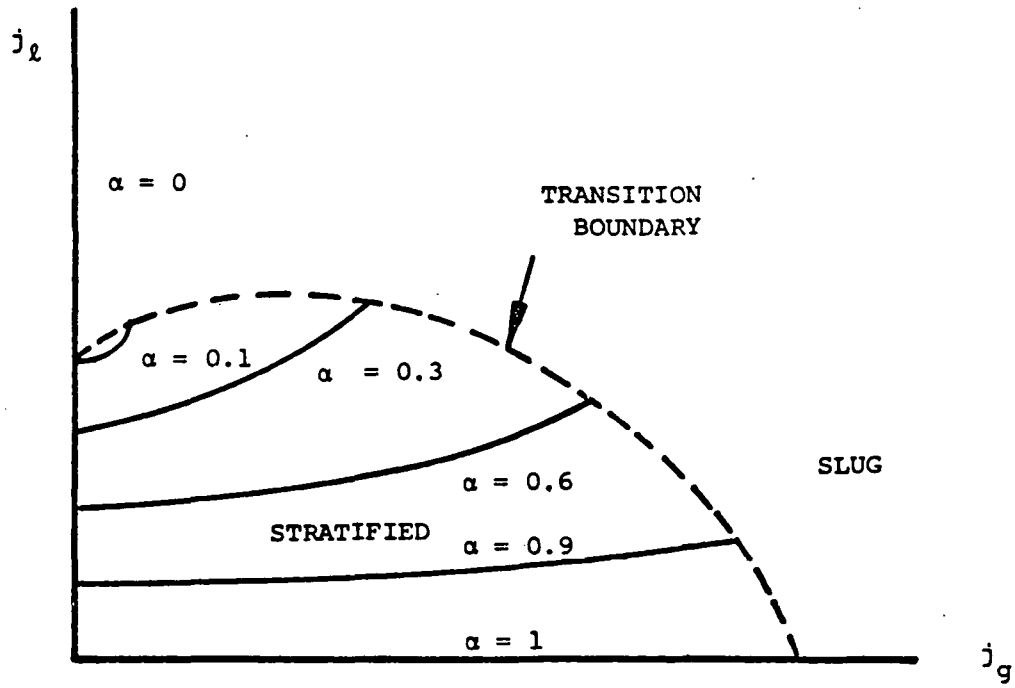

Figure 30. TRANSITION BOUNDARY FOR INCLINED DOWNFLOW WITH VISCOUS LIQUID

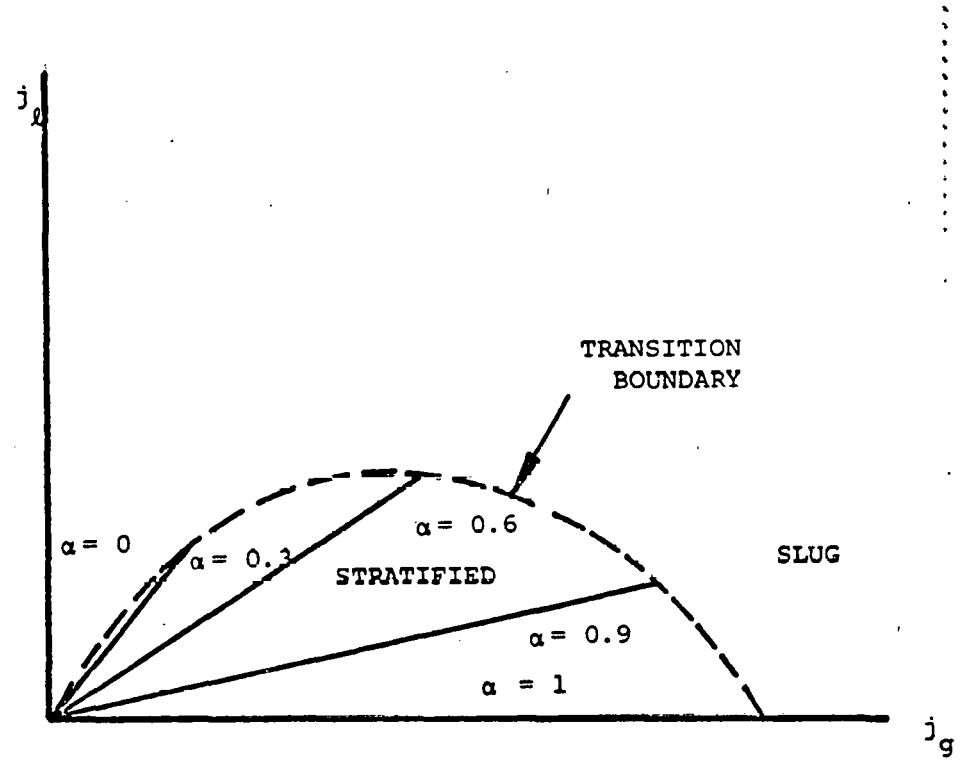

Figure 31. TRANSITION BOUNDARY FOR HORIZONTAL FLOW

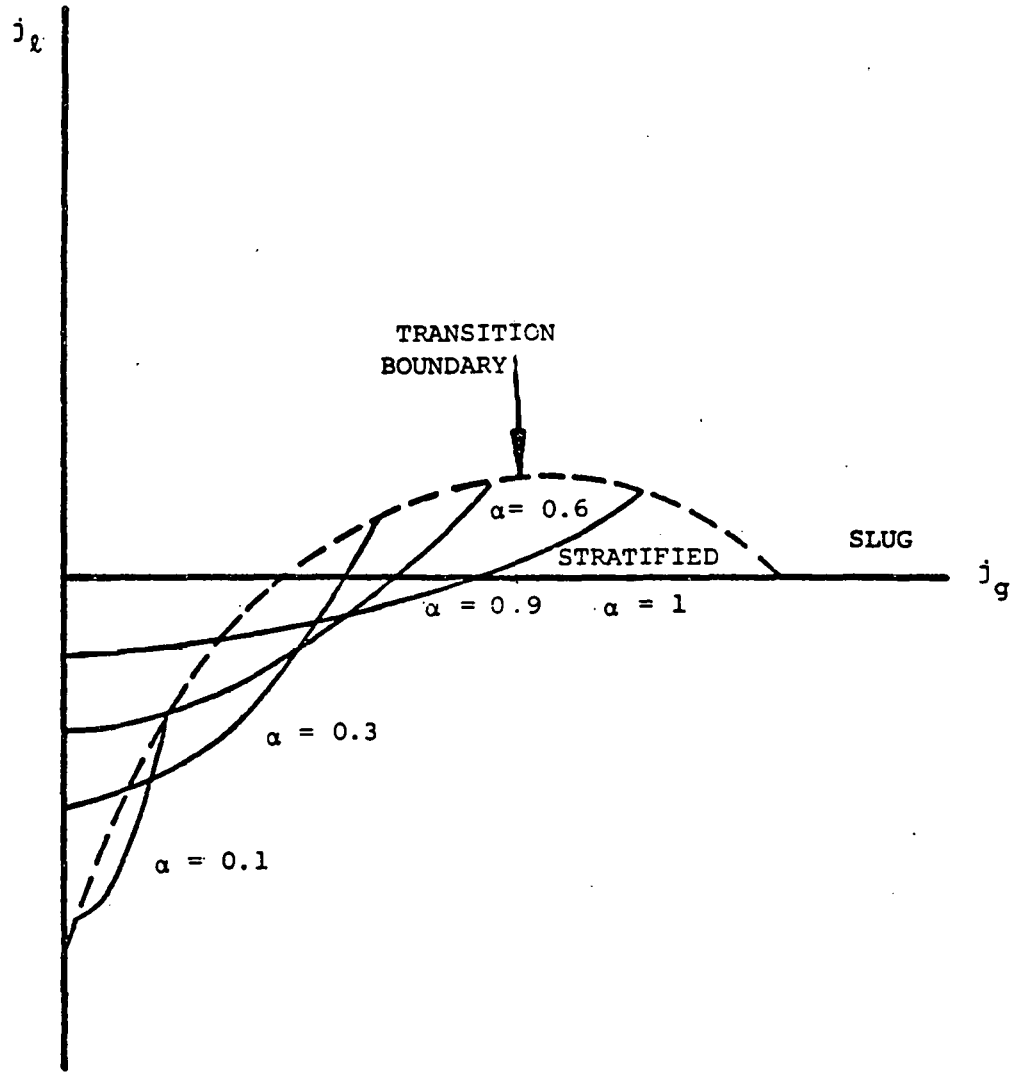

Figure 32. TRANSITION BOUNDARY FOR INCLINED UPFLOW

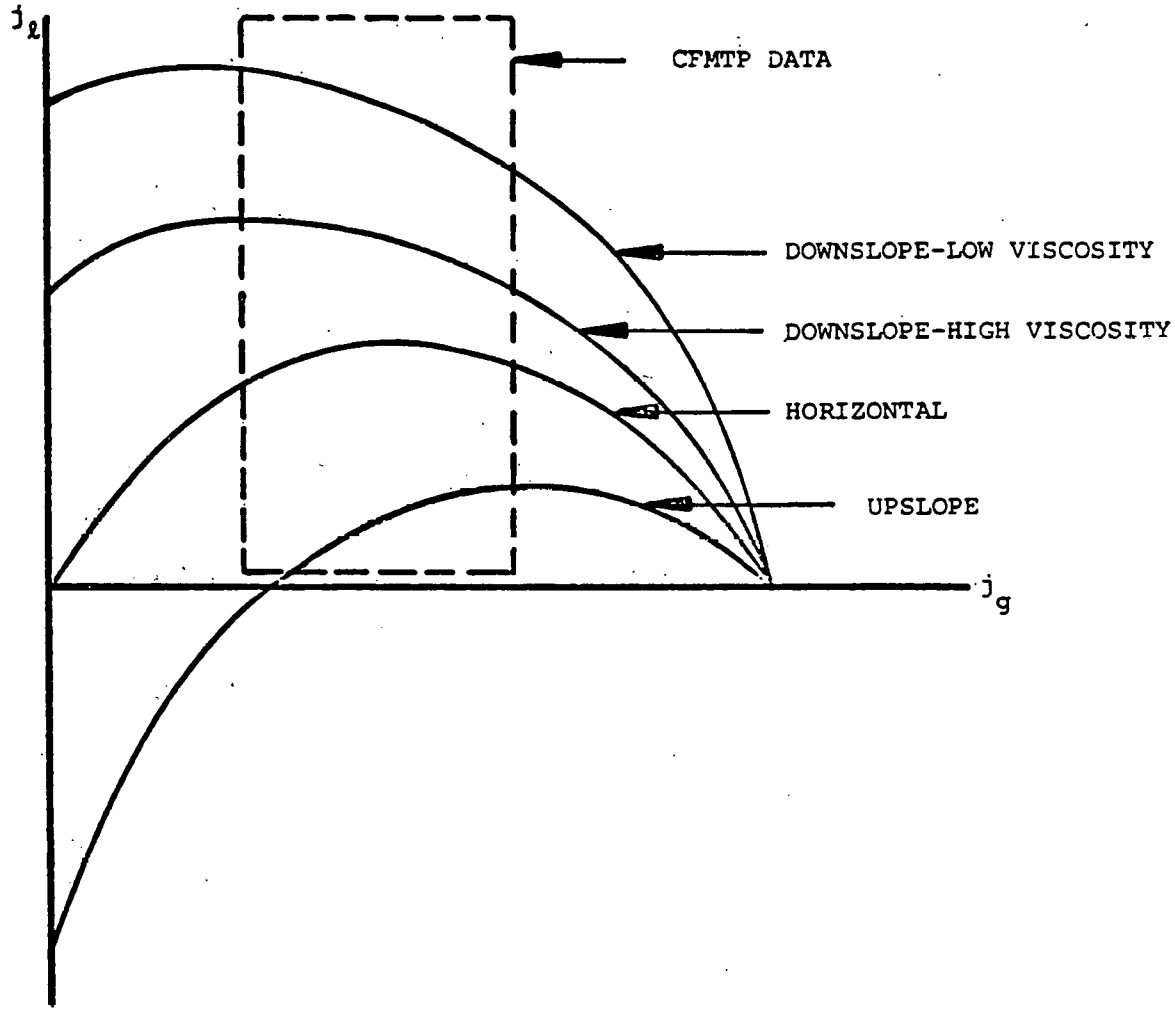

Figure 33. SUMMARY OF TRANSITION BOUNDARIES FOR VARIOUS INCLINATIONS AND LIQUID VISCOSITIES

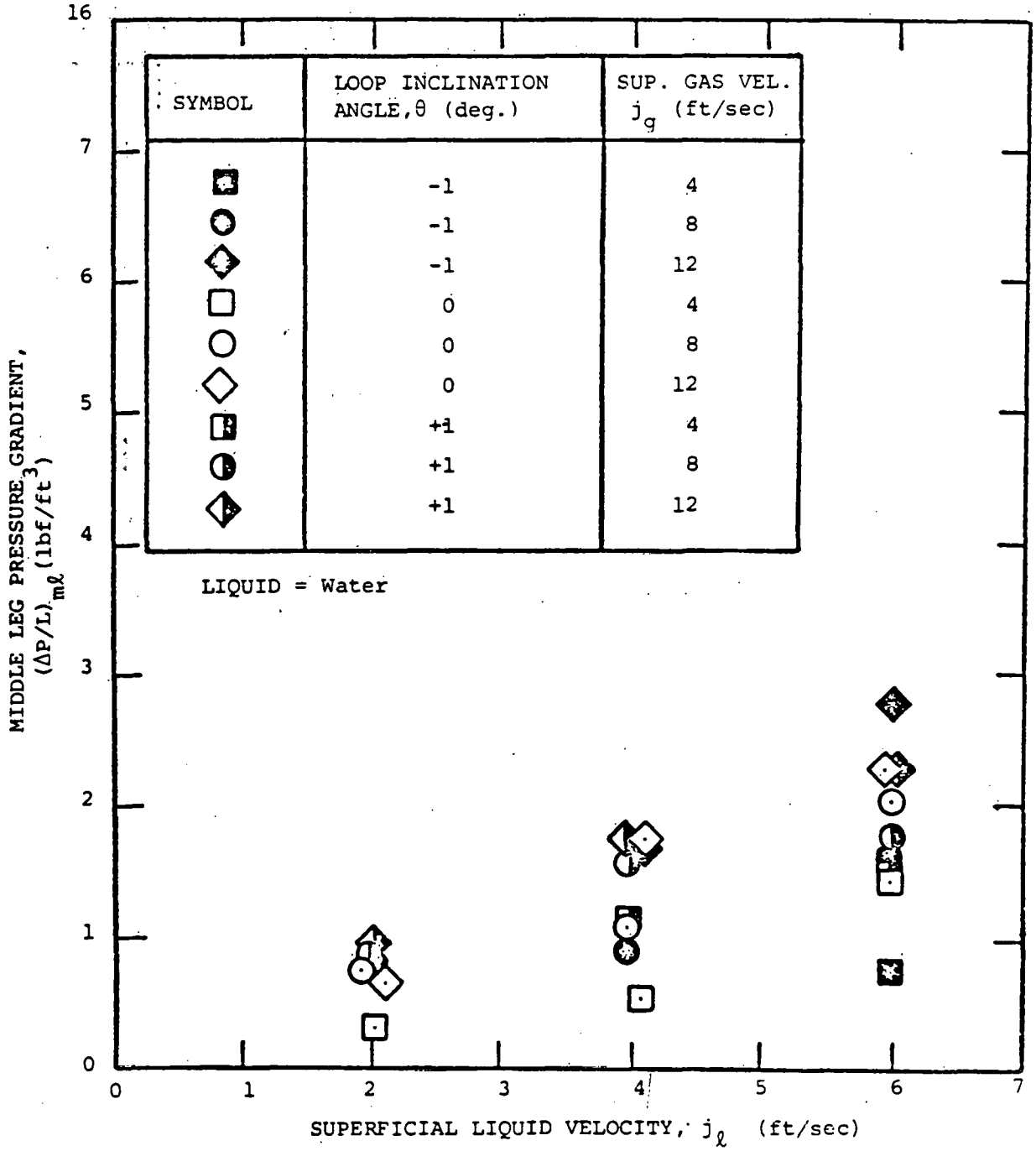

Figure 34. MIDDLE LEG PRESSURE GRADIENT DATA OBTAINED WITH WATER

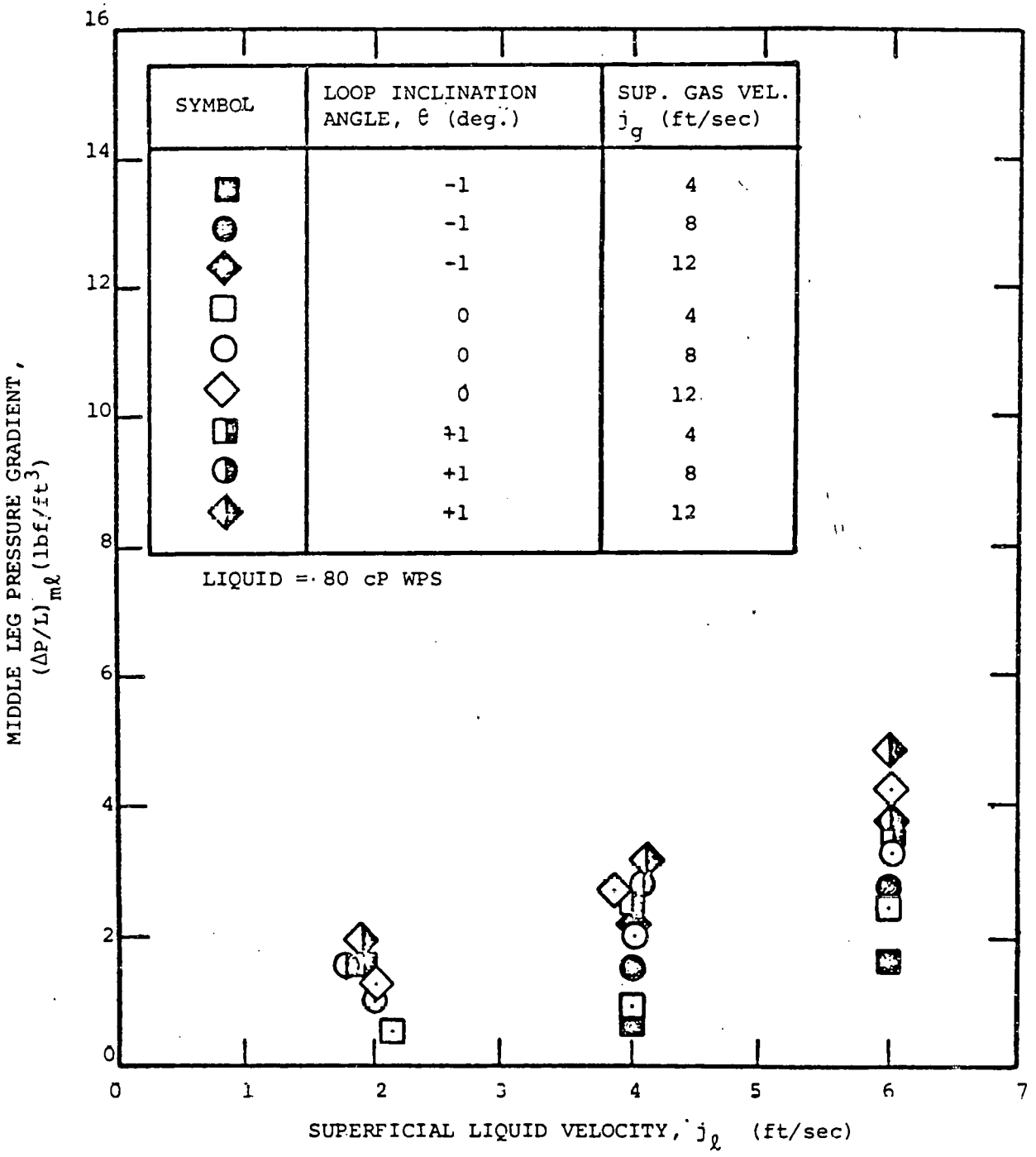

Figure 35. MIDDLE LEG PRESSURE GRADIENT DATA OBTAINED WITH 80 cP WPS

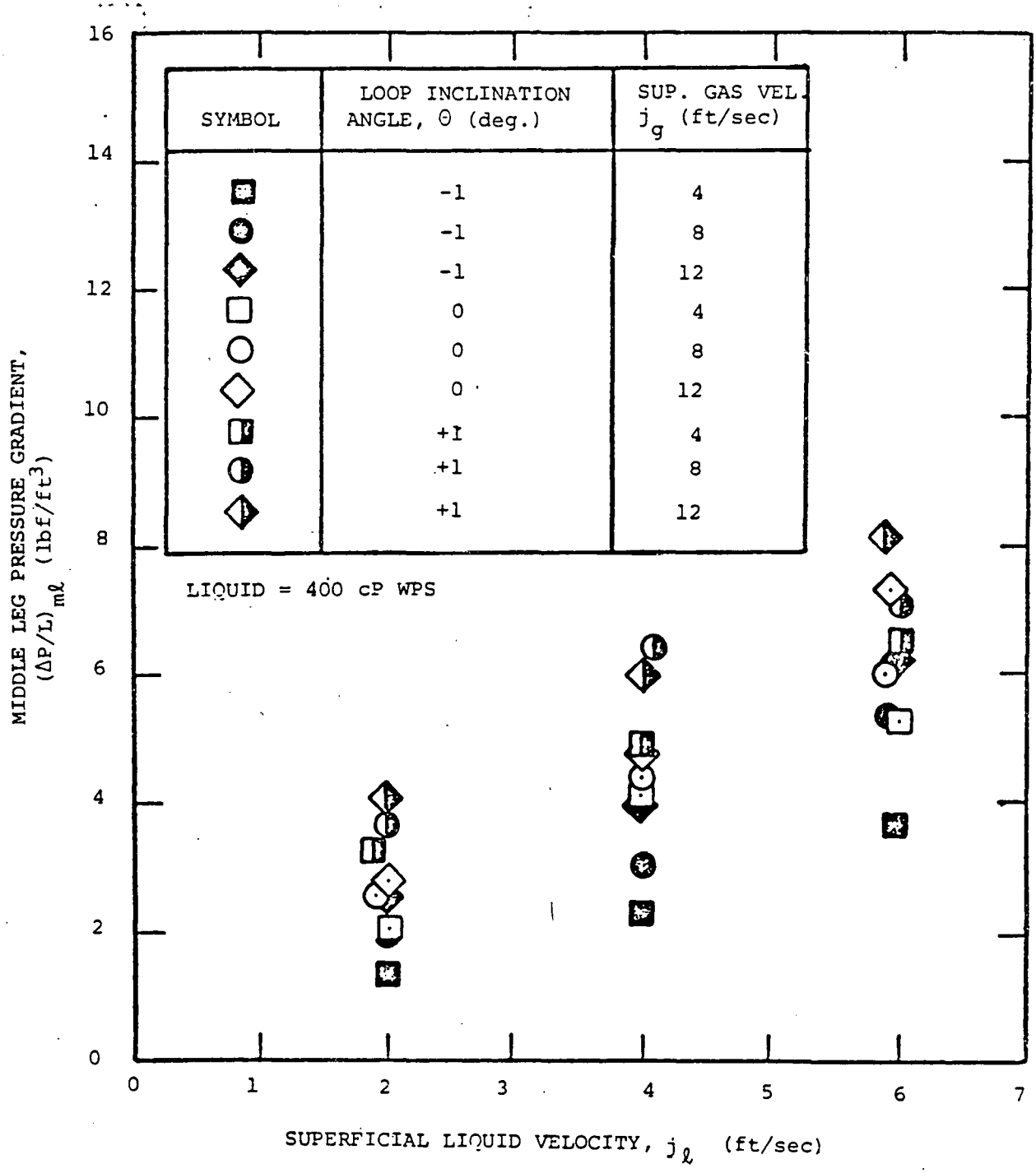

Figure 36. MIDDLE LEG PRESSURE GRADIENT DATA OBTAINED WITH 400 cP WPS

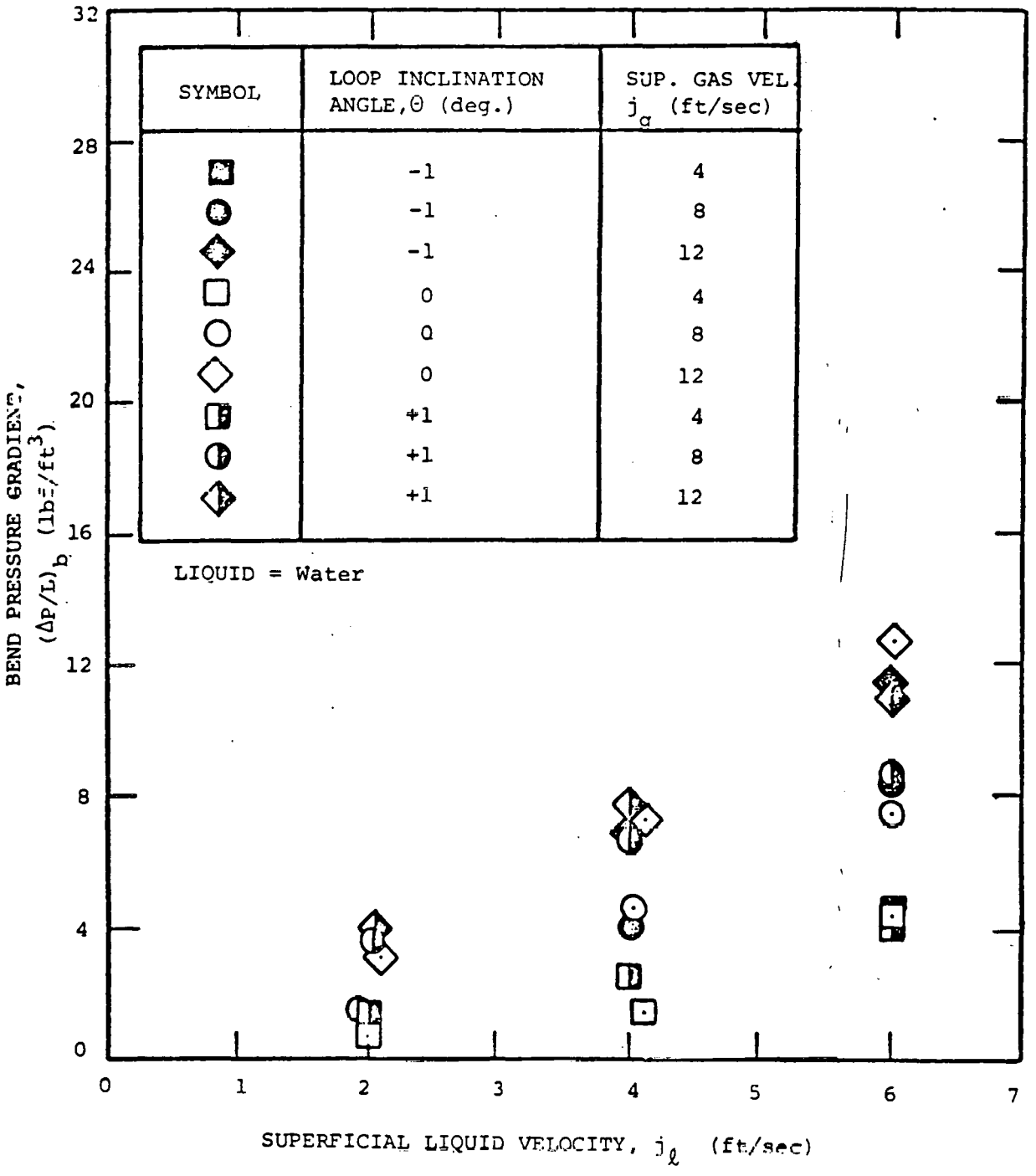

Figure 37. BEND PRESSURE GRADIENT DATA OBTAINED WITH WATER

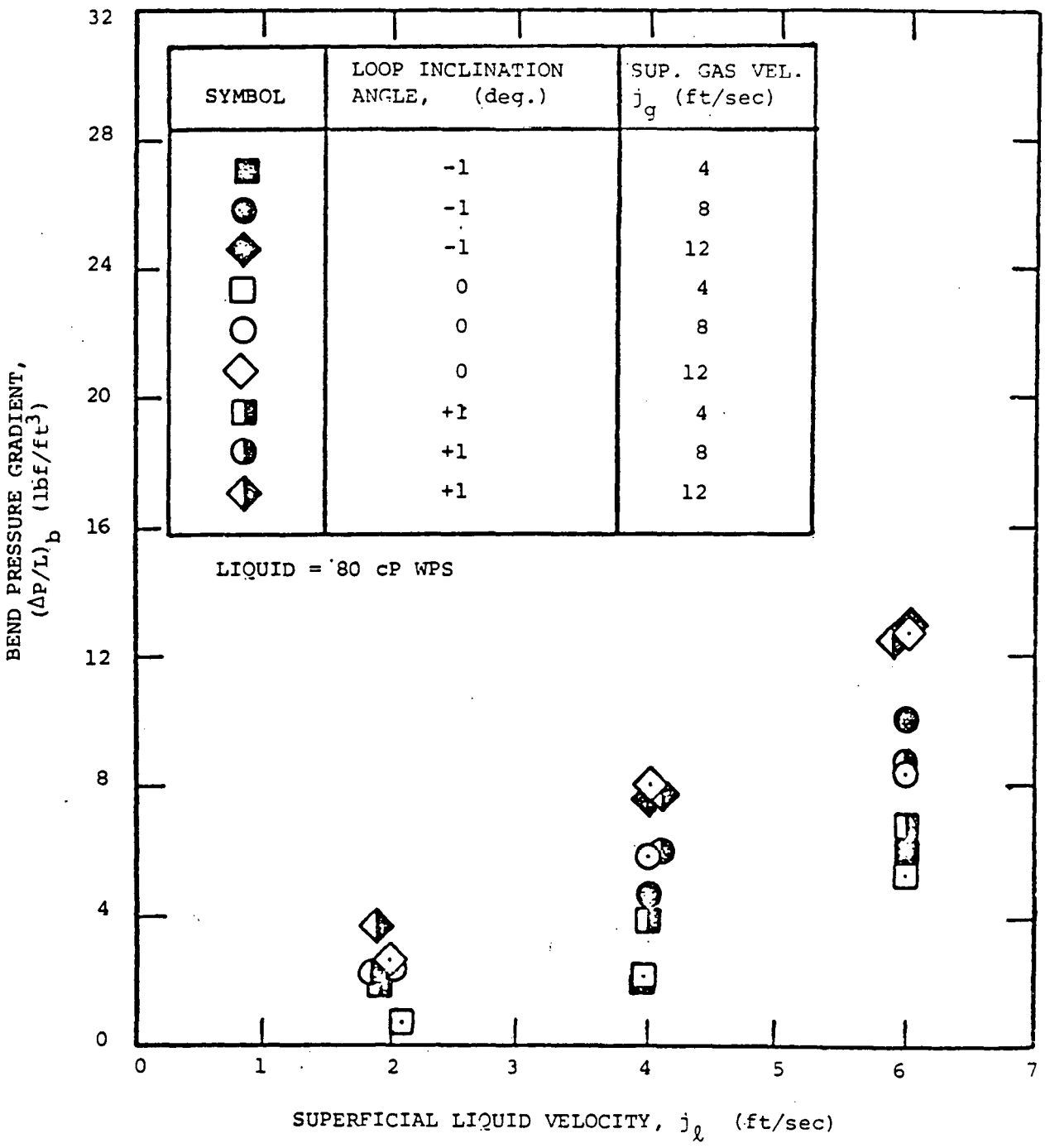

Figure 38. BEND PRESSURE GRADIENT DATA OBTAINED WITH 80 cP WPS

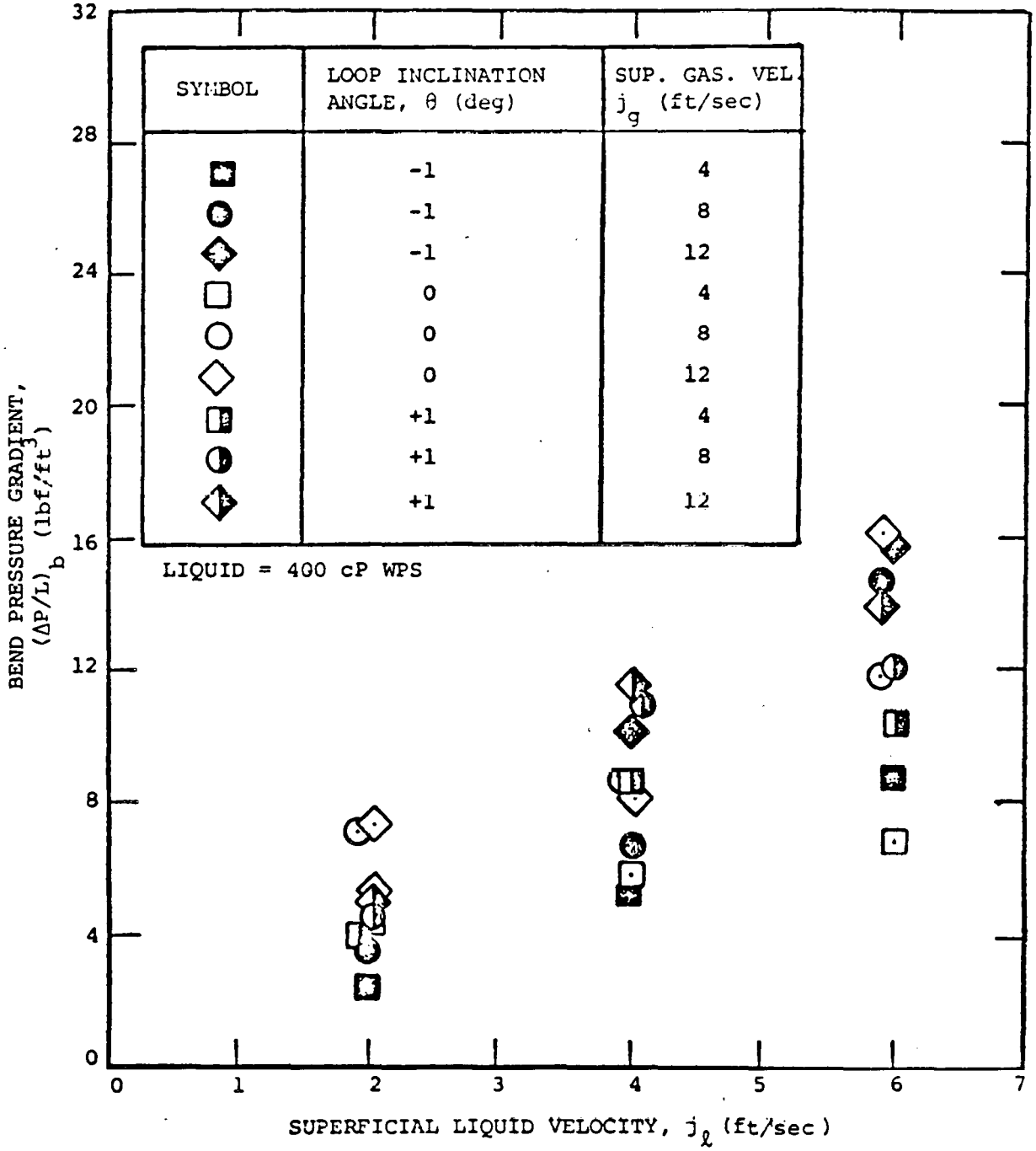

Figure 39. BEND PRESSURE GRADIENT DATA OBTAINED WITH 400 cP WPS

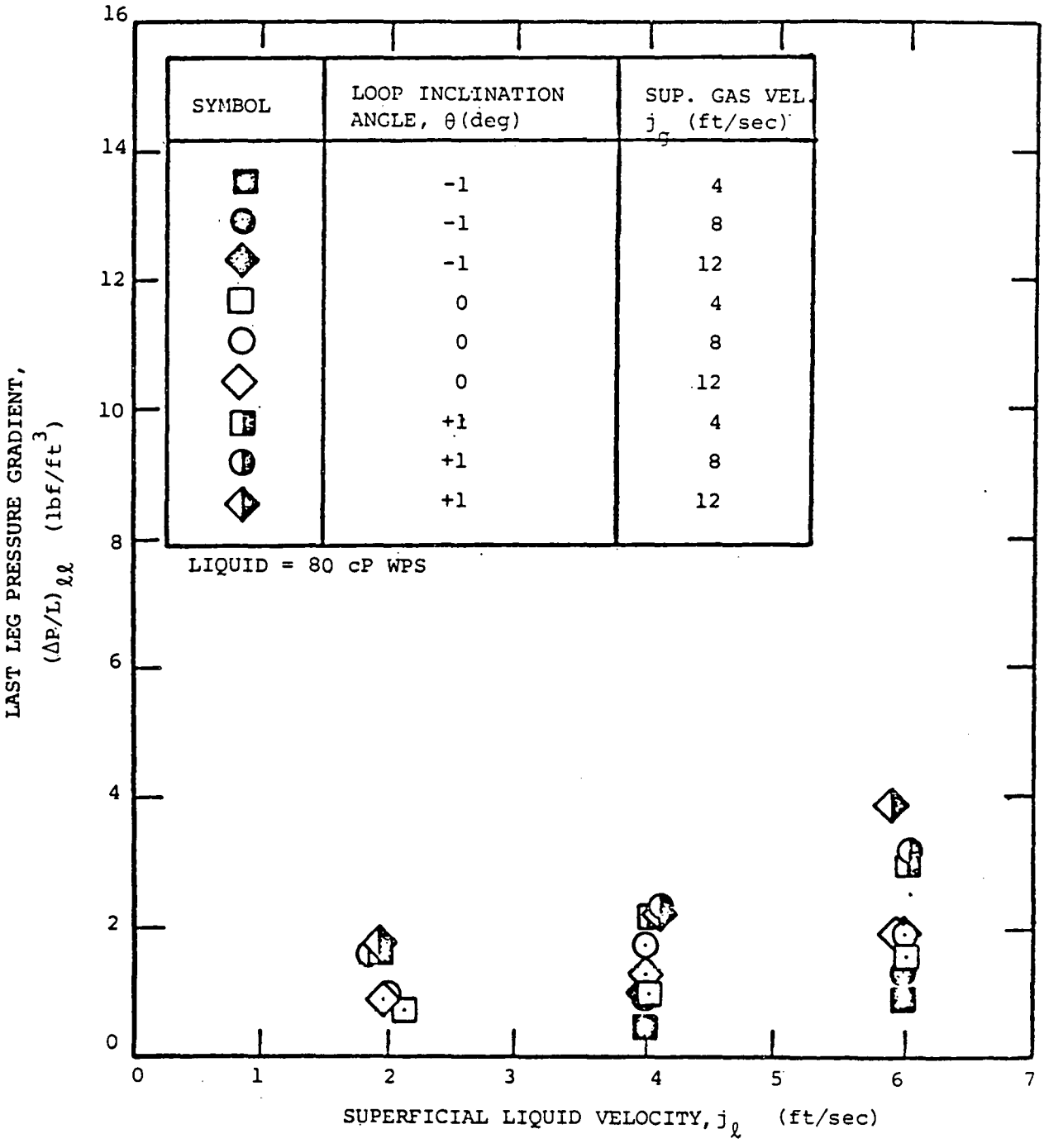

Figure 40. LAST LEG PRESSURE GRADIENT DATA OBTAINED WITH 80 cP WPS

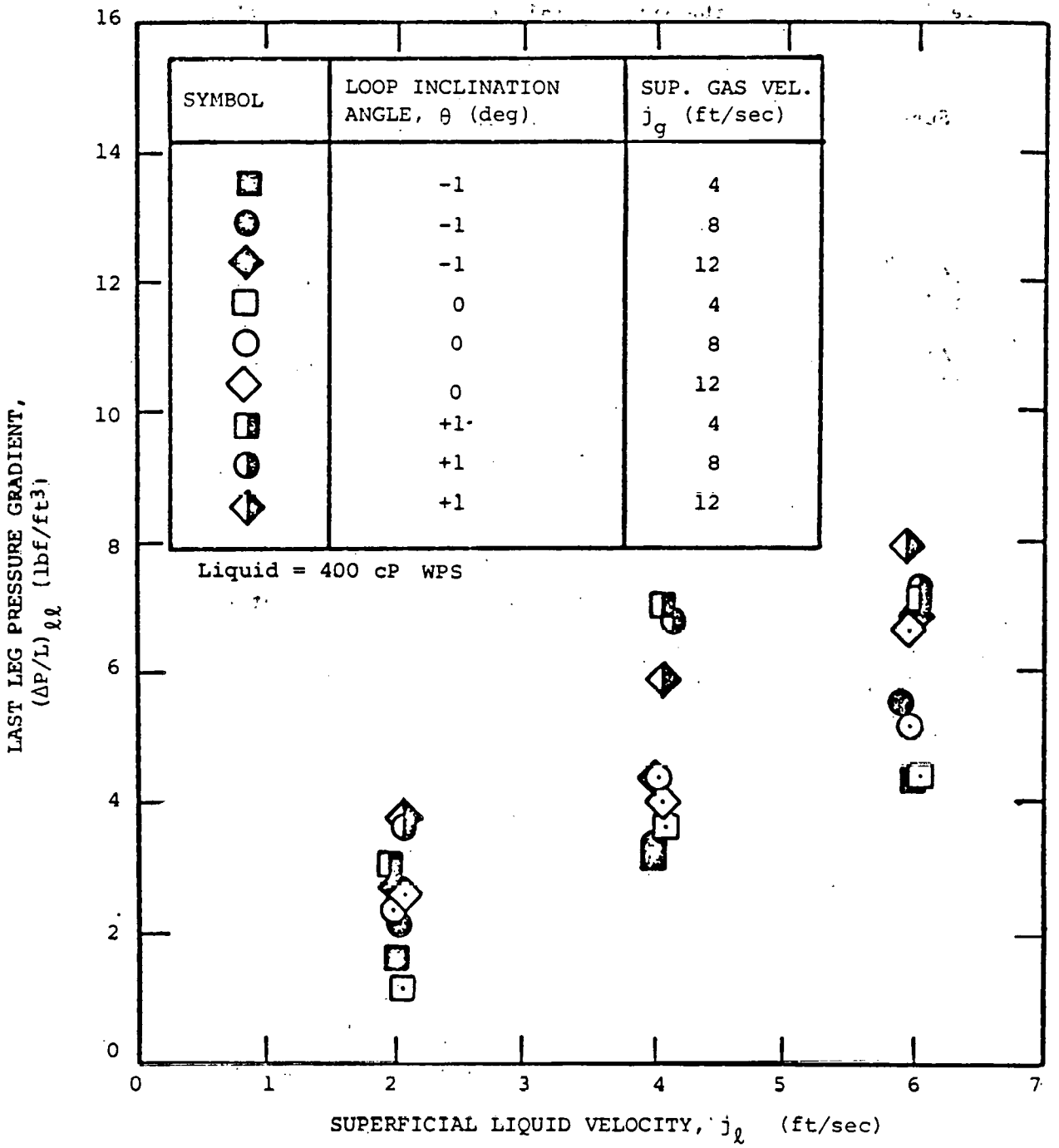

Figure 41. LAST LEG PRESSURE GRADIENT DATA OBTAINED WITH 400 cP WPS

The overall mass flux G is:

$$G = \rho_\ell j_\ell + \rho_g j_g \cong \rho_\ell j_\ell \tag{5}$$

while J is the sum of the superficial velocities of each phase:

$$J = j_\ell + j_g \tag{6}$$

Substituting Eq. 5 and Eq. 6 into Eq. 4 yields:

$$\frac{\Delta P}{L} = \frac{2f}{D} \rho_\ell j_\ell (j_\ell + j_g) \tag{7}$$

Therefore, if f is approximately constant, the pressure gradient can easily be related to the fluxes.

As shown in Figure 42, the Freon/water, middle leg pressure gradient data can be fit quite well by Eq. 7, namely:

$$\frac{\Delta P}{L} = 0.029\ j_\ell (j_\ell + j_g) \tag{8}$$

This implies f = 0.004 which is a reasonable value since a friction factor for turbulent flow can be correlated by $f = 0.046(Re_\ell)^{0.2}$ and Reynolds numbers are of the order 1×10^5 (based on the superficial velocity of the liquid phase in these experiments).

For the bend pressure gradient, a similar approach gives quite good correlation if 0.029 is replaced by 0.1, reflecting an increased friction coefficient because of the pipe curvature (see Figure 43).

For the 400 cP WPS, the Reynolds number is low so that the flow may be laminar. In laminar flow, the friction factor is given by:

$$f = \frac{16}{Re_\ell} = \frac{16\mu_m}{\rho_m D\ j_\ell} \tag{9}$$

substituting in Equation 7,

$$\frac{\Delta P}{L} = 32\mu_m J/D^2 \tag{10}$$

and the problem becomes how to determine the "effective viscosity" of the mixture, μ_m.

For single-phase liquid flow $\mu_m = \mu_\ell$ and Eq. 10 becomes

$$\frac{\Delta P}{L} = 0.85\ j_\ell \tag{11}$$

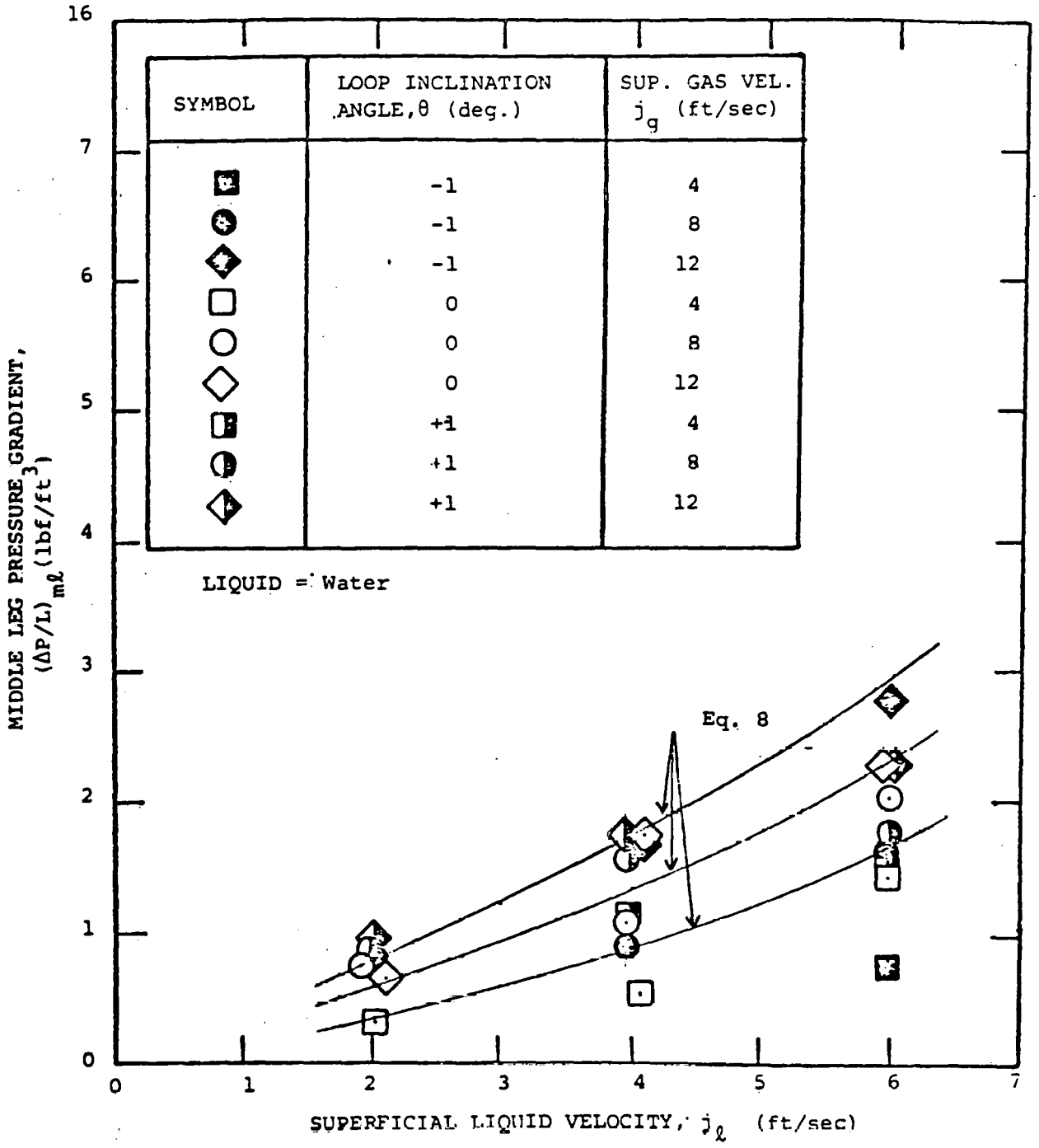

Figure 42. COMPARISON OF HOMOGENEOUS FLOW MODEL WITH MIDDLE LEG PRESSURE GRADIENT DATA WITH WATER

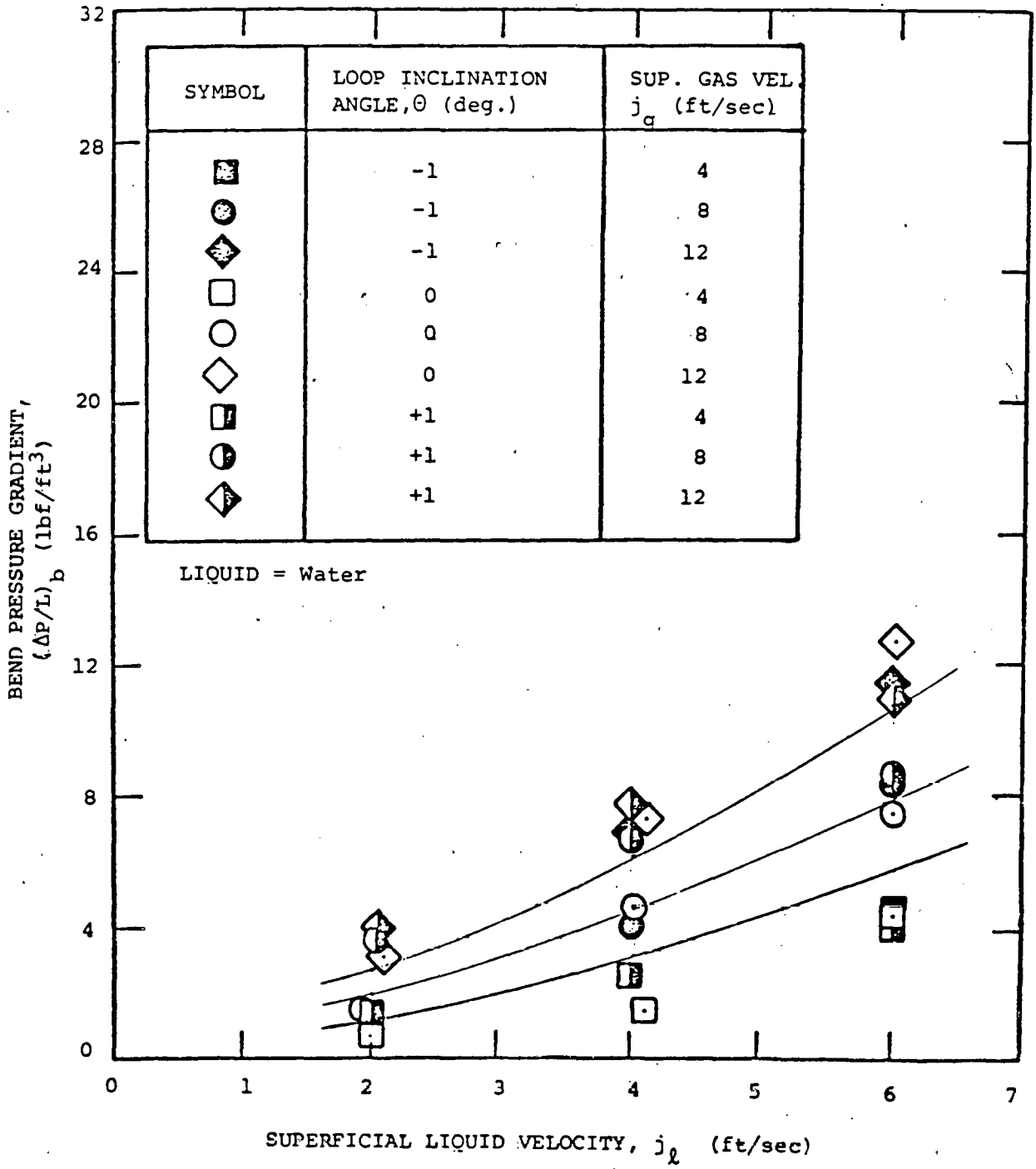

Figure 43. COMPARISON OF HOMOGENEOUS FLOW MODEL WITH BEND PRESSURE GRADIENT DATA WITH WATER

if the fluid is considered Newtonian with μ_ℓ = 400 cP. Eq. 11 fits the single-phase data previously reported [1] when the coefficient is increased to 0.95 to reflect the non-Newtonian characteristics of the fluid.

The two-phase pressure drop data obtained with the 400 cP WPS do not support Eq. 10, with μ_m postulated to be a function of j_g/j_ℓ. The middle leg pressure gradient are correlated quite well

$$\frac{\Delta P}{L} = 0.63\ j_\ell\ (1 + 0.066 j_g) \qquad (12)$$

as shown in Figure 44. This model reflects the linear dependence on j_ℓ with constant j_g as seen in the data. Since Eq. 12 results in a lower value than the observed single-phase pressure gradient when j_g is small (about 4 ft/sec or less) the apparent viscosity actually appears to be reduced by adding a small amount of gas. Since the "apparent viscosity" does not seem to be predictable from a simple physically-based theory, a mechanistic model for the slug flow regime should be developed. Some initial work along this line is described below.

Slug Flow

A mechanistic model for slug flows observed in the CFMTP would consider the following contributions to the pressure gradient:

- wall shear in the liquid slug,
- wall shear in the liquid carpet,
- wall shear in the gas bubble,
- interfacial shear between the gas bubble and the liquid carpet, and
- acceleration ("scooping up") of liquid from the carpet into the liquid slug.

Previous models developed by Shu [3], Vermeulen and Ryan [4], and Dukler and Hubbard [5] include terms for wall shear due to the liquid and the scooping up of liquid ahead of the slug. The wall shear in the gas bubble and the interfacial shear are typically neglected, i.e. the pressure drop in the gas bubble is neglected. Shu and Vermeulen and Ryan also assume the liquid carpet velocity is zero, leading to large values for the acceleration term. Evaluation of the CFMTP data via a material balance suggests that liquid carpet velocities may be significant. The model proposed by Dukler and Hubbard accounts for the carpet velocity, V_c, in the acceleration term. This acceleration term is:

$$\left.\frac{\Delta P}{\Delta L}\right|_{acc} = \frac{\rho_\ell\ E_\ell\ (J-V_c)\ (V_s-V_c)}{g(L_s + L_b)} \qquad (13)$$

and gives smaller values than the other models. This model reduces to the other models when the carpet velocity is zero.

Wallis suggests a model for wall shear in the liquid regions which may explain the apparent decrease in pressure drop with the addition of small amounts of gas. This model is discussed below.

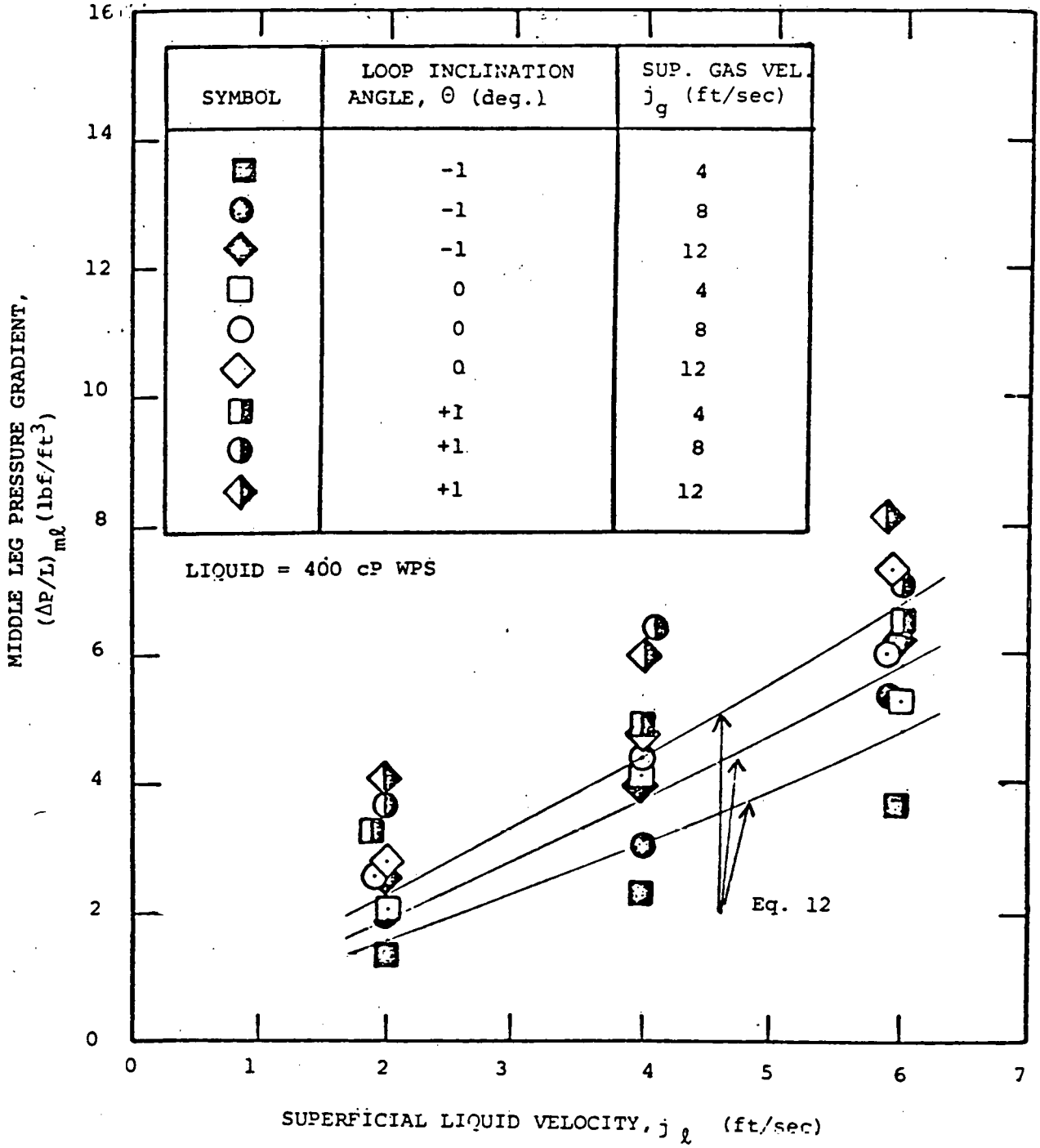

Figure 44. COMPARISON OF HOMOGENEOUS FLOW MODEL WITH MIDDLE LEG PRESSURE GRADIENT DATA WITH 400 cP WPS

In the classical view, horizontal slug flow (based on observations in small pipes) can be represented as a series of "unit cells" consisting of one large bubble and one liquid slug, as shown in Figure 45. The unit cell can be imagined to start and end at any equivalent point in the sequence. The bubble is at constant pressure, if its density and viscosity are low, and therefore the pressure drop occurs entirely in the liquid slug. If the slug is long enough, a fully-developed single-phase liquid velocity profile is developed. The pressure drop can therefore be computed for a series of single-phase liquid slugs with average speed $C_o J$ and an effective length that exceeds the slug length by an amount necessary to account for entrance effects at the nose and tail of adjacent slugs. For example, Wallis [2] suggests the following equation for the frictional pressure gradient:

$$\left.\frac{\Delta P}{\Delta L}\right|_f = \frac{2f}{D} j_\ell J \frac{L_s + 4D}{L_s + L_b} \tag{14}$$

For laminar flow, $f = 16/Re_\ell$ so Eq. 14 becomes:

$$\left.\frac{\Delta P}{\Delta L}\right|_f = \frac{32\mu_\ell}{D^2} J \left[\frac{L_s + 4D}{L_s + L_b}\right] \tag{15}$$

However, since L_s has been measured but not L_b, an indirect approach is necessary. The measured slug velocity appears to be represented quite well by Eq. 1

$$V_s = C_o J = C_o (j_\ell + j_g) \tag{1}$$

with $C_o \cong 1.4$ for water and 1.4 to 1.6 for the 400 cP WPS.

From Eq. 1, the void fraction is:

$$\alpha = j_g / V_s = j_g / (C_o J) \tag{16}$$

If the average fraction of the tube cross-section occupied by the liquid in the bubble is E_ℓ, the void fraction can also be expressed as

$$\alpha = \frac{L_b (1-E_\ell)}{L_b + L_s} \tag{17}$$

From Eq. 16 and 17,

$$\frac{L_s}{L_b + L_s} = 1 - \frac{j_g}{C_o J (1-E_\ell)} \tag{18}$$

Eq. 18 can be used in Eq. 15 to give an underestimate of the pressure gradient (since the influence of D is larger if slugs are shorter). Making this substitution,

$$\left.\frac{\Delta P}{\Delta L}\right|_f < \frac{32\mu_\ell}{D^2} \left[J - \frac{j_g}{C_o (1-E_\ell)}\right] \tag{19}$$

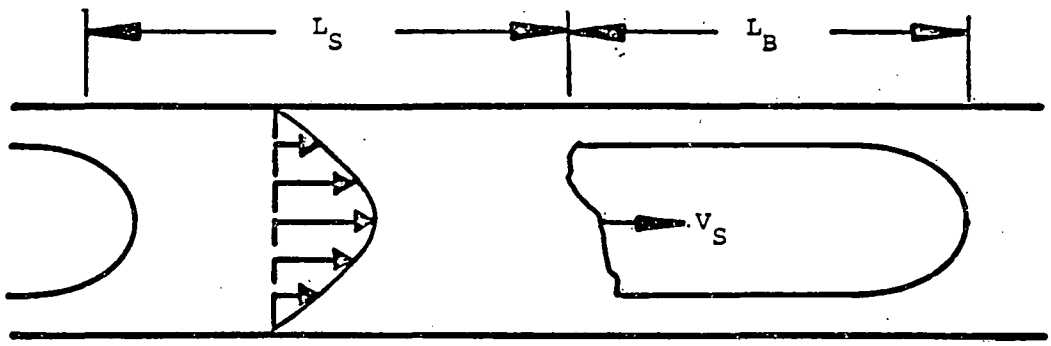

Figure 45. TYPICAL UNIT CELL

or expanding this equation with Eq. 6,

$$\left.\frac{\Delta P}{\Delta L}\right|_f < \frac{32\mu_\ell}{D^2}\left[j_\ell + j_g\left(1 - \frac{1}{C_o(1-E_\ell)}\right)\right] \qquad (20)$$

Depending on the values of C_o and E_ℓ, the effect of adding gas is to either increase or decrease the pressure gradient. For instance, with $C_o = 1.6$, $E_\ell = 0.5$

$$\left.\frac{\Delta P}{\Delta L}\right|_f = \frac{32\mu_\ell}{D^2}\left[j_\ell - 0.25\, j_g\right] \qquad (21)$$

which may explain, in part, how the pressure drop decreases when some gas is added.

If $C_o = 1.6$, $E_\ell = 0.7$ had been used, Eq. 21 would have become:

$$\left.\frac{\Delta P}{\Delta L}\right|_f = \frac{32\mu_\ell}{D^2}(j_\ell + 0.11\, j_g) \qquad (22)$$

If, in general, Eq. 21 is presented by

$$\left.\frac{\Delta P}{\Delta L}\right|_f = \frac{32\mu_\ell}{D^2}(j_\ell + Bj_g) \qquad (23)$$

which, in view of Eq. 11, for the 400 cP WPS gives

$$\left.\frac{\Delta P}{\Delta L}\right|_f = 0.85\,(j_\ell + Bj_g) \qquad (24)$$

the two-phase flow data fit a range

$$-0.25 < B < 0.2 \qquad (25)$$

suggesting that this form of empirical correlation to the theory may be useful to explain trends in the data.

In order to evaluate the friction and acceleration terms (Equations 20 and 13) additional information from each test, particularly the liquid fraction in the carpet, is needed to evaluate these terms. Future analysis efforts should include these data.

The models for the friction and acceleration terms are also somewhat idealized. Visual observations do not always indicate distinct slugs, but rather large waves that come close to the top of the pipe and sometimes appear to bridge it entirely. The interface between the carpet and the gas in the "bubbles" is quite wavy and there may be significant interfacial drag, influenced by the high gas density, which violates the assumption of constant pressure in the bubble. Future analysis efforts should also include evaluation of the interfacial shear terms, perhaps supported by experimental measurements.

REFERENCES

1. Sam, R.G., Patel, B.R. and Crowley, C.J.; COLD FLOW MODELLING TEST PROGRAM, FINAL REPORT; TN-358, Creare R&D Inc., July 1983.

2. Wallis, G. B.; ONE-DIMENSIONAL TWO-PHASE FLOW; New York, NY: McGraw-Hill, 1969, pg. 303.

3. Shu, M. T.; HORIZONTAL TWO-PHASE FLOW OF GASES AND NON-NEWTONIAN LIQUIDS; Drexel University; October 1981.

4. Vermeulen, L. R. and Ryan, J.T.; TWO-PHASE SLUG FLOW IN HORIZONTAL AND INCLINED TUBES; The Canadian J. of Chem. Eng.; Vol 49, April 1971, pg. 195-201.

5. Dukler, A.E., and Hubbard, M. G.; A MODEL FOR GAS-LIQUID SLUG FLOW IN HORIZONTAL AND NEAR HORIZONTAL TUBES; Ind. Eng. Chem., Fundam, Vol. 14, No. 4, 1975, pg. 337-347.

APPENDIX A

Mixing and Downslope Configuration Experiment

Data Tables

Test Numbering Convention:

8 Character Name: 1 2 34 5 678

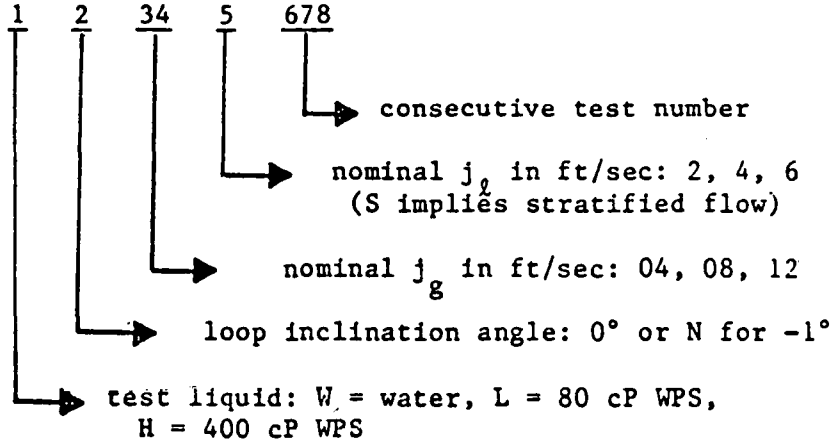

TABLE A-1
SINGLE-PHASE FLOW MIXING RESULTS

TEST LIQUID	LOOP FLOW VEL., V(ft/sec)	MEASURED CONCENTRATION, X(%) LOCATION, H/D			FULLY MIXED CALCULATED CONCENTRATION, X_T (%)
		0	0.5	1.0	
Water	2	5.92	1.59	0	3.29
	4	2.03	0.48	0.03	1.46
	6	1.67	0.73	0.24	1.06
400 cP WPS	2	15.60	0.22	0.25	3.08
	4	7.16	0.71	0.41	2.81
	6	2.99	0.31	0	0.70

TABLE A-2
TWO-PHASE FLOW MIXING RESULTS

TEST LIQUID	TEST NUMBER	MEASURED CONCENTRATION, X(%) LOCATION, H/D			FULLY MIXED CALCULATED CONCENTRATION, X_T (%)
		0	0.5	1.0	
Water	W0046096	2.06	1.56	0.70	1.26
	W0044097	2.36	1.91	1.59	1.77
	W0042098	3.59	0.05	ns	3.33
	W0082099	2.55	1.73	ns	3.24
	W0084100	0.97	0.82	0.46	1.29
	W0086101	0.89	0.66	0.50	1.18
	W0126102,1*	1.09	0.85	0.57	1.14
	W0126102,2*	0.93	0.71	ns	1.27
	W0126102,3*	1.27	0.88	ns	1.17
	W0126102,C	1.00	-	-	1.49
	W0124103	1.38	0.98	ns	1.57
	W0122104	1.48	1.27	ns	3.06
400 cP WPS	H0126105	0.47	0.51	0.20	1.00
	H0126105,C	2.20	-	-	2.36
	H0086106	0.95	0.86	0.92	1.68
	H0086106,C	2.25	-	-	1.89
	H0044107	4.60	1.06	0.44	2.00
	H0044107,C	2.26	-	-	3.67
	H0046108	4.01	0.38	0.20	0.63
	H0046108,C	2.11	-	-	1.43
	H0084109	1.62	0.07	0.16	1.73
	H0084109,C	2.57	-	-	1.75
	H0124110	1.15	0.36	0.33	1.73
	H0124110,C	1.54	-	-	1.69
	H0042111	8.38	0.08	0	2.53
	H0042111,C	5.77	-	-	3.57
	H0082112	3.61	1.11	1.24	2.66
	H0082112,C	4.89	-	-	2.04
	H0122113	3.77	2.31	ns	3.98
	H0122113,C	12.49	-	-	3.09

* 1,2,3 are repeatability tests
C designates carpet measurement test
ns implies no sample could be obtained

TABLE A-3 SUMMARY OF SLUG CHARACTERISTIC DATA

TEST NO:	SLUG VELOCITY V_s (ft/sec)	SLUG FREQUENCY f_s (1/sec)	AVE. SLUG LENGTH L_{sa} (ft)	INDIVIDUAL SLUG LENGTHS L_s (ft)
WN084118	16.0	0.21	2.4	1.0, 4.5, 1.3, 1.3, 3.2, 1.3, 2.7, 3.5, 4.3, 2.4, 1.9, 2.2, 1.9
WN086119	19.2	0.61	2.4	3.7, 1.5, 3.7, 3.1, 4.2, 2.1, 5.0, 4.0, 1.0, 2.5, 1.5, 1.2, 1.0, 1.2, 1.5, 2.7, 2.5, 1.0, 2.3, 2.7, 2.1, 3.7, 2.9, 2.5, 2.3, 4.2, 1.3, 1.7, 3.3, 1.7, 1.2, 2.5, 1.5, 1.5, 3.1, 1.2, 3.3
WN126120	23.8	0.30	1.6	2.9, 2.9, 1.0, 1.2, 1.9, 1.0, 1.0, 1.9, 1.7, 1.9, 1.2, 3.8, 1.0, 1.0, 1.0, 1.0, 1.4, 1.2
WN124121	22.0	0.11	2.2	3.3, 1.1, 1.8, 2.4, 1.1, 4.6, 1.1
WN046122	15.2	0.62	2.9	2.7, 2.4, 2.4, 2.3, 2.1, 3.5, 5.8, 4.7, 2.1, 2.4, 2.6, 3.6, 4.3, 2.1, 4.1, 2.7, 1.8, 1.3, 2.4, 2.0, 2.7, 2.3, 2.4, 2.4, 1.5, 2.7, 2.6, 3.8, 2.9, 2.6, 3.0, 1.8, 8.7, 2.3, 2.1, 4.9, 2.4, 2.1
LN086128	20.5	0.70	3.4	2.5, 2.3, 4.5, 2.0, 7.6, 4.9, 2.9, 5.5, 5.3, 2.0, 3.5, 2.5, 1.0, 6.1, 3.1, 1.4, 2.5, 1.2, 1.6, 7.6, 1.6, 4.5, 1.6, 1.8, 3.1, 2.3, 3.1, 2.3, 6.8, 1.2, 5.7, 4.9, 3.3, 1.8, 4.9, 2.5, 5.9, 1.2, 7.4, 2.7, 3.9, 2.9, 1.4
LN084129	15.2	0.26	2.7	4.4, 1.1, 1.2, 5.3, 1.7, 2.3, 1.2, 3.0, 2.0, 1.7, 1.1, 2.6, 4.7, 2.4, 1.7, 6.8
LN124130	18.9	0.21	1.8	2.3, 1.7, 1.1, 1.3, 2.8, 1.1, 1.5, 1.1, 3.0, 1.1, 2.1, 1.3, 2.3
LN126131	22.7	0.25	2.0	1.1, 3.2, 3.4, 2.3, 3.9, 2.3, 1.8, 2.7, 1.4, 1.1, 1.1, 1.6, 1.8, 1.8, 1.1
LN044132	12.2	0.34	4.3	13.4, 5.9, 4.3, 1.3, 7.6, 1.3, 2.0, 1.6, 3.2, 2.4, 2.6, 6.8, 5.6, 5.6, 2.7, 6.0, 3.4, 1.1, 5.1, 6.8, 2.4
LN046133	16.4	0.79	7.8	3.3, 9.2, 3.4, 3.6, 11.6, 6.2, 3.4, 7.4, 9.2, 9.0, 11.0, 3.1, 4.3, 8.2, 8.7, 10.8, 6.7, 3.6, 14.8, 13.6, 9.8, 9.7, 8.4, 10.3, 7.7, 3.3, 8.4, 4.4, 14.6, 13.3, 8.2, 2.8, 11.5, 13.8, 7.2, 3.8, 8.7, 14.6, 11.8, 11.0, 3.8, 6.4, 6.9, 4.8, 5.9, 3.8, 5.1, 5.1
HN042137	8.0	0.36	4.8	4.5, 7.6, 5.3, 5.9, 5.2, 3.6, 2.8, 5.2, 4.4, 7.0, 5.9, 6.2, 6.7, 1.5, 5.4, 6.0, 6.9, 1.2, 1.7, 6.8, 4.9, 1.6
HN082138	13.5	0.30	2.9	1.5, 3.0, 5.0, 3.0, 3.4, 1.6, 3.5, 2.7, 2.3, 3.2, 2.0, 2.0, 2.6, 1.0, 1.3, 1.9, 6.7, 5.7
HN122139	19.7	0.05	1.5	2.2, 1.4, 1.0
HN124140	22.7	0.18	2.5	1.6, 1.4, 5.5, 2.0, 1.8, 1.8, 1.6, 3.0, 2.5, 1.6, 5.2
HN084141	19.2	0.56	3.6	3.0, 8.0, 3.2, 4.2, 3.5, 2.0, 2.5, 4.0, 1.0, 1.7, 1.0, 5.3, 2.3, 2.7, 1.5, 1.7, 7.0, 1.8, 4.2, 7.0, 3.5, 1.8, 3.2, 4.8, 6.2, 1.3, 4.3, 7.3, 2.0, 1.5, 6.0, 3.0, 7.2, 1.0
HN044142	12.3	0.38	11.3	9.2, 10.2, 9.1, 16.6, 13.8, 9.2, 6.0, 13.0, 12.5, 12.8, 17.0, 13.0, 7.5, 7.0, 9.6, 12.8, 11.2, 17.5, 11.8, 9.7, 10.1, 9.1, 10.9
HN046143	INSTRUMENT FAILURE			
HN086144	21.6	0.74	3.3	5.2, 3.0, 2.2, 1.9, 3.7, 2.4, 4.1, 3.9, 3.2, 1.7, 4.3, 3.0, 2.6, 3.0, 1.1, 1.7, 2.2, 2.2, 3.2, 5.2, 6.5, 3.5, 2.2, 2.4, 3.2, 3.2, 6.1, 3.5, 8.0, 2.2, 4.1, 2.6, 2.2, 2.8, 3.7, 4.3, 7.1, 1.7, 2.6, 3.7, 1.1, 3.0, 5.2, 1.3, 3.9
HN126145	27.2	0.31	1.8	2.2, 2.4, 1.6, 1.9, 1.4, 1.6, 1.6, 1.4, 1.1, 3.8, 1.6, 2.4, 2.2, 1.6, 1.6, 1.4, 1.1, 2.2, 1.1

TABLE A-4
SUMMARY OF TRANSITION VELOCITIES

LIQUID	SUPERFICIAL GAS VEL., j_g (ft/sec)	SUPERFICIAL LIQUID VEL. AT TRANSITION, $j_{\ell t}$ (ft/sec)
Water	4.0	4.9
	8.0	3.4
	11.9	2.8
	6.0	4.0
	10.0	3.2
80 cP WPS	4.0	3.6
	8.1	2.7
	11.9	2.1
	6.0	3.1
	10.0	2.3
400 cP WPS	4.1	1.2
	7.8	1.5
	12.0	1.7

TABLE A-5
PRESSURE GRADIENT DATA FOR -1° DOWNSLOPE LOOP CONFIGURATION

TEST NUMBER	SUP. GAS VEL. j_g (ft/sec)	SUP. LIQ. VEL. j_ℓ (ft/sec)	PRESSURE GRADIENT, $\Delta P/L$ (lbf/ft^3)		
			Middle Leg	Bend	Last Leg
WN12S116	11.9	2.8	0.95	4.29	↑
WN046117	4.1	6.0	0.77	4.67	↑
WN084118	8.1	4.0	0.90	4.13	Instrument
WN086119	8.0	6.0	1.67	8.64	Failure
WN126120	11.5	6.0	2.84	11.81	↓
WN124121	11.8	4.0	1.81	7.08	↓
LN04S123	4.0	3.6	0.35	1.39	0.15
LN08S124	8.1	2.7	0.65	2.03	0.36
LN12S125	11.9	2.1	0.92	3.43	0.57
LN044126	4.1	4.0	0.58	2.03	0.36
LN046127	4.1	6.0	1.59	6.12	0.87
LN086128	8.0	6.0	2.76	10.31	1.33
LN084129	8.2	4.0	1.44	4.72	0.87
LN124130	11.8	4.0	2.20	7.73	0.91
LN126131	11.5	6.0	3.85	13.31	1.88
HN04S134	4.1	1.2	0.54	0.75	0.53
HN08S135	7.8	1.5	1.52	2.46	1.71
HN12S136	12.0	1.7	2.31	4.56	2.52
HN042137	4.0	2.0	1.29	2.36	1.59
HN082138	8.0	2.0	1.97	3.32	2.10
HN122139	11.9	2.0	2.50	5.26	2.73
HN124140	11.4	4.0	4.01	10.31	4.42
HN084141	8.1	4.0	3.06	6.76	3.37
HN044142	4.1	4.0	2.31	5.26	3.20
HN046143	4.0	6.0	3.67	8.91	4.42
HN086144	8.1	5.9	5.47	15.03	5.61
HN126145	10.9	6.0	6.34	16.00	7.03

APPENDIX B

Comparison of Slug Characteristic Data Obtained From Movies and Liquid Level Indicators

TABLE B-1

NEW SLUG CHARACTERISTIC DATA OBTAINED WITH THE LIQUID LEVEL PROBES AND THE HORIZONTAL LOOP CONFIGURATION

Test Liquid	Test Number	Slug Velocity V_s (ft/sec)	Slug Frequency f_s (1/sec)	Ave. Slug Length L_{ss} (ft)	Individual Slug Lengths L_s (ft)
Water	W0046096	13.8	1.02	4.1	8.3, 2.4, 2.1, 4.0, 3.7, 4.7, 3.9, 6.8, 5.0, 8.0, 4.2, 1.1, 1.1, 3.7, 1.5, 5.8, 4.0, 1.7, 1.5, 3.0, 4.8, 2.1, 3.5, 2.9, 6.1, 4.6, 4.0, 3.9, 6.4, 5.4, 4.6, 4.4, 3.2, 8.0, 1.9, 4.8, 1.2, 1.5, 2.4, 4.7, 5.1, 1.2, 4.8, 3.6, 6.0, 3.3, 6.1, 5.5, 1.5, 4.7, 1.9, 9.0, 2.9, 4.3, 4.2, 6.4, 1.1, 3.3, 7.1, 7.9, 4.3, 2.4
	W0044097	11.7	0.46	4.0	3.1, 1.9, 3.6, 2.6, 3.6, 5.1, 2.8, 5.1, 2.6, 3.3, 4.2, 4.8, 1.0, 4.7, 4.8, 3.0, 4.4, 3.7, 5.6, 6.6, 5.5, 3.5, 5.5, 2.2, 4.5, 5.6, 4.9, 4.2
	W0042098	8.6	0.11	1.5	2.0, 1.3, 1.0, 1.2, 1.3, 1.2, 2.4
	W0082099	12.7	0.05	1.8	1.9, 2.5, 1.0
	W0084100	16.5	0.43	3.6	4.1, 3.1, 4.4, 4.6, 7.6, 3.6, 1.3, 4.3, 1.3, 4.9, 2.3, 2.8, 2.5, 1.8, 1.8, 3.0, 3.5, 2.3, 4.9, 3.5, 7.9, 1.0, 4.3, 4.9, 6.7, 1.6
	W0086101	19.6	0.80	3.6	2.0, 2.2, 4.1, 3.8, 3.7, 3.1, 4.1, 2.0, 3.9, 4.3, 4.1, 3.5, 5.9, 4.5, 5.9, 2.2, 3.5, 2.2, 1.6, 5.3, 2.0, 2.3, 4.3, 2.0, 5.0, 4.1, 4.5, 3.9, 2.0, 6.3, 1.7, 2.5, 1.6, 5.1, 4.9, 5.1, 1.6, 5.9, 4.5, 2.0, 3.7, 2.3, 2.5, 4.1, 3.7, 4.5, 2.0, 4.9, 5.9
	W0126102	24.4	0.54	2.1	1.5, 3.9, 2.2, 1.7, 2.4, 1.0, 1.5, 1.0, 2.7, 2.2, 3.9, 1.9, 1.0, 2.2, 1.9, 2.2, 2.7, 1.9, 1.0, 1.5, 1.9, 1.9, 1.0, 2.9, 1.2, 6.3, 2.4, 1.0, 1.2, 1.0, 1.5, 2.7, 2.4
	W0124103	23.1	0.25	2.4	3.0, 3.0, 2.8, 2.5, 2.3, 2.8, 1.4, 1.8, 4.4, 1.6, 2.3, 1.4, 3.2, 1.2, 2.3
	W0122104	15.8	0.02	1.4	1.4
400 cP WPS	H0126105	27.9	0.72	8.1	9.2, 8.6, 1.4, 11.7, 5.9, 6.1, 2.5, 10.0, 5.6, 8.6, 9.8, 9.5, 7.3, 8.1, 4.5, 8.6, 8.6, 12.6, 10.3, 3.6, 9.5, 6.1, 10.6, 3.9, 15.9, 10.0, 10.6, 10.0, 2.2, 8.4, 13.4, 4.2, 8.9, 3.6, 12.3, 11.7, 5.0, 8.1, 9.5, 9.2, 3.9, 5.0, 10.9, 8.9
	H0086106	21.8	0.51	9.2	7.2, 7.8, 8.5, 8.3, 3.9, 9.6, 10.0, 5.5, 6.8, 8.7, 12.0, 7.0, 12.6, 5.2, 10.5, 10.5, 5.2, 9.6, 8.3, 8.7, 7.4, 9.8, 6.5, 7.0, 18.1, 16.4, 5.2, 8.5, 18.3, 7.0, 14.8
	H0044107	Instrument Failure			
	H0046108	Instrument Failure			
	H0084109	18.8	0.48	7.6	7.5, 7.5, 6.8, 8.3, 6.8, 8.6, 3.4, 11.7, 7.3, 2.1, 11.5, 1.1, 6.4, 6.6, 7.5, 6.8, 9.0 8.3, 10.2, 10.9, 10.3, 6.6, 7.3, 10.9, 3.2, 10.0, 8.1, 7.7, 7.1
	H0124110	25.4	0.52	7.0	7.9, 6.6, 1.8, 7.9, 9.7, 4.1, 7.9, 8.9, 2.3, 6.1, 10.4, 1.5, 8.1, 10.2, 9.1, 2.5, 11.2, 9.7, 7.6, 5.6, 2.8, 12.7, 3.0, 11.7, 5.3, 7.9, 7.1, 9.9, 5.6, 7.9, 4.3, 6.6
	H0042111	11.2	0.36	6.7	9.1, 4.6, 4.0, 3.6, 5.8, 8.1, 9.5, 8.3, 5.2, 7.2, 7.7, 2.2, 4.0, 8.3, 3.6, 9.4, 6.6, 4.3, 10.5, 10.5, 10.4, 5.2
	H0082112	14.4	0.30	5.7	4.6, 4.6, 1.4, 6.2, 8.1, 5.9, 3.5, 6.6, 4.8, 6.0, 3.9, 3.7, 7.9, 10.2, 7.8, 3.0, 7.9, 7.2
	H0122113	21.6	0.33	3.6	1.7, 3.5, 6.9, 3.0, 1.7, 3.2, 3.7, 5.6, 2.2, 3.7, 3.2, 3.0, 2.4, 8.4, 6.3, 2.6, 6.5, 1.1, 1.1, 1.5

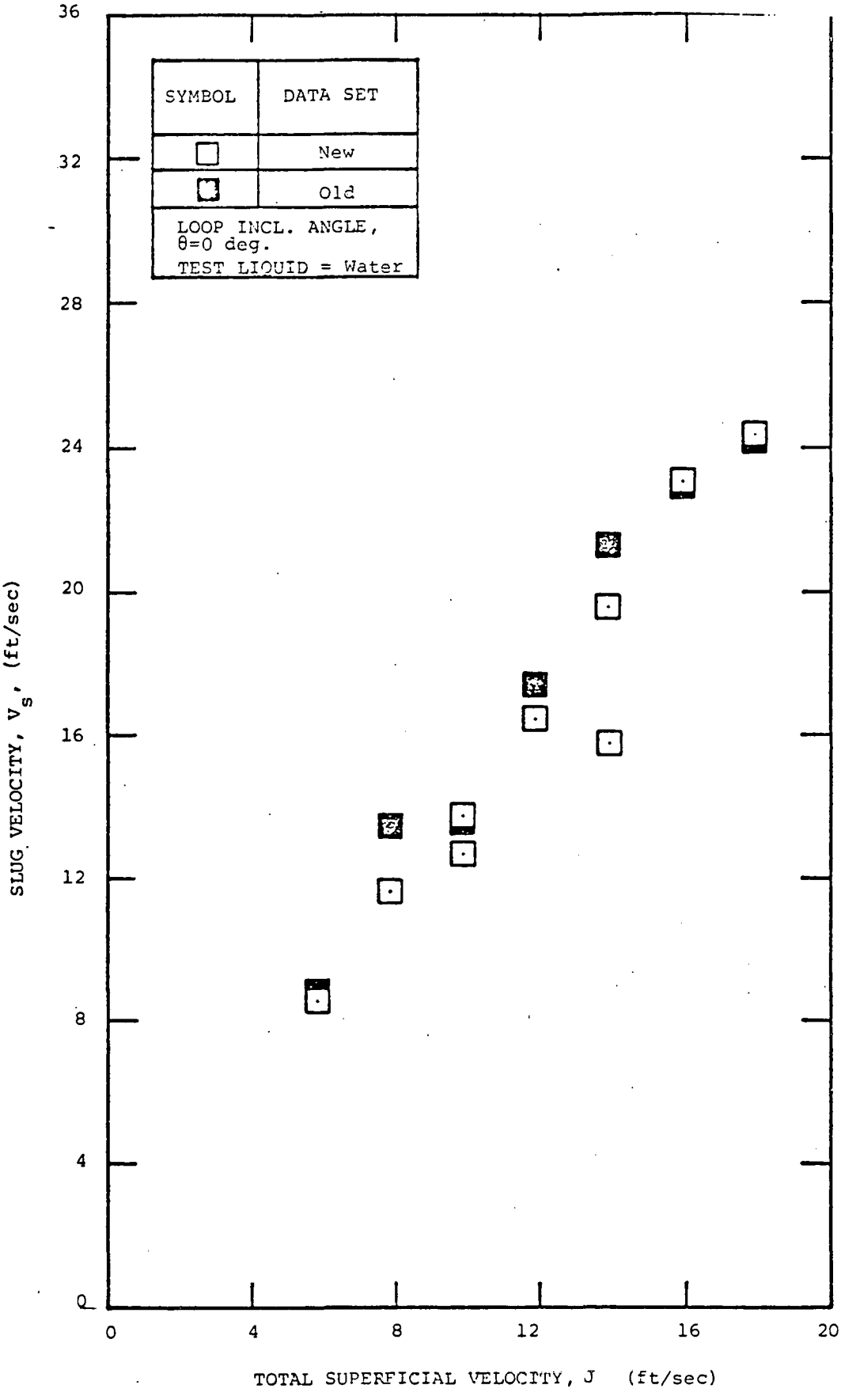

Figure B-1. SLUG VELOCITY DATA OBTAINED WITH WATER AS A FUNCTION OF TOTAL SUPERFICIAL VELOCITY

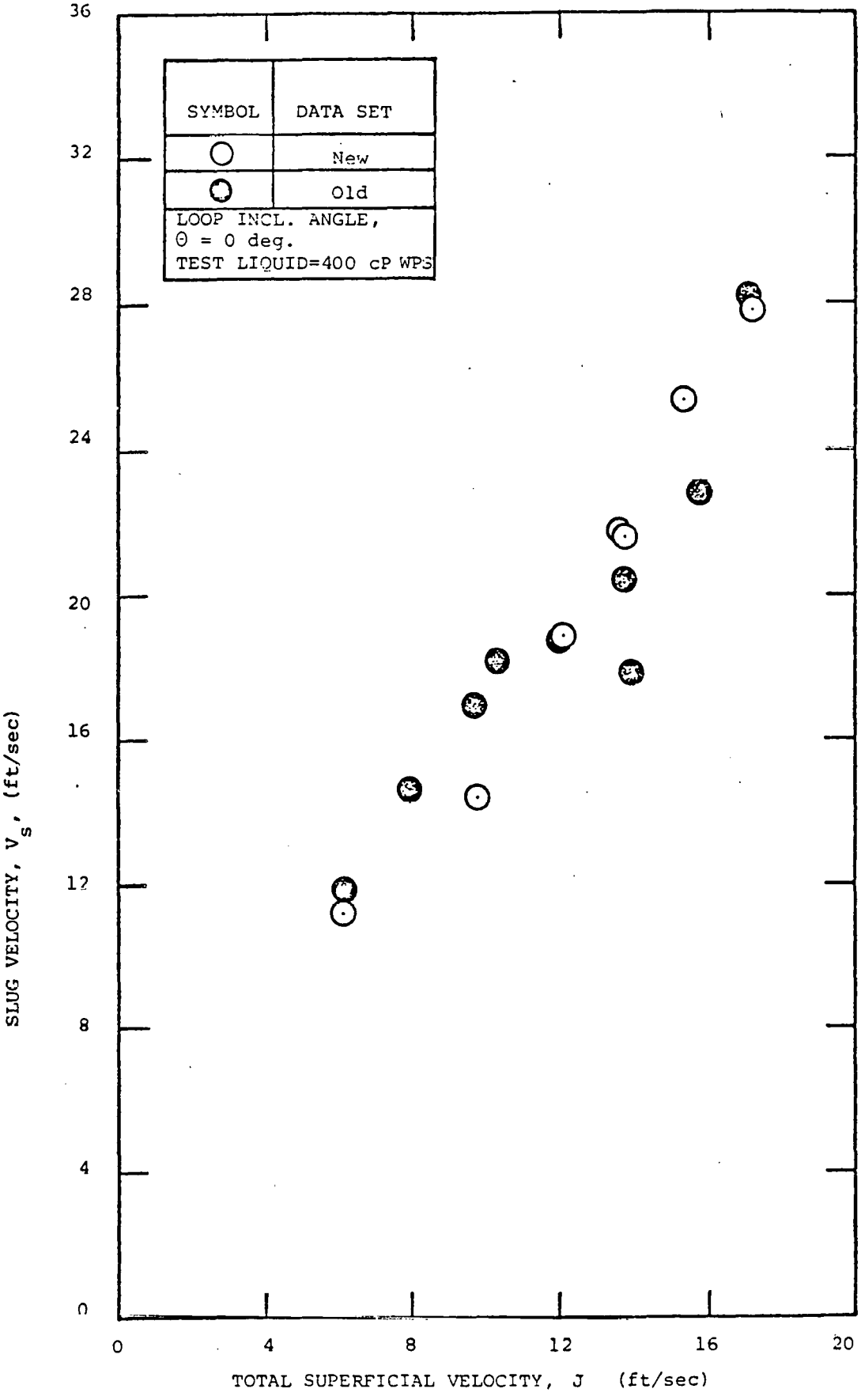

Figure B-2. SLUG VELOCITY DATA OBTAINED WITH 400 cP WPS AS A FUNCTION OF TOTAL SUPERFICIAL VELOCITY

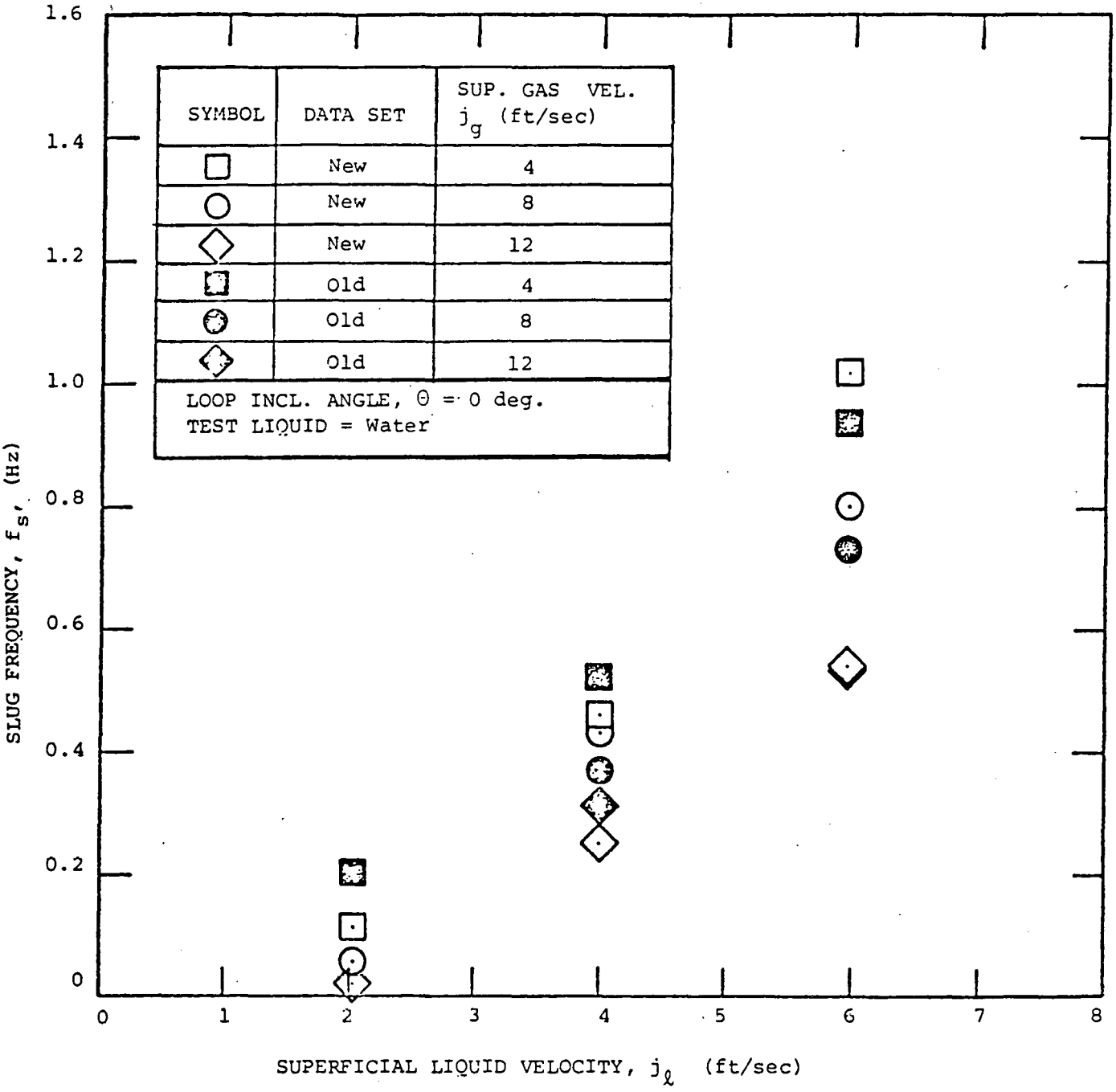

Figure B-3. SLUG FREQUENCY DATA OBTAINED WITH WATER

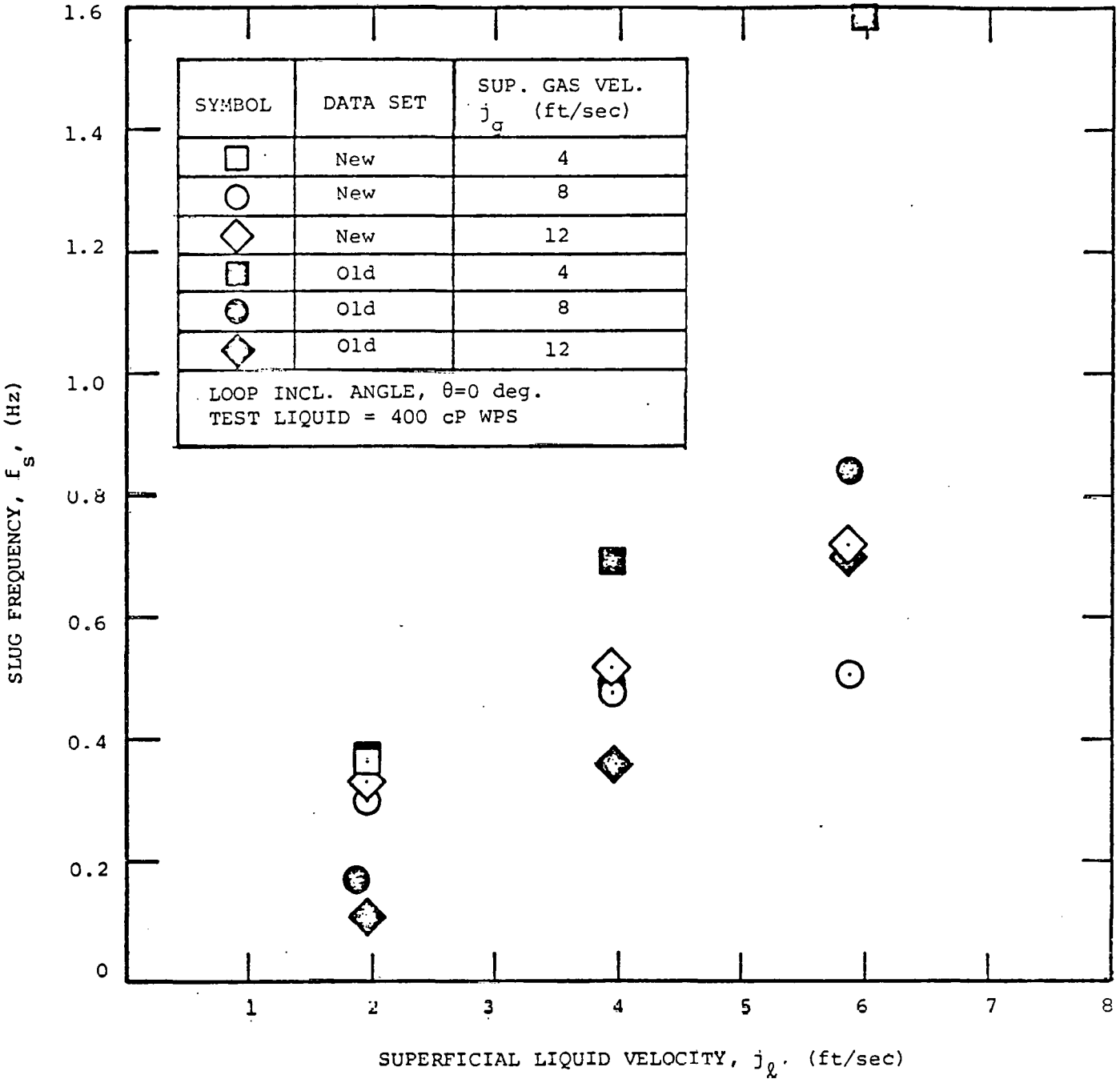

Figure B-4. SLUG FREQUENCY DATA OBTAINED WITH 400 cP WPS

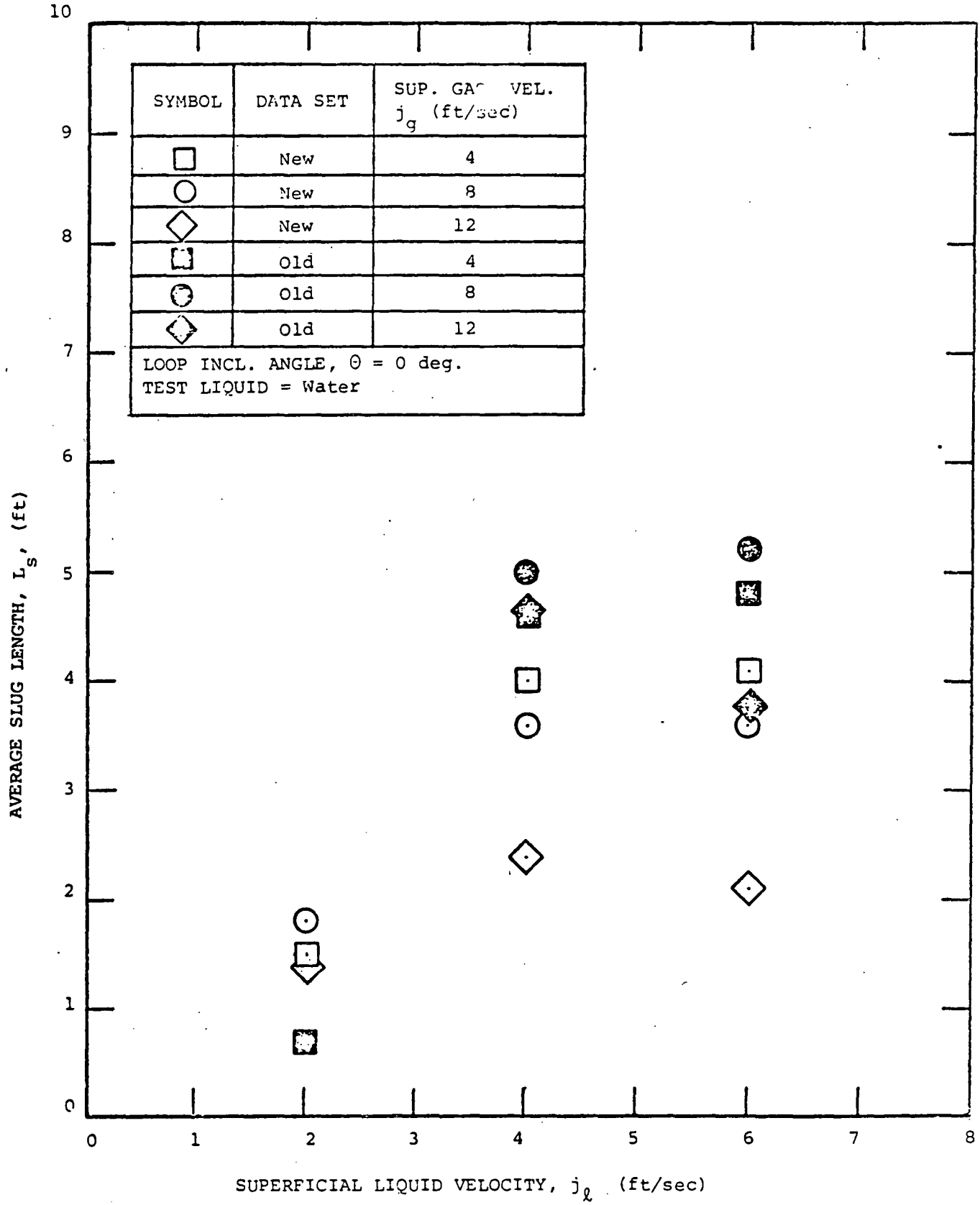

Figure B-5. AVERAGE SLUG LENGTH DATA OBTAINED WITH WATER

APPENDIX C

Comparison of New Pressure Drop Data Obtained In The Horizontal Loop Configuration With Previous Results

TABLE C-1
NEW LOOP PRESSURE GRADIENT DATA OBTAINED
WITH THE HORIZONTAL LOOP CONFIGURATION

Test Liquid	Test Number	Sup. Gas Vel. j_g (ft/sec)	Sup. Liq. Vel. j_ℓ (ft/sec)	Pressure Gradient, $\Delta P/L$ (lbf/ft^3)		
				Middle Leg	Bend	Last Leg
Water	W0046096	3.8	6.0	1.58	5.04	
	W0044097	3.9	4.0	0.75	2.35	
	W0042098	4.2	2.0	0.36	1.12	
	W0082099	7.8	2.0	0.53	1.57	Instrument Failure
	W0084100	7.8	4.0	1.37	4.12	
	W0086101	7.8	6.1	2.30	8.40	
	W0126102	11.6	5.9	3.06	12.29	
	W0124103	11.9	4.0	2.00	6.27	
	W0122104	11.8	1.9	0.90	3.36	
400 cP WPS	H0126105	11.4	5.9	6.22	15.46	7.21
	H0086106	7.9	5.9	5.42	10.98	5.84
	H0044107	4.1	4.0	2.75	5.15	3.25
	H0046108	4.0	5.9	4.33	7.84	4.87
	H0084109	8.1	4.0	3.80	7.17	4.19
	H0124110	11.4	4.0	4.22	9.41	4.85
	H0042111	4.0	2.0	1.43	1.90	1.73
	H0082112	7.7	2.0	2.26	3.19	2.31
	H0122113	11.8	1.9	2.03	3.81	2.67

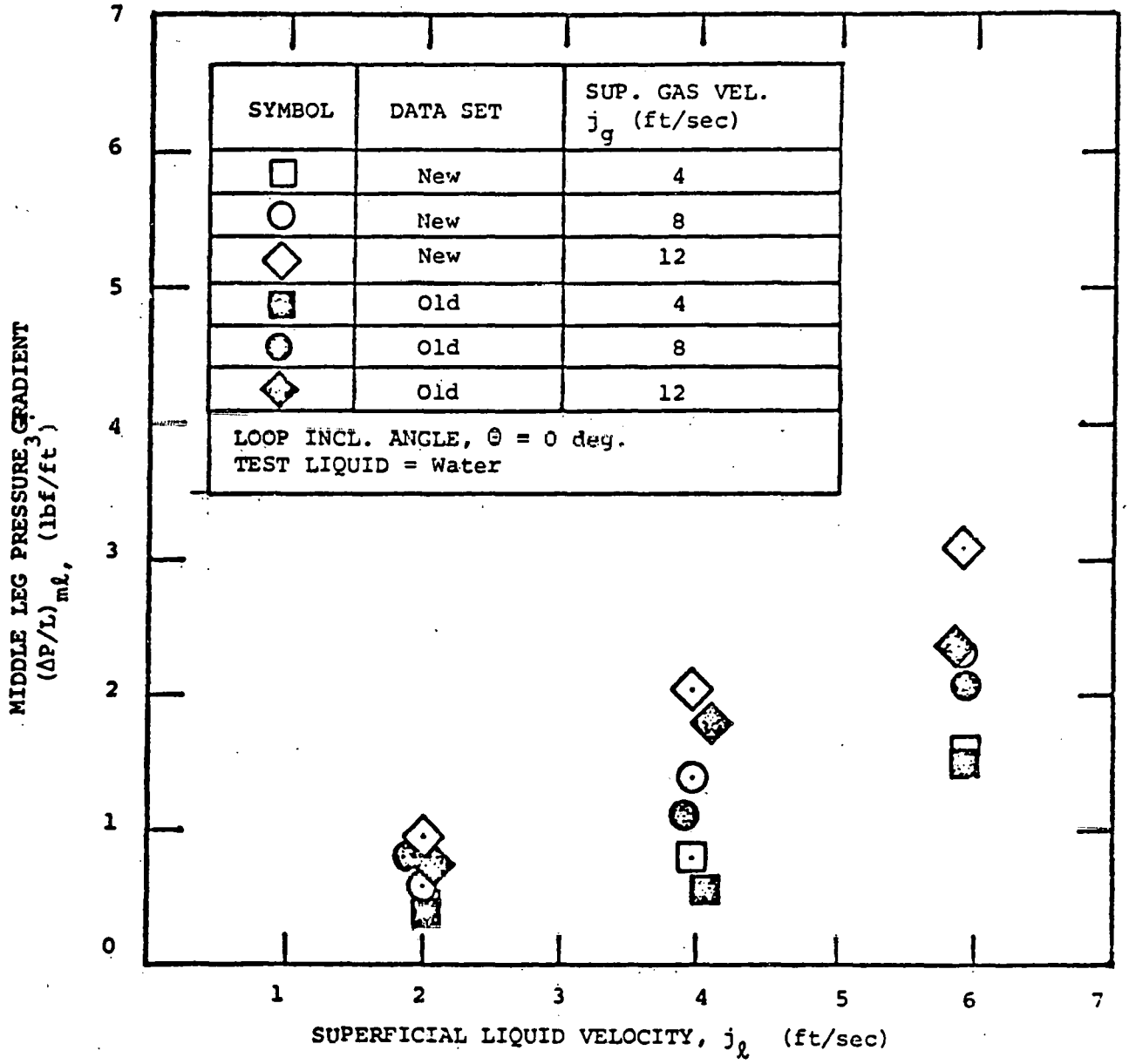

Figure C-1. MIDDLE LEG PRESSURE GRADIENT DATA OBTAINED WITH WATER

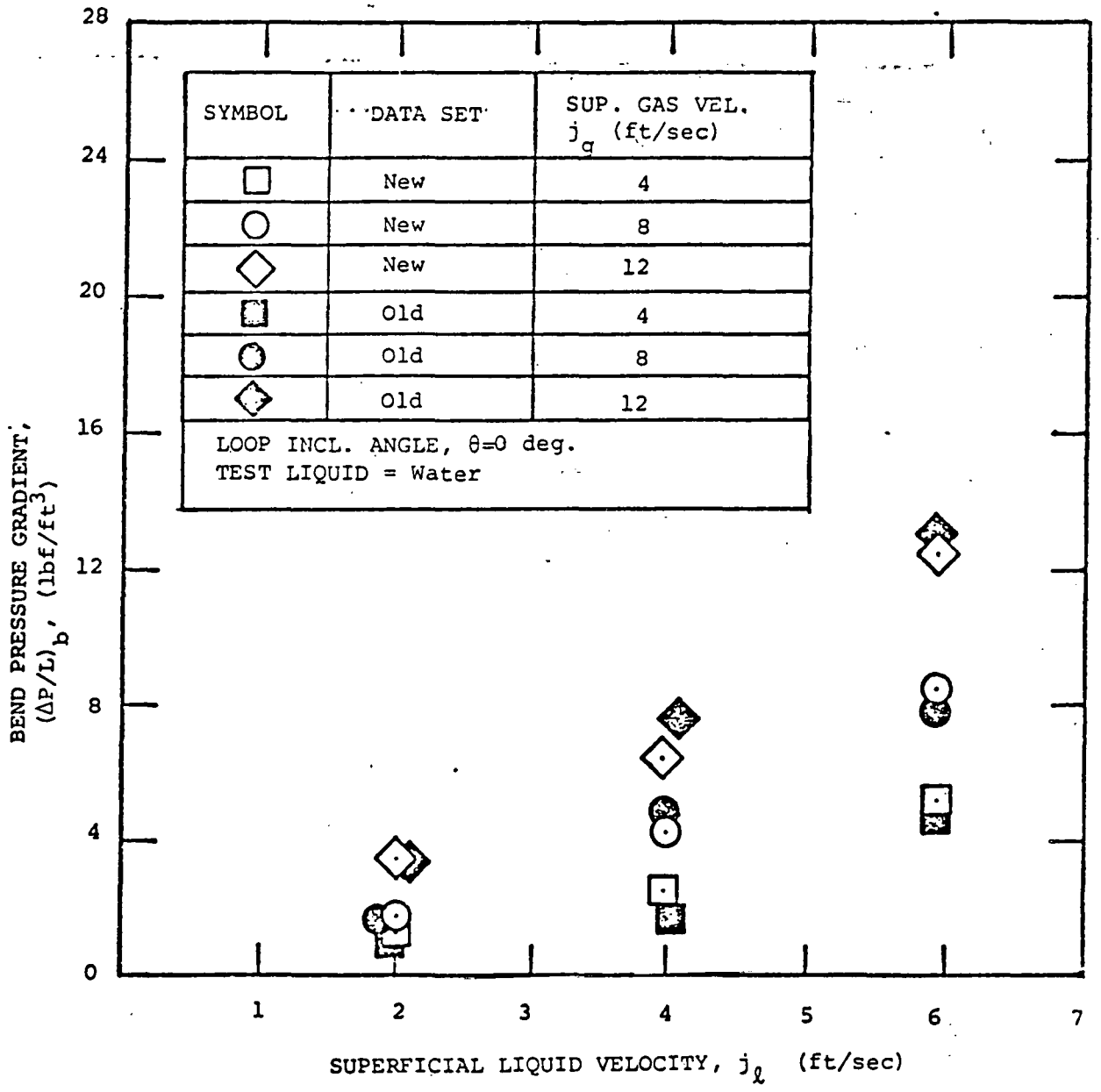

Figure C-2. BEND PRESSURE GRADIENT DATA OBTAINED WITH WATER

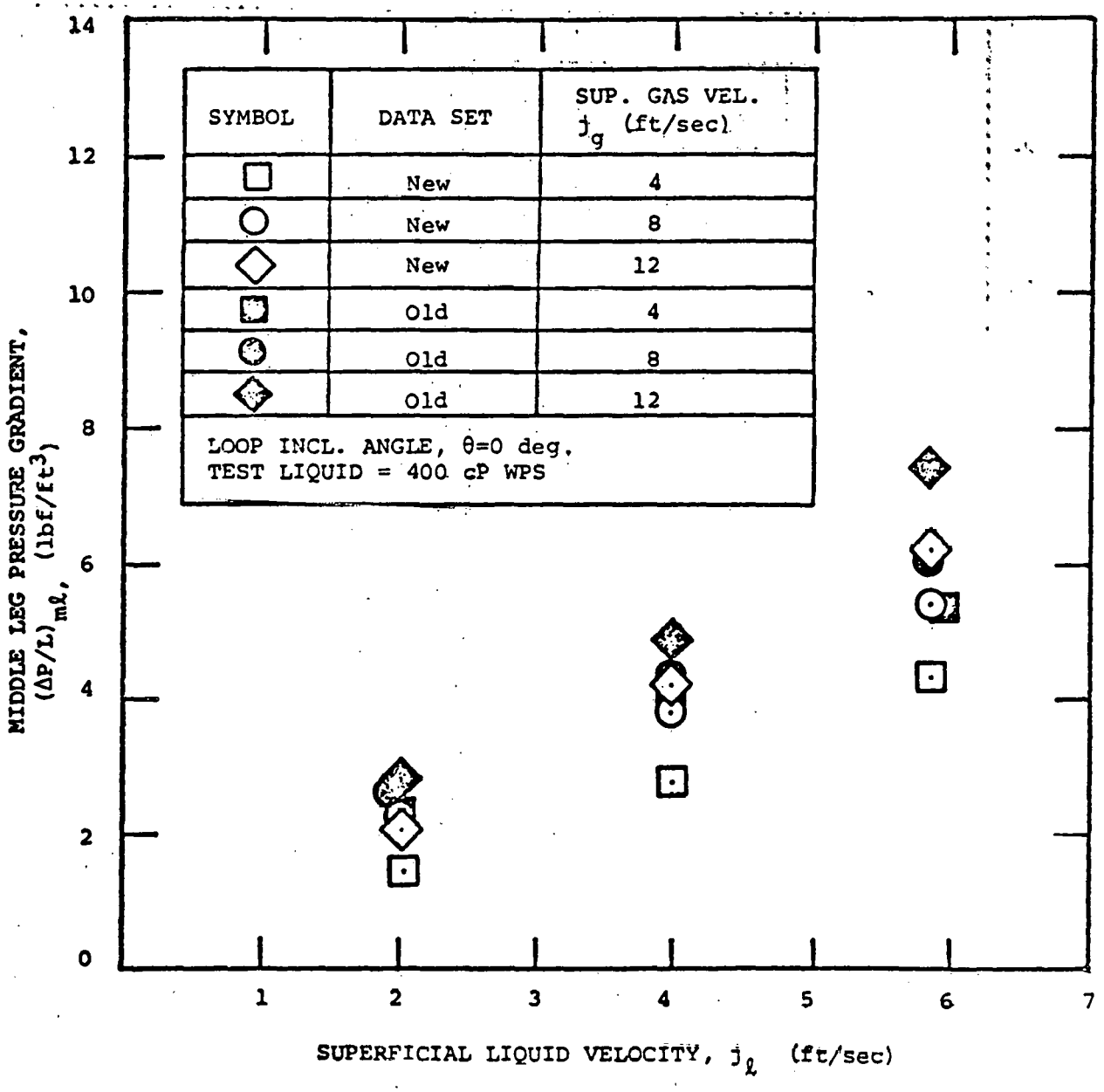

Figure C-3. MIDDLE LEG PRESSURE GRADIENT DATA OBTAINED WITH 400 cP WPS

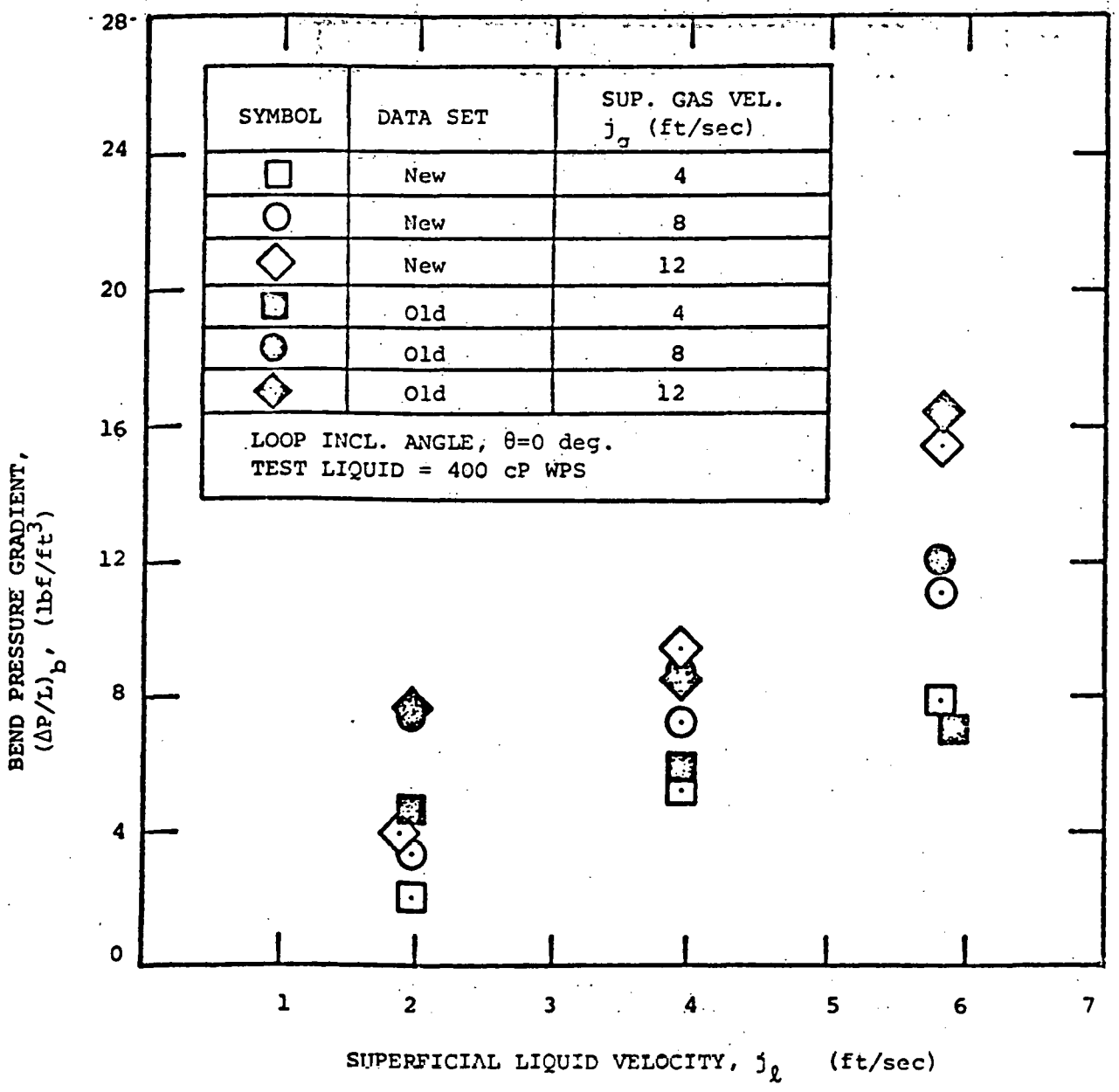

Figure C-4. BEND PRESSURE GRADIENT DATA OBTAINED WITH 400 cP WPS

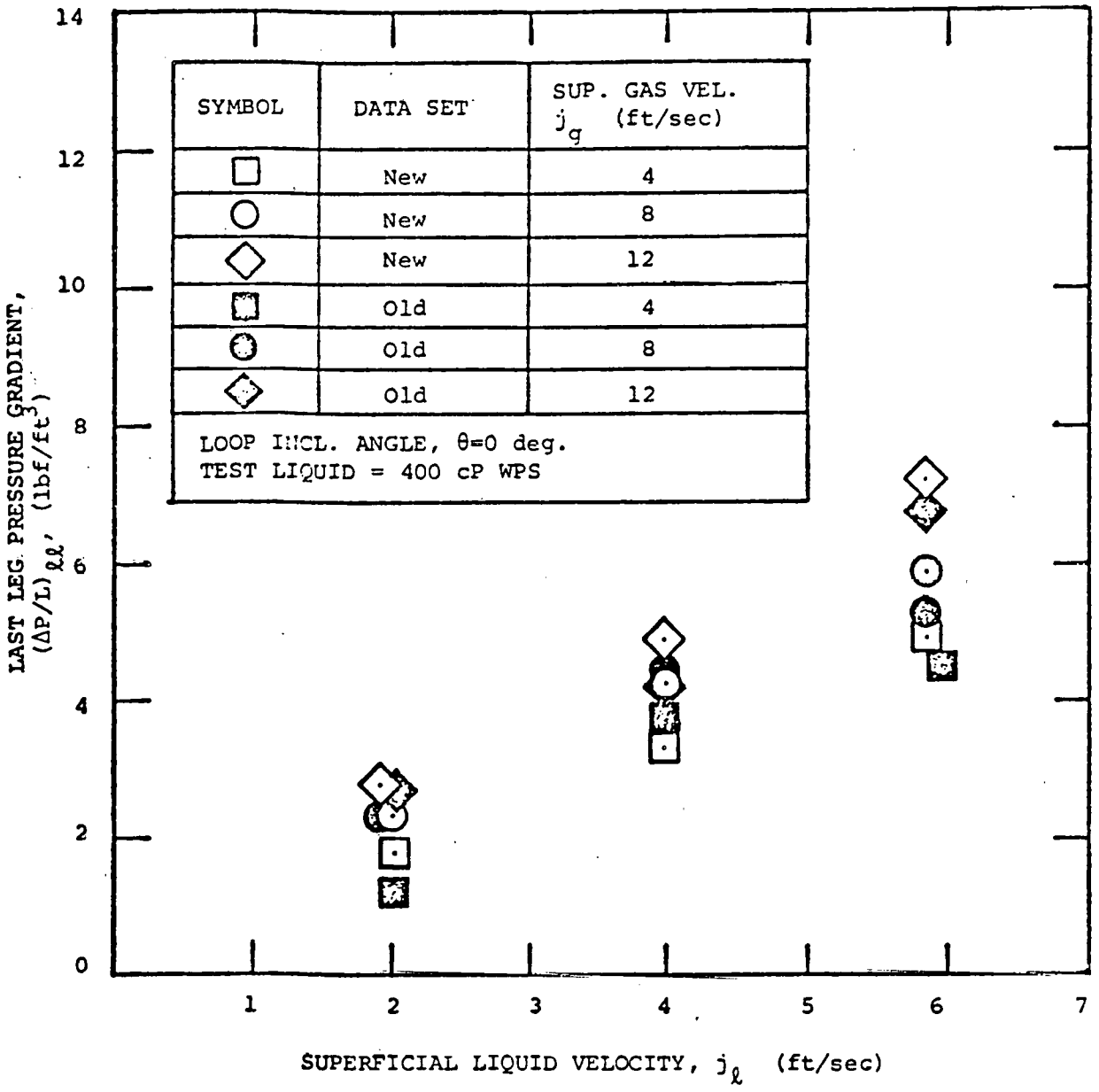

Figure C-5. LAST LEG PRESSURE GRADIENT DATA OBTAINED WITH 400 cP WPS

• U. S. GOVERNMENT PRINTING OFFICE: 1984-544-063/10279